POTENTIAL USE OF SFLT-1 AND PTERIN TO PREDICT THE CLINICAL OUTCOME OF CARDIOVASCULAR DISEASE

A thesis submitted in partial fulfilment of the requirements for the Degree of

Master of Science

in Biochemistry

School of Biological Sciences

University of Canterbury

New Zealand

Edward C.A. Marks

June 2015

Contents

List of figures. **V**

List of tables. **VII**

Acknowledgements. **IX**

Abstract. **X**

Abbreviations. **XII**

1 Introduction. **1**

1.1 Atherosclerotic plaque progression. 1

Pathophysiology of cardiovascular disease. 1

Epidemiology/ of cardiovascular disease in relation to heart failure and stroke. 5

1.2 VEGF and its receptors in cardiovascular disease. 6

The vascular endothelial growth factor (VEGF) pathway. 6

Utility of sFlt-1as a prognostic marker of CVD. 8

Current method of measurement. 9

Evaluation of Elisa kits for quantification of sFlt-1. 10

Assessment of clinical utility. 11

Development of sFlt-1 standards. 12

1.3 Cells mediating inflammation in CVD. 13

T-cell activation in atherosclerotic plaques. 13

Macrophage activation in atherosclerotic plaques. 15

1.4 Neopterin and 7,8-NP. 18

7,8 NP and neopterin in cardiovascular disease. 18

Synthesis of 7,8NP and neopterin. 18

Clinical utility of 7,8NP and neopterin. 20

1.5 Objectives of study. 22

2 Materials and methods. **24**

2.1 Reagents, kits, media and buffers. 24

Reagents. 24

Kits. 25

Media. 25

Buffers and solutions. 25

2.2 Plaque culture technique. 26

Endarterectomy plaque and plasma collection. 26

Sterile conditions. 26
Collection of human serum for use in Culture media. 27
Preparation of cell and plaque culture medium. 27
Plaque culture procedure. 28
2.3 Human monocyte derived macrophage culture. 28
Lymphocyte isolation. 28
HMDM seeding and feeding. 30
2.4 IFN-γ stimulation of macrophages and live plaque. 30
2.5 PMA stimulation of live plaque. 31
Alternative procedure. 32
2.6 Lactic acid assay. 32
2.7 sFlt-1 assay. 33
Alternative sample preparation. 34
2.8 Neopterin and 7,8-NP HPLC method. 35
HPLC setup. 35
Neopterin standard curve preparation. 35
Acidic iodide oxidizing potential testing. 36
Plasma and cell culture sample preparation and injection. 37
2.9 Statistical methods. 37
Patient population CDCS. 37
General linear model analysis. 38
Cox regression proportional hazards model and Kaplan-Meier analysis. 38
Endarterectomy statistics. 39
3 Results. 40
3.1 Cardiovascular disease cohort study (CDCS) 40
3.1.1 Statistical Power of CDCS in comparison with Matsumoto et al., 2013. 41
3.1.2 Relationship between CVD variables and biomarkers. 43
3.1.3 Direct correlations between Biomarkers and significant variables. 47
3.1.4 Survival analysis of CDCS patients. 49
3.2 Carotid endarterectomy cohort. 73
3.2.1 Plasma analysis. 74
3.2.2 Correlations. 78
3.2.3 IFN-γ treated HMDM analysis (positive control). 81
3.2.4 Dead IFN-γ treated plaque analysis (negative control). 83

3.2.5 Live untreated plaque analysis. 84
3.2.6 Live IFN-γ treated plaque analysis. 87
3.2.7 Live PMA treated plaque analysis. 93
3.2.8 Live IFN-γ and PMA treated plaque analysis. 97
4 General discussion, conclusions and future work. 101
4.1 Direct associations in the CDCS plasma between alcohol consumption and BNP versus the measured biomarkers neopterin, 7,8 NP and sFlt-1. 101
4.2 Predictive capacity of sFlt-1, neopterin, 7,8 NP and total neopterin in determining ACD TCVE and CVD death. 103
4.3 Plasma levels of sFlt-1, 7,8 NP, total neopterin, and neopterin in patients with late stage atherosclerosis in the carotid artery. 106
4.4 The presence of live inflammatory cell populations within atherosclerotic plaques. 107
4.5 Summary. 111
5 Bibliography. 112
6 Appendix. 124

List of figures

1 Introduction.

Fig 1. The response to injury hypothesis. 1

Fig 2. The oxidative modification hypothesis. 2

Fig 3. The response to retention hypothesis. 3

Fig 4. Progression of atherosclerosis. 4

Fig 5. VEGF receptors and the corresponding angiogenic machinery. 7

Fig 6. Regulation of VEGF signalling. 8

Fig 7. T-cell lineages in atherosclerosis. 15

Fig 8. Endothelial activation, macrophage migration and foam cell formation. 16

Fig 9. Biological 7,8 NP triosphosphate pathways. 19

Fig 10. Oxidation of 7,8 NP. 20

2 Methods.

Fig 2.1 Post centrifuged blood. 29

Fig 2.2 IFN-γ Procedure for macrophages and atherosclerotic plaque. 31

Fig 2.3 PMA procedure for atherosclerotic plaque. 32

Fig 2.4 Neopterin linear regression (standard curve). 36

3 Results.

Fig 3.1.1 Distribution Schematic. 41

Fig 3.1.2 Total neopterin ACD Kaplan-Meier analysis. 49

Fig 3.1.3 Total neopterin TCVE Kaplan-Meier analysis. 51

Fig 3.1.4 Total neopterin CVD death Kaplan-Meier analysis. 53

Fig 3.1.5 Neopterin ACD Kaplan-Meier analysis. 55

Fig 3.1.6 Neopterin TCVE Kaplan-Meier analysis. 57

Fig 3.1.7 Neopterin CVD death Kaplan-Meier analysis. 59

Fig 3.1.8 7,8 NP ACD Kaplan-Meier analysis. 61

Fig 3.1.9 7,8 NP TCVE Kaplan-Meier analysis. 63

Fig 3.1.10 7,8 NP CVD death Kaplan-Meier analysis. 65

Fig 3.1.11 sFlt-1 ACD Kaplan-Meier analysis. 67

Fig 3.1.12 sFlt-1 TCVE Kaplan-Meier analysis. 69

Fig 3.1.13 sFlt-1 CVD death Kaplan-Meier analysis. 71

Fig 3.2.1 sFlt-1 measured in endarterectomy plasma vs age and gender matched control plasma. 74

Fig 3.2.2 Neopterin measured in endarterectomy plasma vs age and gender matched control plasma. 73
Fig 3.2.3 7,8 NP measured in endarterectomy plasma vs age and gender matched control plasma. 75
Fig 3.2.4 Total neopterin measured in endarterectomy plasma vs age and gender matched control plasma. 76
Fig 3.2.5 Bivariate analysis of sFlt-1 vs 7,8 NP in endarterectomy patient plasma. 78
Fig 3.2.6 Bivariate analysis of sFlt-1 vs neopterin in endarterectomy patient plasma. 79
Fig 3.2.7 Bivariate analysis of sFlt-1 vs total neopterin in endarterectomy patient plasma. 80
Fig 3.2.8 HMDM vulnerability testing (positive control). 81
Fig 3.2.9 HMDMs total neopterin and neopterin production with IFN-γ treatment. 82
Fig 3.2.10 Dead plaques total neopterin production with IFN-γ treatment. 83
Fig 3.2.11 Total neopterin production per gram of untreated live plaque. 84
Fig 3.2.12 7,8 NP production per gram of untreated liv plaque. 85
Fig 3.2.13 Neopterin per gram of untreated live plaque. 86
Fig 3.2.14 Lactate produced per gram of IFN-γ treated live plaque. 87
Fig 3.2.15 Total neopterin produced per gram of IFN-γ treated live plaque. 89
Fig 3.2.16 7,8 NP produced per gram of IFN-γ treated live plaque. 90
Fig 3.2.17 Neopterin produced per gram of IFN-γ treated live plaque. 91
Fig 3.2.18 sFlt-1 produced per gram of IFN-γ treated live plaque. 92
Fig 3.2.19 Total neopterin produced per gram of PMA treated live plaque. 93
Fig 3.2.20 7,8 NP produced per gram of PMA treated live plaque. 94
Fig 3.2.21 Neopterin produced per gram of PMA treated live plaque. 95
Fig 3.2.22 Total neopterin produced per gram of PMA and IFN-γ treated live plaque. 97
Fig 3.2.23 7,8 NP produced per gram of PMA and IFN-γ treated live plaque. 98
Fig 3.2.24 Neopterin produced per gram of PMA and IFN-γ treated live plaque. 99

List of Tables

Table 3.1.1 General summary of CDCS patients 40
Table 3.1.2 Commonly associated variables expressed in a general linear model with sFlt-1 as the dependent variable. 43
Table 3.1.3 Commonly associated variables expressed in a general linear model with both neopterin and 7,8 NP combined as the dependent variable. 44
Table 3.1.4 Commonly associated variables expressed in a general linear model with Neopterin as the dependent variable. 45
Table 3.1.5 Commonly associated variables expressed in a general linear model with 7,8 NP as the dependent variable. 46
Table 3.1.6 Correlations observed between significant factors. 47
Table 3.1.7 Test for equality of survival distributions for the different levels of total neopterin. 50
Table 3.1.8 Cox proportional hazards model for ACD vs total neopterin, BNP age at baseline and drinks per week. 50
Table 3.1.9 Test for equality of TCVE distributions for the different levels of total neopterin. 51
Table 3.1.10 Cox proportional hazards model for TCVE vs total neopterin, BNP, age at baseline and drinks per week. 52
Table 3.1.11 Test for equality of CVD death distributions for the different levels of total neopterin. 53
Table 3.1.12 Cox proportional hazards model for CVD death vs total neopterin, BNP, age at baseline and alcohol consumption. 54
Table 3.1.13 Test for equality of survival distributions for the different levels of neopterin. 55
Table 3.1.14 Cox proportional hazards model for ACD vs neopterin, BNP, age at baseline and drinks per week. 56
Table 3.1.15 Test for equality of TCVE distributions for the different levels of neopterin. 57
Table 3.1.16 Cox proportional hazards model for TCVE vs neopterin, drinks per week, BNP and age at baseline. 58
Table 3.1.17 Test for equality of CVD death distributions for the different levels of Neopterin. 59

Table 3.1.18 Cox proportional hazards model for CVD death vs neopterin BNP, drinks per week and age at baseline. 60
Table 3.1.19 Test for equality of survival distributions for the different levels of 7,8 NP. 61
Table 3.1.20 Cox proportional hazards model for ACD vs 7,8 NP, drinks per week, BNP and age at baseline. 62
Table 3.1.21 Test for equality of TCVE distributions for the different levels of 7,8 NP. 63
Table 3.1.22 Cox proportional hazards model for TCVE vs 7,8 NP, drinks per week, BNP and age at baseline. 64
Table 3.1.23 Test for equality of CVD distributions for the different levels of 7,8 NP. 65
Table 3.1.24 Cox proportional hazards model for CVD death vs 7,8 NP, drinks per week, BNP and age at baseline. 66
Table 3.1.25 Test for equality of survival distributions for the different levels of sFlt-1. 67
Table 3.1.26 Cox proportional hazards model for ACD vs sFlt-1, drinks per week, BNP and age at baseline. 68
Table 3.1.27 Test for equality of TCVE distributions for the different levels of sFlt-1. 69
Table 3.1.28 Cox proportional hazards model for TCVE vs sFlt-1, drinks per week, BNP and age at baseline. 70
Table 3.1.29 Test for equality of CVD death distributions for the different levels of sFlt-1. 71
Table 3.1.30 Cox proportional hazards model for CVD death vs sFlt-1, BNP, drinks per week and age at baseline. 72
Table 3.2.1 General summary of endarterectomy patient's plasma. 73
Table 6.1 General summary of endarterectomy patients. 124
Table 6.2 General summary of endarterectomy patient's plasma. 125
Table 6.3 Age and gender matched healthy control patient plasma. 126

Acknowledgements

Mum and Dad if you can sit through this 140 page sleeping pill I will be impressed. Thank you eternally for all your support and time, this thesis is for you.

To Dr Barry Palmer and Associate Professor Steven Gieseg my appreciation of your guidance and thoughts will not be forgotten, as wherever I may end up, you will always remain in mine.

Neil Pattinson and Maurice Owen, thank you for your valuable advice and funding for this project, without you much of what was achieved would not have been possible.

Thank you to the Free Radical Biochemistry Department of Canterbury University and Justin Roake of the Christchurch Vascular Surgery Department. This study would not have been possible without you.

Lastly thank you to Craig Galilee whose efforts provided the departmental and regulatory means necessary to carry out this thesis.

Abstract

Formation of functional collateral circulation, to repair blocked or damaged arterial blood flow, is an important process in amending adverse outcomes after acute coronary occlusion events. Inadequate capillary growth during pressure overloads impairs myocardial perfusion, often contributing to the progression of coronary heart disease and ischaemia. Considered to be the critical rate-limiting step in physiological angiogenesis, the binding of VEGF (vascular endothelial growth factor) to VEGFR (vascular endothelial growth factor receptors) is essential for the growth and repair of arteries. Conversely, VEGF mediated angiogenesis has also been shown to promote atherosclerosis through arterial wall thickening. However, an alternatively spliced soluble form of VEGFR-1 (sFlt-1) has been shown to inhibit VEGF activity. sFlt-1 binds and sequesters free extracellular VEGF and/or heterodimerizes with VEGFR preventing the angiogenic pathway occurring. As a result, the primary pathway of angiogenesis does not occur. In recent years this has led to debate over the nature of sFlt-1 in the VEGF system. However, the level of sFlt-1 found in cardiovascular disease (CVD) patients, as well as its stability in plasma, has allowed for current research into its involvement with ischemic disorders to take place.

Enhanced T-cell activity that results in increased production of interferon-γ has been shown to have involvement in the pathogenesis of CVD. 7,8-dihydroneopterin (7,8 NP) production by monocytes and macrophages is primarily in response to stimulation by interferon-γ (IFN-γ) released by activated T-lymphocytes. When combined with neopterin, the oxidised product of 7,8 NP, the total neopterin is accounted for which is a measure of the total macrophage activation by interferon-γ. Therefore, the levels of total neopterin observed may reflect the level of cell-mediated immunity within individuals which could contribute to mortality post CVD event.

Progression of coronary heart disease is often clinically silent, without signs or symptoms. For this reason, the ability of markers to monitor progression is a powerful tool for predicting cardiovascular risk and the level of preventative treatment required. This study shows, that in 514 stable post-ACS (MI or unstable angina) patients, above median baseline sFlt-1, total neopterin and 7,8 NP levels, were strong predictors of mortality over a median 5 year period. Furthermore, above median sFlt-1 levels were specifically predictive of CVD death ($p=0.001$). This suggests that sFlt-1, total neopterin and 7,8 NP may be useful markers

for risk prediction in CVD patients, post-acute event, with potential to aid prognosis in previously diagnosed patients.

In support of these findings, levels of sFlt-1 measured in plasma taken from patients, immediately prior to undergoing carotid endarterectomy procedures (n=27), were significantly raised in comparison to age and gender matched healthy controls ($p<0.001$). Furthermore, levels of sFlt-1 in patient and control groups were shown to be independent of both age and gender.

Another aspect of the study, analysis of excised live plaque tissue from carotid endarterectomy patients, showed the presence of live inflammatory cell populations. Macrophages, in the plaque sections, could be stimulated in the presence of IFN-γ to produce significantly elevated ($p<0.01$) levels of the antioxidant 7,8 NP. Since bivariate analysis of 7,8 NP and sFlt-1, in plasma from the endarterectomy patients, yields a positive correlation ($r=0.323$, $p<0.01$), further analysis of live plaque may give insight into the association between inflammation and hypoxic up-regulation of sFlt-1.

It is now generally accepted, in diseases with complex pathogenesis, that particular biomarkers are predominantly indicative of only a single variable in a wide range of contributing factors. The data generated in this study highlights the potential for sFlt-1, neopterin and 7,8 NP to be used as contributing biomarkers in the prognosis of patients suffering from CVD, which if confirmed, may have important clinical implications in the medical community.

Abbreviations

AAP - Amino Antipyrine

ACD - All Cause Death

ACN – Acetonitrile

ACS - Acute Coronary Syndrome

$AmPO_4$ - Ammonium Phosphate

Apo-B - Apolipoprotein B

BMI - Body Mass Index

BNP - B Type Natriuretic Peptide

CD - Cluster differentiation

CDCS - Cardiovascular Disease Cohort Serum

CRP - C Reactive Protein

CSA - Chronic Stable Angina

CVD - Cardiovascular Disease

DMSO - Dimethy Sulphoxide

ELISA - Enzyme Linked Immunosorbent Assay

Flt-1 - FMS like Tyrosine Kinase-1

GTP - Guanosine Triphosphate

GTPCH-1 - Guanosine Triphosphate Cyclohydrolase-1

Ha - Hypothesis (actual)

HCL - Hydrochloric Acid

HIF-1 - Hypoxia Inducible Factor-1

HIHS - Heat Inactivated Human Serum

HMDM - Human Monocyte Derived Macrophage

$HO^{\bullet}$ - Hydroxyl Radical

Ho - Hypothesis (observed)

HOCL - Hypochlorous Acid

HPLC - High Performance Liquid Chromatography

I - Iodine

ICA - Internal Carotid Artery

IFN-γ - Interferon Gamma

Ig - Immunoglobulin

KDR - Kinase Insert Domain Receptor

KI - Potassium Iodide

LDL - Low Density Lipoprotein

LOD - Limit of Detection

MI - Myocardial Infarction

mRNA - messenger Ribose Nucleic acid

MW - Molecular Weight

NKT - Natural Killer T Cells

PBS - Phosphate Buffered Saline

PLGF - Placental Growth Factor

PMA - Phorbol 12-Myristate 13-Acetate

POD - Peroxidase

PRR - Pattern Recognition Receptor

PTS - 6-pyruvol-tetrahydropterin synthase

$ROO^{\bullet}$ - Peroxyl Radical

RPMI - Roswell Park Memorial Institute medium

SCX - Strong Cation Exchange

SEM - Standard Error of Mean

sFlt-1 - Soluble FMS like tyrosine kinase-1

$sPLA_2$ - Secretory Phospholipase A_2

TCVE - Total Cardiovascular Events

TFH - Follicular Helper T Cells

Th - T Helper Cells

TIA - Transient Ischaemic Attacks

TNF-α - Tumour Necrosis Factor Alpha

T_{Reg} - Regulatory T Cells

VEGF - Vascular Endothelial Growth Factor

VEGFR - Vascular Endothelial Growth Factor Receptor

7,8 DXP - 7,8-Dihydro-xanthopterin

7,8 NP - 7,8 Dihydroneopterin

1

Introduction

1.1 Atherosclerotic plaque progression

Pathophysiology of Cardiovascular disease

Major advances in understanding the underlying pathophysiology behind atherosclerosis have been achieved over the last 30 years. Previously considered a lipid storage disease, atherosclerosis, thought to be the leading cause of coronary artery disease, is now viewed as an inflammatory disorder (Siegel et al., 2013).

Acute myocardial ischaemia, like other manifested disorders of cardiovascular and cerebrovascular disease such as unstable angina and strokes, usually occurs following development of a fibrolipid plaque. However, the initial mechanism of atheroma development, prior to formation of an arterial fatty streak, is still under debate over three main hypotheses (Stocker & Keaney Jr, 2004).

The "response to injury hypothesis" first proposed in 1977 by Ross and Glomset, contradicted prior hypotheses of passive lipid and fibrin deposition, suggesting instead that prolonged damage to the arterial endothelium may be responsible. This repeated or chronic injury of the endothelium is said to upset the vascular homeostatic balance, resulting in distinct sites of smooth muscle proliferation and sequestering of lipid at the site of injury (Ross, Glomset, & Harker, 1977) (Fig. 1).

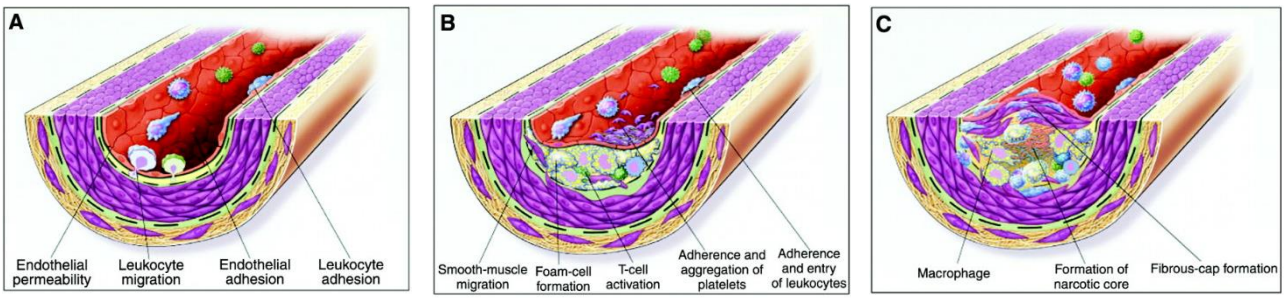

Fig 1. The response to injury hypothesis (Ross et al., 1977). A: Increased endothelial permeability occurs as a result of prolonged damage to the arterial endothelium resulting in

LDL accumulation in the sub-endothelial space. This promotes the adhesion and migration of inflammatory cells into the sub-endothelial space. B: Foam cell formation occurs following macrophage uptake of modified LDL in the sub-endothelial space. T-cell activation further promotes the migration of inflammatory cells to the sub-endothelial space advancing the atherosclerotic plaque formation. C: A fully formed fibro-lipid plaque. Characterised by continued macrophage accumulation, a necrotic core and a fibrous cap (Stocker & Keaney Jr, 2004).

The "oxidative modification hypothesis" was originally proposed on the basis of two different experiments. Firstly that injury to cells by LDL was dependent upon its oxidation (Hessler, Morel, Lewis, & Chisolm, 1983; Morel & Chisolm, 1984; Morel, Hessler, & Chisolm, 1983) and secondly that cultured cells could modify native LDL in media, to a form recognized by scavenger receptors on macrophages, which was shown to be a result of oxidative modification (Henriksen, Mahoney, & Steinberg, 1981, 1983) (Fig. 2).

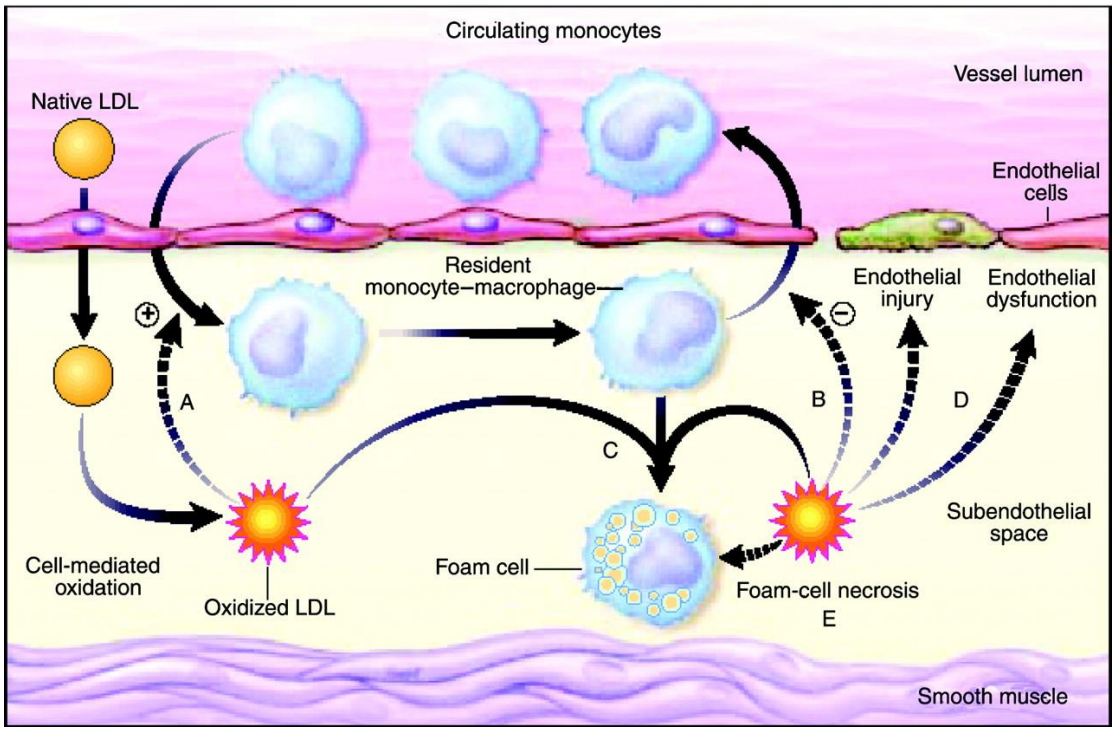

Fig. 2 The oxidative modification hypothesis (Henriksen et al., 1981, 1983; Hessler et al., 1983; Morel & Chisolm, 1984; Morel et al., 1983). A: Circulating LDL accumulates in the sub-endothelial space where it is subject to oxidative modification. B&C: This oxidised LDL stimulates monocyte chemotaxis eventually causing foam cell formation as it is engulfed by macrophages. D: Oxidised LDL also results in endothelial dysfunction contributing to the necrotic core (Epstein, Diaz, Frei, Vita, & Keaney Jr, 1997).

Lastly the "response to retention hypothesis" suggests that arterial lipoprotein retention is the defining event in atherosclerotic initiation (Williams & Tabas, 1995). Hyperlipidemia is said to cause lesion development at specific points in the artery, which express apolipoprotein B (ApoB) retentive molecules. Therefore ApoB containing lipoproteins are somewhat restricted at these points, where they may encroach on the sub-endothelial tissue via transcytosis (Proctor, Vine, & Mamo, 2002). This accumulated lipoprotein may then prompt a chemotaxic event, triggering an inflammatory response, which results in the recruitment of monocytes and other inflammatory cells to the arterial intima (Fig. 3).

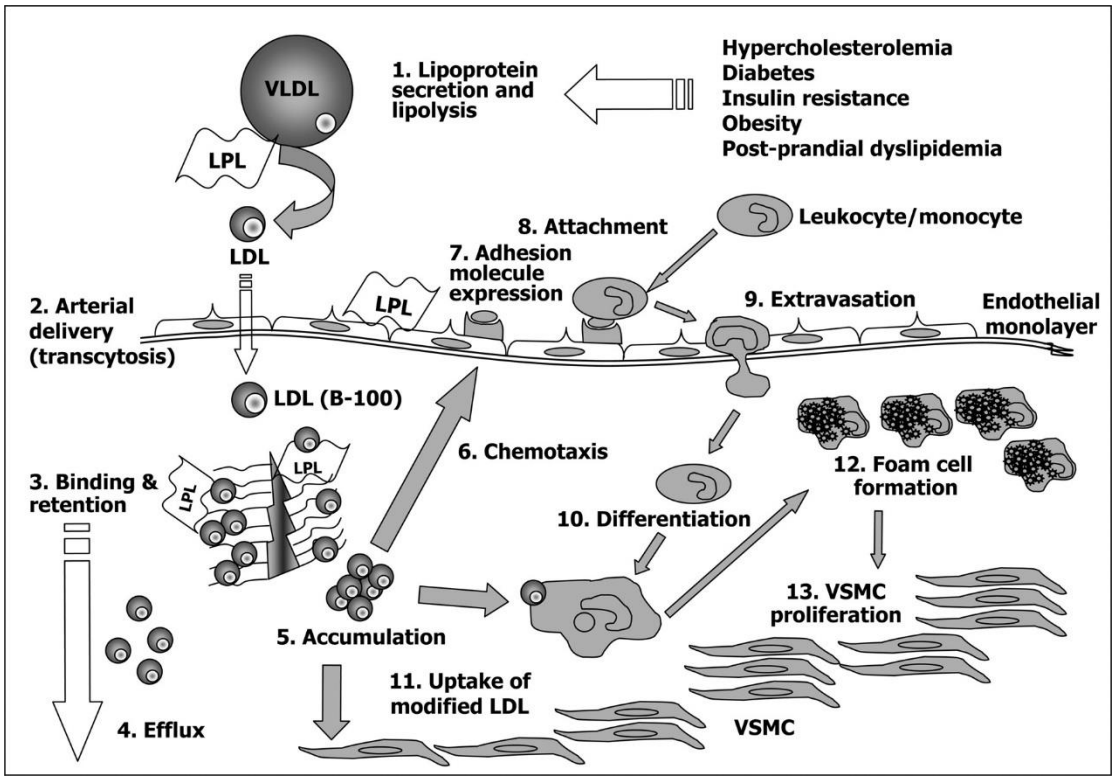

Fig 3. The response to retention hypothesis (Williams & Tabas, 1995). Apolipoprotein B (Apo-B) retentive molecules within the artery lead to accumulation and aggregation of LDL (1-5). Accumulation of the apolipoprotein B containing lipoproteins is then thought to further promote pro-inflammatory cascades in the sub-endothelial space (Stocker & Keaney Jr, 2004).

Though all three hypotheses have merit, lipoprotein retention, oxidative damage and chronic inflammation are all intimately related to the early progression of atherosclerotic plaques. Therefore, atherosclerotic initiation is now more commonly noted as a unified model of these three concepts (Fuster, Moreno, Fayad, Corti, & Badimon, 2005).

Although there is still debate over the initial stages of plaque formation, it is now well documented that the inflammatory response comes as a result of lipid filled inflammatory cells (mainly macrophages) and T-cells within the arterial wall. These cells, more often than not, are highly activated producing pro-coagulant and inflammatory mediators such as tumour necrosis factor-α (TNF-α) and IFN-γ. This inflammatory cell accumulation and subsequent death leads to asymmetrical focal thickening of the arterial intima, forming what is known as an atherosclerotic plaque (Hegyi, Skepper, Cary, & Mitchinson, 1996).

If growth of the plaque is unrelieved, destabilization can occur resulting in plaque rupture and release of highly thrombogenic materials such as tissue factor, fragments of collagen and crystalline surfaces which accelerate the process of blood coagulation (Davies, 2000). The two mechanisms by which the plaque may rupture (tearing of the fibrous cap or breakdown of the fibrous cap by proteases released by macrophages) are both a reflection of the enhanced inflammatory activity within the plaque (Davies, 2000). When exposed to the artery lumen blood coagulation and thrombogenic factors cause aggregation of activated platelets, which occlude the artery, restricting blood flow and reducing the efficiency of oxygen transport. Furthermore, whilst blood flows past the occluding thrombus, activated platelets are swept into distal arteries which may result in the formation of emboli and further artery occlusion (Libby, 2001) (Fig. 4)

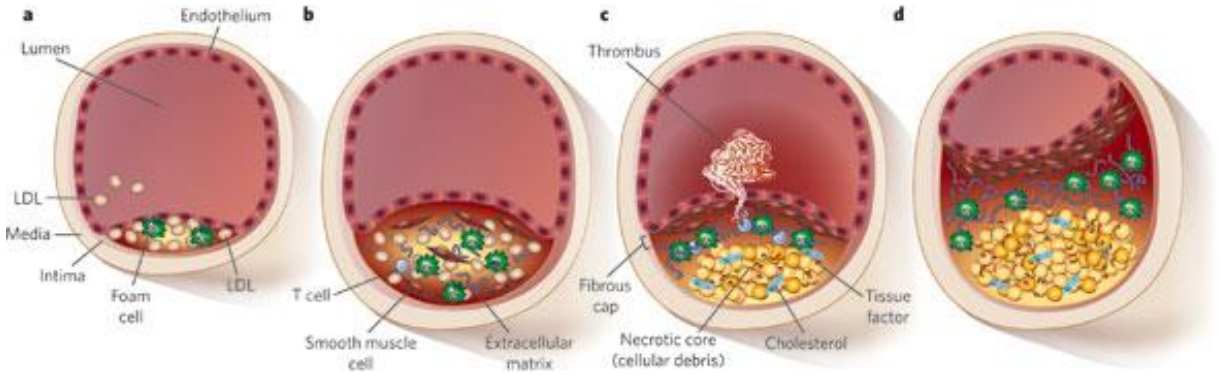

Fig 4. Progression of atherosclerosis. A: LDL enters the arterial intima, where it is modified by oxidation or enzymatic activity and aggregates within the sub-endothelial space, this promotes its uptake by macrophages. Unregulated uptake of lipoproteins by macrophages leads to the generation of foam cells. The accumulation of foam cells leads to the formation of fatty streaks. B: Vascular smooth muscles contribute to the inflammatory process via cytokine driven recruitment of further inflammatory cells to the arterial intima. As the plaque grows compensatory remodelling takes place, narrowing the arterial lumen diameter, which restricts blood flow and increases blood pressure. C: Foam cells eventually die resulting in the release

of cellular debris and crystalline cholesterol. As well as contributing to the necrotic core, this process results in further macrophage recruitment. This advanced plaque is prone to rupture releasing thrombogenic material, including tissue factor, resulting in the formation of a thrombus in the artery lumen. If the thrombus is large enough it can block the artery preventing downstream oxygen supply, ultimately resulting in clinically observable manifestations, such as myocardial infarction (MI). D: Alternatively, the plaque may not rupture but continue to grow. This results in a silently occlusive process which often manifests as angina (Rader & Daugherty, 2008).

A loss of oxygen perfusion to the myocardial tissue, as a result of thrombus formation, may result in clinical manfestations of CVD such as MI. Likewise the loss of blood flow in arteries which perfuse the brain causing strokes is another manifestation of atherosclerosis. However, this is often referred to as cerebrovascular disease. In order to simplify the pathology of these two clinical syndromes, coronary artery disease and cerebrovascular disease are referred to collectively as CVD (Stocker & Keaney Jr, 2004).

Epidemiology/ of CVD in relation to heart failure and stroke

In New Zealand alone, CVD, characterized mostly by clinical manifestation events such as strokes, MI, unstable angina and heart failure, is second only to all forms of cancer, in the rate of mortality caused by disease (Hay, 2002). Furthermore, recent studies have indicated that approximately 25% of patients who are discharged following treatment of a CVD event are re-admitted within one year (Ross et al., 2009; Selim, Velankar, Soghier, & Zolty, 2011). For this reason research into the development of diagnostic tools for the early detection and prognosis in CVD patients has been of great interest.

Challenges in the diagnosis of CVD, and an increased prevalence with advancing age (Gross, Chaudhry, Leo-Summers, & Fried, 2011), often makes intervention prior to a CVD event difficult. With the notion that abnormal ischemic events play a detrimental role in the development of CVD; mediators of vascular function and their receptors may provide valuable prognostic information as biomarkers of the disease.

In accordance with various health statistics, repeated ischemic events in the myocardium, characterized by an inadequate supply of oxygen-rich blood to the heart muscles, is generally associated with CVD. This suggests that recurrent ischemic events may be one of

the dominant mechanisms leading to exacerbation of and progression of heart failure (Khand, Gemmell, Rankin, & Cleland, 2001).

Recent heart disease and stroke statistics highlight the importance of accurate diagnosis and reliable prognostic markers of cardiovascular disease. According to the most recent summary by the American Heart Association, CVD events still account for one in every three of all the 2,437,163 deaths per year in the USA, with 1 in every 6 and 1 in every 19 from coronary artery disease and strokes, respectively. Overall, CVD accumulates a cost of approximately US$312.6 billion annually to the US economy, further highlighting the need to identify early signs of the disease so adequate preventative measures can be taken such as cessation of smoking and monitoring of dietary and exercise habits (Go et al., 2013).

1.2 VEGF and its receptors in CVD

The vascular endothelial growth factor (VEGF) pathway

New blood vessel growth and repair is a highly complex process, thought to require sequential activation via a series of ligands and their corresponding receptors. However, VEGF signalling is known as the critical rate limiting step in physiological angiogenesis (Ferrara, Gerber, & LeCouter, 2003).

VEGF-A is one of five related growth factors, including VEGF-B, VEGF-C, VEGF-D and placenta growth factor (PlGF), which bind primarily to three tyrosine kinase receptors with differing affinity. In addition to these five factors, a series of VEGF-A splice variants may bind to corresponding VEGF receptors, but fail to evoke any response and have therefore been described as anti-angiogenic (Harper & Bates, 2008).

The structurally related VEGF receptors, denoted VEGFR1/FMS-like tyrosine kinase-1 (Flt-1), VEGFR2/Kinase insert domain receptor (KDR) and VEGFR3 (Flt-4) have an overlapping, but distinct expression pattern, with Flt-1 in monocytes, macrophages and vascular endothelial cells, KDR in vascular endothelial cells and Flt-4 in lymphatic endothelial cells (Koch & Claesson-Welsh, 2012). However, the complexity of these receptors is increased further by alternative splicing (Fig. 5).

Hypoxic tension, in such circumstances as stenosis caused by CVD, mediates the regulation and expression of several VEGF family ligands and receptors via Hypoxia inducible factor-1 (HIF-1) (Banai et al., 1994; Germain, Monnot, Muller, & Eichmann, 2010; Vissers, Gunningham, Morrison, Dachs, & Currie, 2007). This up-regulation in hypoxic conditions leads to increased expression in states of growth (embryonic development) and disease (cancer and CVD).

Flt-1, the first receptor tyrosine kinase to be identified as a VEGF receptor, is also up-regulated by hypoxia in a HIF-1-dependent mechanism (Sandner, Wolf, Bergmaier, Gess, & Kurtz, 1997). Although Flt-1 binds VEGFA, VEGFB and PIGF its kinase activity is poor (Eichmann & Simons, 2012; Koch & Claesson-Welsh, 2012). It has therefore been hypothesised that Flt-1 is not required as an endothelial signalling receptor, but may instead serve to capture VEGFA in order to mediate formation of angiogenic sprouts through KDR (Kappas et al., 2008). In support of this, mouse models with deletion of the Flt-1 tyrosine kinase domain are compatible with vascular development (Hiratsuka et al., 2001). However, this is not to say that Flt-1 may not still be able to signal via formation of a heterodimer (Rahimi, 2006).

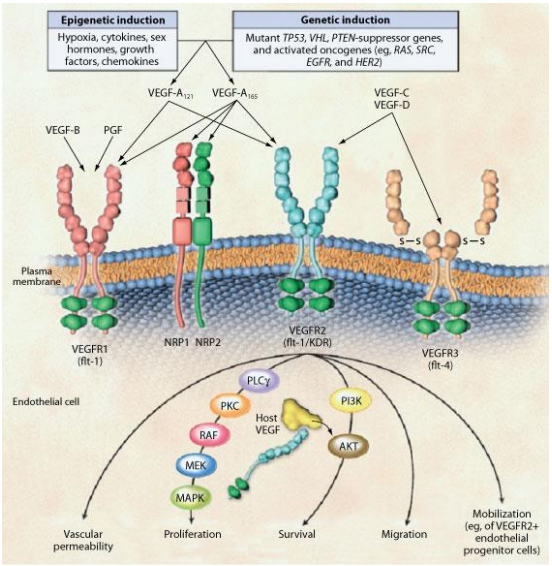

Fig 5. VEGF receptors and the corresponding angiogenic machinery. Binding of vascular growth factors to KDR is shown to elicit pathways necessary for angiogenic up regulation.(Kerbel, 2008)

Although the exact function of Flt-1 is still under debate, it is well known and documented that binding of VEGF-A to KDR promotes the growth of vascular endothelial cells, prompting a potent angiogenic response to hypoxic conditions. This results in the remodelling of arteries, production of new blood vessels and vasodilatation (Ku, Zaleski, Liu, & Brock, 1993) to relieve stress caused by disorders such as CVD (Schaper & Buschmann,

1999). Furthermore, mouse model studies have shown that KDR knockout is not compatible with vascular development (Cai, Jiang, Ahmed, & Boulton, 2006).

Soluble Flt-1 (sFlt-1) is an alternatively spliced circulating form of Flt-1 with equal affinity for VEGF. However, in contrast to Flt-1, sFlt-1 is produced mainly by endothelial cells and deposited in their extracellular matrix (Orecchia et al., 2003).

Acting as a decoy, sFlt-1 (also up-regulated by hypoxia) binds VEGF in the blood, inhibiting the angiogenic action which occurs from VEGF binding to membrane bound KDR on endothelial cells in the artery (Belgore, Blann, & Lip, 2001). Consequently it has been implicated as a negative regulator of angiogenesis (Fig. 6). It is therefore not surprising that elevated levels of sFlt-1, following acute myocardial ischemia in CVD patients, have been associated with increased risk of future CVD events as neovascularization is hindered (Hochholzer et al., 2011; Kapur et al., 2011; Kim et al., 2011). However, contrary to this, gene delivery of sFlt-1 has been shown to inhibit intra-plaque angiogenesis which supresses atherosclerotic plaque development (Wang et al., 2011).

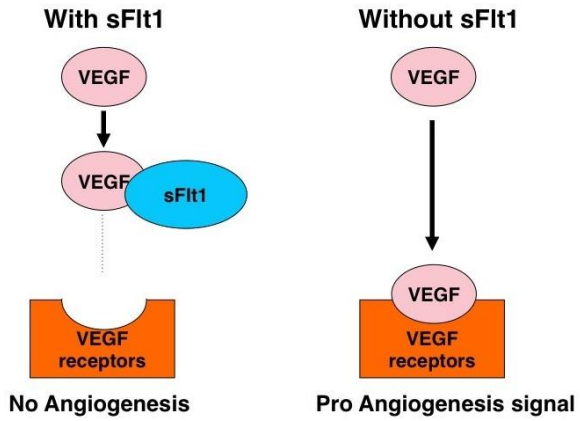

Fig 6. Regulation of VEGF signalling. Strict regulation of VEGF signalling occurs through sFlt-1. sFlt-1 binds and sequesters VEGF from cell-surface VEGF receptors, subsequently the VEGF modulated pro-angiogenic signal is inhibited (L. Xu, Kanasaki, Kitada, & Koya, 2012).

Despite these contrary findings in varying diseases, where a balance of anti- angiogenic and angiogenic factors play a key role in the context of their pathology, such as MI (Searle et al., 2012) and pre-eclampsia (Seki, 2014), s-Flt-1 has been shown to be a valuable diagnostic and prognostic marker. In support of its potential utility patients referred for emergent percutaneous coronary revascularization and active chest pain, with acute coronary occlusion, exhibited significantly elevated sFlt-1 serum levels (Kapur et al., 2011).

Utility of sFlt-1as a prognostic marker of CVD

An imbalance of anti-angiogenic and angiogenic factors, causing abnormal vascular growth, plays a major role in the progression of CVD (Lip & Chung, 2005). Alteration in angiogenic growth factors (such as VEGF) results in endothelial cell dysfunction and a lack of vascularization, also causing an increase in pressure and afterload putting strain on the heart (Carmeliet, 2005). It has been shown, and is now well documented, that Flt-1 as well as sFlt-1 are upregulated during ischemia (Gerber, Condorelli, Park, & Ferrara, 1997; Koch & Claesson-Welsh, 2012).

Since levels of sFlt-1 are associated with inhibition of VEGF activity, there have been studies into sFlt-1's potential for biomarker use in CVD (Searle et al., 2012). However, not all studies have provided the same results. Recent reports have shown that plasma levels of sFlt-1 are associated with increased disease severity in chronic CVD (Kim et al., 2011; Ky et al., 2011). Furthermore, other work has shown the prognostic utility of sFlt-1 in predicting the clinical outcome of post-percutaneous coronary intervention MI patients (Searle et al., 2012). On the other hand, data obtained by Kodama et al. indicates that plasma sFlt-1 is lower in patients with acute MI (Kodama et al., 2006). These contradictory findings are difficult to explain. However, there is an overwhelming body of data in support of sFlt-1's association with CVD events (Hochholzer et al., 2011; Kapur et al., 2011; Onoue et al., 2009). Furthermore, past evidence also indicates that levels of Flt-1, as well as sFlt-1 are significantly increased in the acute phase of myocardial ischemia (Kapur et al., 2011; Xu et al., 2001).

Since HIF-1 binding in the Flt-1 promoter region is responsible for the hypoxia induced up-regulation of Flt-1, sFlt-1 mRNA is also up-regulated under hypoxic conditions. This has led to the general consensus that sFlt-1 increases during acute CVD as a result of alternative Flt-1 splicing under hypoxic conditions (Onoue et al., 2009). This hypothesis of sFlt-1 up-regulation, along with large scale studies demonstrating the prognostic impact of sFlt-1 in patients with CVD and MI (Hochholzer et al., 2011; Matsumoto et al., 2012), indicates the potential that sFlt-1 has as a biomarker, with respect to CVD and other ischaemic conditions.

Current method of measurement

Based on the current literature; identifying sFlt-1's role in CVD, there have been many assays developed. Currently the gold standard for the detection and measurement of sFlt1 in the plasma is by enzyme linked immunosorbent assay (ELISA). Studies by Belgore et al. and

Hornig et al. outline the use of modified double-sandwich, non-competitive ELISA designs for the detection of sFlt-1 (Belgore et al., 2001; Hornig, Behn, Bartsch, Yayon, & Weich, 1999).

In recent years the use of commercially available ELISA kits has been preferred, for their efficiency, as opposed to designing assays from scratch. However, most rely on the same electrochemiluminescence technology for detection as the ELISA assays designed by Belgore and Hornig. Whilst many successful ELISAs have been developed for experimental use, evidence for their use in a clinical setting is lacking.

A recent study has outlined the use of the Roche ELISA kit to successfully determine reference ranges of sFlt-1 for the assessment of pre-eclampsia (Verlohren et al., 2010), a hypertensive medical condition seen in pregnant women, suggesting that a similar method could be used following hypertensive crisis resulting from ischemic events such as in CVD. This being said, recent attempts to derive reference values for the prognosis of ischaemic heart conditions have yielded varied results.

Three recent studies obtained values of approximately 72pg/ml, 500pg/ml and 379pg/ml respectively (Kim et al., 2011; Ky et al., 2011; Onoue et al., 2009), for patients suffering varying forms of ischaemic heart disease. Furthermore, Kim et al. determined that the level of sFlt-1 in CVD patients was not significantly different to those found in the healthy controls. However, it has been shown recently, that above median baseline levels of sFlt-1 (>300 pg/ml) measured in CVD patients prior to coronary angiography, were predictive of all-cause mortality, but not necessarily CVD events, supporting sFlt-1's prognostic utility, but not its ability for prediction of CVD events (Ky et al., 2011). Therefore, due to the lack of consistent results and reference points, required for the prognosis of CVD in a clinical setting, further research is required into the development of a successful protocol for measurement and accurate reference standards for comparison.

Evaluation of ELISA kits for quantification of sFlt-1

Advances in the purification and measurement of proteins have led to a better understanding of the molecular principles behind health and disease. From a clinical perspective, the selection of appropriate protein detection is essential, as the quantitative changes in expression must be accurately measured before a diagnostic outcome can be achieved. The ideal procedure for protein detection must cater for the biological question being

analysed, in order to achieve a low limit of detection (LOD) and an optimal signal to noise ratio (Westermeier & Marouga, 2005).

Detection and quantification of sFlt-1 using ELISA methods has been used extensively to determine its potential association with CVD severity (Kim et al., 2011; Matsumoto et al., 2012; Onoue et al., 2009). However, although an association between CVD and sFlt-1 levels has been established, bioanalytical methods must be optimized before valid reference standards can be produced for use in a clinical setting. In an article submitted by Hantash *et al*. (2009), a procedure for the optimization, validation and development of an ELISA method for the binding of an IgG1 monoclonal antibody to the epidermal growth factor receptor, similar to VEGR-1 was outlined (Hantash, Smidt, & Bowsher, 2009). Using the same method of accuracy assessment; assay kits for the measurement of analytes, such as sFlt-1, relating to disease progression may be compared and contrasted for their efficiency.

The major concern of the ELISA assay is that protein levels typically vary much more between individuals than within one individual over time. As a result, longitudinal studies across a large subject group are useful in controlling for this biomarker variability across a population (Gonzalez et al., 2008). Furthermore, this research also demonstrates the importance of a stringent assay protocol and the value of optimizing antibody specificity, in order to avoid saturation and resulting uncertainty of analyte levels at higher concentrations. Studies using ELISA have shown its potential for use in candidate biomarker validation, due to its exceptional specificity as a result of the two antibody analyte detection system (Zangar, Varnum, & Bollinger, 2005).

Once an appropriate selective assay has been identified methods of quantification for the desired biomarker can be employed. However, in order to achieve a definitive quantitative assay, yielding accurate and precise values to be assessed in a clinical setting, healthy and unhealthy reference ranges must first be defined.

Assessment of clinical utility

Aside from the limitations of the ELISA method, all biological and environmental factors affecting the subject populations must be taken into account, before statements on the clinical outcome and early diagnosis of patients (with reference to a biomarker) can be made. A recent study, identifying the impact of sFlt-1 serum levels for early diagnosis in patients with

suspected acute MI, demonstrated that baseline characteristics of the subject population such as previous heart failure, smoking and diabetes played a role in the levels of biomarker measured and were therefore highly relevant (Hochholzer et al., 2011).

Although recent findings have found a significant correlation between CVD events and sFlt-1 levels, reference values for healthy and CVD patients have not yet been established. Furthermore, values of sFlt-1 in patients at risk of CVD differ widely across various studies (Hochholzer et al., 2011; Kim et al., 2011; Ky et al., 2011; Matsumoto et al., 2012; Onoue et al., 2009). Therefore the repeatability of recent findings is difficult to verify, highlighting the need for development of sFlt-1 reference standards in order to ascertain reproducible results.

Development of sFlt-1 standards

A definitive quantitative assay is defined as the use of calibrators fitted to a regression model in order to determine the quantitative values of unknown samples. However, such assays are only possible when the reference standards are well defined and fully representative of the endogenous biomarker (Lee et al., 2006).

It has been shown that basal levels of sFlt-1 will vary between healthy populations and those suffering from CVD, as well as in individuals, depending upon their current health status in relation to variables such as previous coronary injury, smoking or diabetes (Matsumoto et al., 2012). Therefore, in order to determine an individual's or population's potential risk via sFlt-1, the reference ranges established must take into account variables affecting each individuals sFlt-1 levels. Furthermore, in order for the ranges to be clinically and statistically viable, they must be obtained from a large subject group (Lee & Hall, 2009). Once these ranges have been established assay standards may be generated for comparison to patient levels, indicating potential risk of CVD events.

The recombinant form of the protein analyte is most commonly used as a reference material, as this serves as a relative measurement to the endogenous species. Once a standard curve is established from the reference material, specific parameters of the analyte material can be derived such as concentration and molar equivalence (Lee & Hall, 2009). Such a procedure is now standard practice for the determination of an unknown protein biomarker concentration.

1.3 Cells mediating inflammation in CVD

T-cell activation in atherosclerotic plaques

Support for the relationship between immunity and inflammation has grown substantially in recent years. As this knowledge has grown, it has been increasingly recognised that both arms of the immune response (innate and adaptive) can either exacerbate or attenuate aspects of atherosclerotic progression (Hansson, 2005). Furthermore, the notion that inflammation plays an instrumental role in plaque growth and rupture has been well supported by studies indicating the presence of active immune subsets in atherosclerotic lesions (George, 2008; Hansson, 2005).

The majority of data supporting activity of the innate and adaptive immune systems in atherosclerosis came, in recent years, from various studies of transgenic mice and from studies on human atherosclerotic plaque. These studies have shown the presence of activated T-lymphocytes, B cells and dendritic cells within the lesions. Moreover, high levels of circulating effector molecules mediating and reflecting immune-cell action have been identified in plaque regions (Gounopoulos, Merki, Hansen, Choi, & Tsimikas, 2007), leading to discussion into the use of inflammatory system by-products as potential markers of CVD (Hansson, 2005; Libby, 2006).

As atherosclerotic lesions mature, T-cells mediate the dominant forces in inflammatory progression. Supporting this, all T-cell subsets ($CD4^+$, $CD8^+$, $TCR\gamma\delta^+$, and NKT cells) have been identified in both human and murine atherosclerotic plaques (Andersson, Libby, & Hansson, 2010; Hansson & Hermansson, 2011; Lahoute, Herbin, Mallat, & Tedgui, 2011; Libby, Ridker, & Hansson, 2011; Tse, Tse, Sidney, Sette, & Ley, 2013).

After proof of the presence of immune cells, and their secreted humoral components within the plaque, came to light an understanding of which auto-immune responses were operating outlined the predominance of $CD4^+$ T cells in comparison to $CD8^+$ T cells accompanied by an increased production of the cytokine IFN-γ (de Boer, van der Wal, Verhagen, & Becker, 1999; Stemme et al., 1995). In conjunction with these findings, patients with acute coronary syndromes have been shown to exhibit an altered T-lymphocyte repertoire

indicated by an increase in IFN-γ produced by $CD4^+$ $CD8^-$ T-cell populations (Liuzzo et al., 1999).

Naïve $CD4^+$ $CD8^-$ T-cell populations include multiple lineages (T_h1, T_h2, T_h17 and T_{reg} cells) which arise in response to varying cytokine proportions in the environment. T_h1 cells in particular occur predominantly in the presence of IL-12, which not only results in IFN-γ and TNF production, but also inhibits IL-4 expression, inhibiting commitment to the T_h2 lineage. IL-18 also promotes the T_h1 phenotype (Tse et al., 2013) (Fig. 7). Interestingly, T_h1 cells exceed T_h2 cells in atherosclerotic plaques and have been designated as pro-atherogenic (Laurat et al., 2001; Mallat, Taleb, Ait-Oufella, & Tedgui, 2009). Furthermore, supporting studies have shown that T-helper (T_h1) subsets, known to provide immunity against intracellular pathogens by secreting cytokines such as IFN-γ, are expanded in acute coronary syndrome patients (Liuzzo et al., 2001).

7,8-Dihydroneopterin (7,8NP), a marker of inflammation and immune cell activation produced by human monocyte-derived macrophages and dendritic cells, is induced by the pro-inflammatory cytokine IFN-γ (Firth, Laing, Baird, Pearson, & Gieseg, 2008; Plata-Nazar & Jankowska, 2011). Therefore measuring 7,8NP, produced by a cellular population after T_h1-cell activation by IL-12 or IL-18, gives an indication of the potential for macrophage and dendritic cell activation by IFN-γ. This technique has proven to be useful in determining the macrophage and dendritic cell activation potential in inflammatory cell populations via T-cell activation with the synthetic protein kinase-C agonist Phorbol 12-myristate 13-acetate (PMA) which, like IL-12 or IL-18, causes IFN-γ up-regulation (Langenkamp, Messi, Lanzavecchia, & Sallusto, 2000).

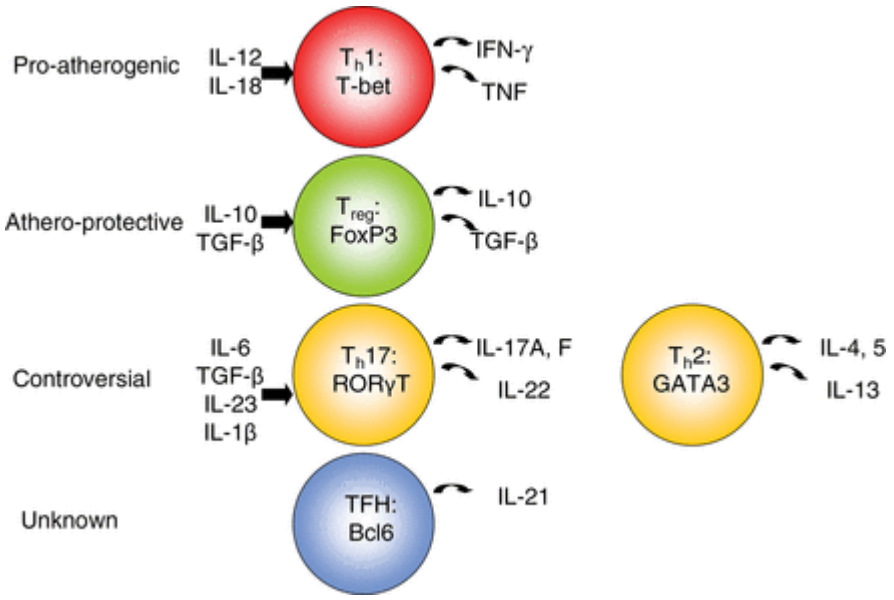

Fig 7. T-cell lineages in atherosclerosis. Pro-atherogenic T_h1: Predominantly formed in the presence of IL-12 and IL-18 from naïve $CD4^+CD8^-$ lymphocytes. IL-12 results in transcription factor, T-bet activation. T-bet activation causes pro-inflammatory cytokine production such as IFN-γ and TNF. IL-10 and TGF-β are required for T_{reg} commitment which have been shown to be athero-protective. T-cells commit to a T_h2 lineage under the influence of IL-4. In a positive feedback loop they also produce IL-4, which inhibits IFN-γ production, as well as IL-13 via the transcription factor GATA3. T_h17 and TFH have functions that are still controversial and largely unknown (Tse et al., 2013).

Macrophage activation in atherosclerotic plaques

Macrophage activation has emerged as a key component of immunology, tissue homeostasis, disease pathogenesis and inflammation (Murray et al., 2014). The innate immune response of atherosclerotic initiation, involving monocyte/macrophage activation in the vessel wall, has been well supported as a mediating factor in cardiovascular disease progression followed by more specific adaptive T cell mediated responses (Moore & Tabas, 2011; Shimada, 2009).

Activation of overlying endothelial cells in a manner which recruits blood-borne macrophages to the arterial intima is noted as one of the key early inflammatory responses to apoB-lipoproteins, which may be enhanced by apoB-lipoprotein oxidation (Glass & Witztum, 2001; Witztum & Steinberg, 2001). As a result of chemoattractant release by the activated endothelium, recruited monocytes are prompted to migrate across the arterial intima (Moore & Tabas, 2011). In support of this process, of monocyte migration, a recent study has identified

that blocking particular chemokines or their cognate receptors stunts atherogenesis in mouse models (Mestas & Ley, 2008). It is therefore likely for this reason that monocytes are found in abundance at the early stages of atherosclerosis.

These cells, stimulated by macrophage colony stimulating factor and other cytokines, differentiate becoming macrophages and upregulate pattern recognition receptors (PRRs) leading to exacerbated lipoprotein uptake and subsequent foam cell formation (Shashkin, Dragulev, & Ley, 2005) (Fig. 8).

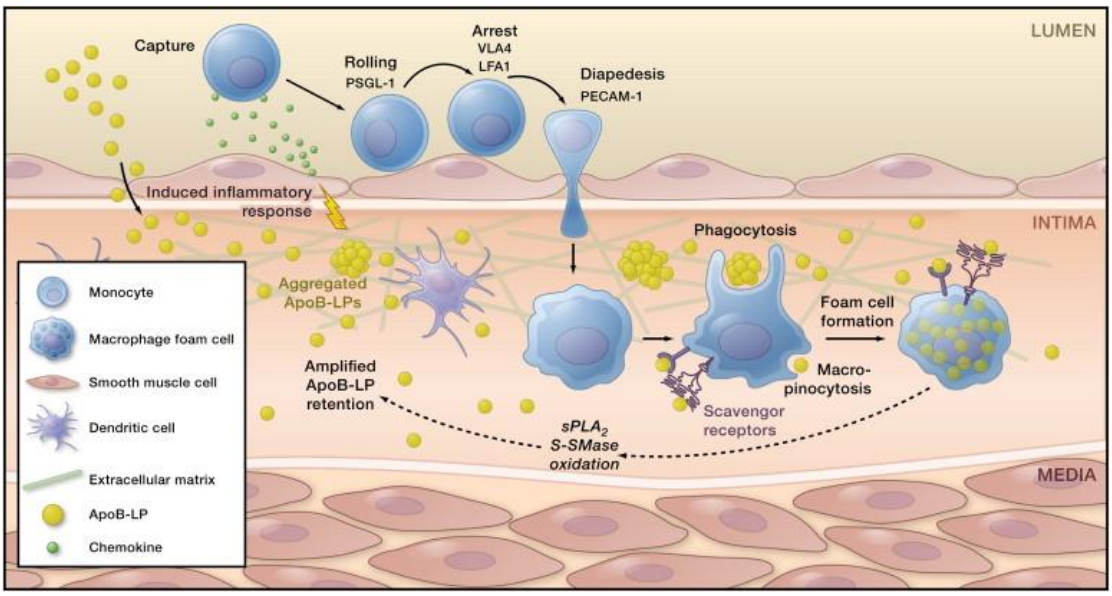

Fig 8. Endothelial activation, macrophage migration and foam cell formation. ApoB-lipoproteins entering the arterial intima bind proteoglycans and undergo both oxidative modification and hydrolysis, most notably by secretory phospholipase A2 ($sPLA_2$). This promotes endothelial activation, characterised by chemokine secretion and altered expression of adhesion molecules, leading to monocyte recruitment into the intima, these monocytes differentiate to macrophages and internalize both native and modified lipoproteins, subsequently forming foam cells. Foam cells may then further amplify lipoprotein retention and oxidation (Moore & Tabas, 2011).

Although it is now well documented that macrophage colony stimulating factor and other differentiation factors promote the differentiation of monocytes to cells with macrophage (and dendritic cell) like features, there is still great interest into the heterogeneity of the cells formed (Johnson & Newby, 2009; Paulson et al., 2010). In recent years in vitro studies, subjecting monocytes or macrophages to various treatments, including cytokines derived from different T helper cells; growth/differentiation factors; transcription factors and atherogenic

lipoproteins, have eluded to two major sub-groups of differentiated macrophages: Pro-inflammatory M1 and M2 macrophages involved in resolution and repair (Johnson & Newby, 2009; Kadl et al., 2010). However, the situation within atherosclerotic plaques in vivo is almost certainly more complex, highlighting the need to characterize specific molecules and molecular networks, which functionally contribute to the activation of macrophages in atherosclerotic plaques.

Localized inflammation occurring as a result of continuous mononuclear cell influx, inefficient efferocytosis, and cell death eventually gives rise to vulnerable atherosclerotic plaque formation with a characteristic necrotic lipid core and a thinning fibrous cap (Thorp, Subramanian, & Tabas, 2011; Thorp & Tabas, 2009). Macrophages at the lesion site are the primary source of the inflammatory cytokine, TNF, responsible for immune cell regulation. TNF fuels the inflammatory cycle within the plaque, by promoting chemokine production, causing recruitment of more T, B (Zhou & Hansson, 1999) and monocyte cells. As well as increased cellular recruitment, healthy endothelial cells in vulnerable plaques have been shown to decrease in number as a result of TNF secretion. In vitro data indicates that macrophages may trigger apoptosis in endothelial cells via activation of the Fas apoptotic pathway, secretion of TNF and secretion of nitric oxide (Boyle, Weissberg, & Bennett, 2003).

As a result of IFN-γ secretion by T_h1 cells, transcription of TNF, nitric oxide and other inflammatory products is enhanced in macrophages (Collart, Belin, Vassalli, De Kossodo, & Vassalli, 1986). This links the process of T_h1 activation to M1 macrophage stimulation and atherosclerotic exacerbation. However, pro-inflammatory molecule production is only one side of the macrophage response to IFN-γ. The biological antioxidant 7,8NP is also a product of IFN-γ induced activation in human macrophage cells. Both 7,8-NP, and especially its oxidized by-product neopterin, have been of substantial scientific and clinical interest recently as markers of macrophage activation and oxidative stress in acute and chronic inflammatory disease (Berdowska & Zwirska-Korczala, 2001; Firth et al., 2008; Sucher et al., 2010).

1.4 Neopterin and 7,8-Dihydroneoptrin

Dihydroneopterin and neopterin in cardiovascular disease

7,8 Dihydroneopterin and neopterin, pteridine derivatives produced as a result of macrophage activation, are known markers of immune activation (Murr, Widner, Wirleitner, & Fuchs, 2002). However, markers of systemic immune system activation have also been associated with vascular inflammation and stenosis, which often lead to the development of severe cardiovascular events (Zouridakis, Avanzas, Arroyo-Espliguero, Fredericks, & Kaski, 2004). Recent studies have shown that neopterin levels are indeed higher in patients with acute MI as opposed to healthy subjects, also a significant correlation between serum neopterin and complex coronary artery stenosis has been found (Avanzas, Arroyo-Espliguero, Quiles, Roy, & Kaski, 2005). Indicating the value of neopterin as a prognostic tool of potential cardiovascular disease.

As well as predicting the progression of inflammatory artery occlusion, neopterin has the potential to predict long term risk of death and recurrent coronary events, with recent studies indicating that high plasma neopterin levels measured after acute coronary syndromes are associated with increased mortality rate and future acute coronary events (Grammer, Fuchs, Boehm, Winkelmann, & Maerz, 2009; Nazer et al., 2011b; Ray et al., 2007; Sasaki et al., 2010).

With large scale studies over the last decade providing substantial evidence confirming the association of neopterin with cardiovascular disease, it can be said with confidence that neopterin is a valuable prognostic tool for the assessment of cardiovascular risk (Fuchs et al., 2009; Go, Chertow, Fan, McCulloch, & Hsu, 2004). Furthermore, the prognostic utility of neopterin also provides the potential for it to be used as a comparative marker for potential new biomarkers of cardiovascular disease.

Synthesis of 7,8NP and neopterin

7,8NP (IUPAC: 2-amino-6-[(1S,2R)-1,2,3-trihydroxypropyl]-7,8-dihydropterin4(3H)-one) is synthesised by the biopterin pathway of human myeloid cells such as: monocytes, macrophages, dendritic cells and to a lesser extent fibroblasts, endothelial cells and kidney cells (Murr et al., 2002; Wirleitner et al., 2002). Through an IFN-γ induced enzyme, guanosine triosephosphate cyclohydrolase-1 (GTPCH-1), GTP is primarily hydrolysed to 7,8NP

triosephosphate. Reflecting the ubiquity of the pathway, in producing alternate reaction products, 7,8NP triosephosphate is then dephosphorylated by a non-specific phosphatase forming 7,8NP (Fuchs et al., 2009; Walter, Schaffner, & Schoedon, 2001). Alternatively, in non-primate and non-human cells, the triosephosphate group of 7,8NP triosephosphate would be removed by the enzyme 6-pyruvol-tetrahydropterin synthase (PTS) prior to further processing by sepiapterin reductase (SR) to tetrahydrobiopterin (Walter et al., 2001). However, due to a lack of PTS activity in human and primate leukocyte cells 7,8NP triosephosphate is sequestered, giving rise to phosphatase mediated 7,8NP production (Leitner et al., 2003) (Fig 9).

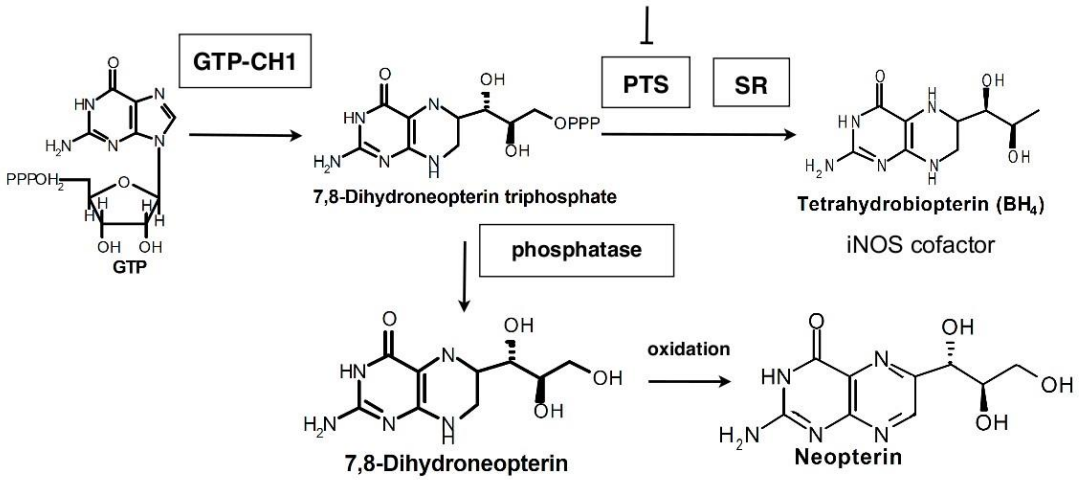

Fig 9. Biological 7,8NP triosphosphate pathways. GTPCH-1 initially converts GTP to 7,8NP triosephosphate, in macrophages, once stimulated by IFN-γ. 7,8NP triosephosphate accumulates due to PTS deficiency in humans. This results in subsequent dephosphorylation of 7,8NP triosephosphate producing 7,8NP. 7,8NP may then be further oxidised to neopterin (Shchepetkina, 2013).

7,8-NP diffuses out of activated macrophages where it can be readily oxidized (in the plasma or within the plaque) (Widner, Mayr, Wirleitner, & Fuchs, 2000), by a range of electrophilic molecules, forming either neopterin or 7,8-dihydroxanthopterin (7,8-DXP). Mainly mediated physiologically by hypochlorous acid (HOCl), neopterin production, like 7,8-DXP occurs during oxidative stress (Fig. 9). However, 7,8-DXP production is not exclusive to 7,8NP oxidation, since it is the main product of most biological pterins it doesn't primarily reflect monocyte and macrophage activation. (Vásquez-Vivar, 2009; Widner et al., 2000).

Neopterin however, being solely derived from 7,8NP (Fuchs et al., 2009), specifically highlights oxidative stress at points of immune system activation.

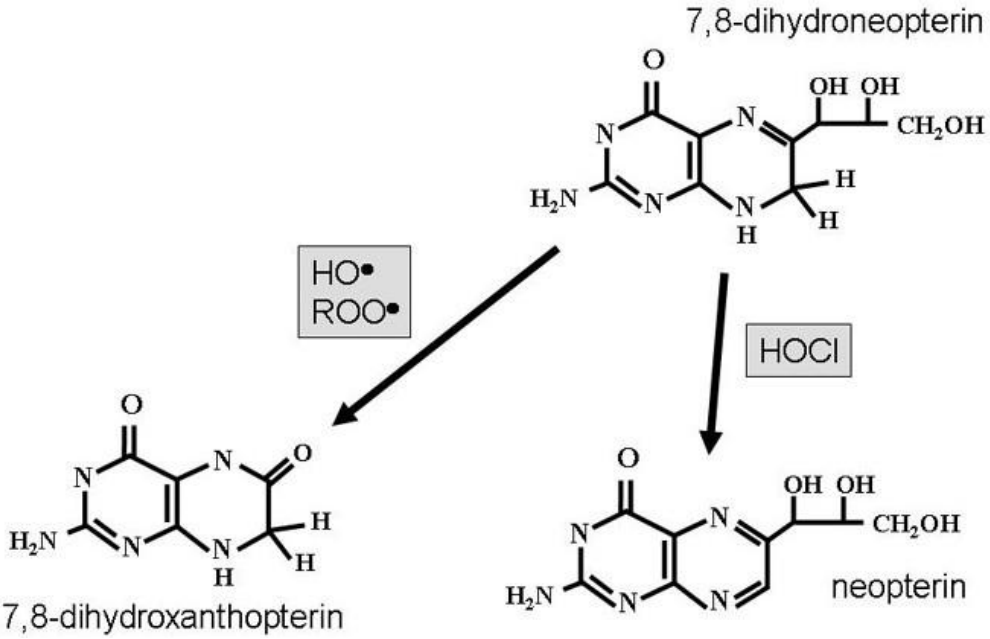

Fig 10. Oxidation of 7,8NP. The oxidation of 7,8NP to neopterin occurs primarily by the action of HOCl. The processing of 7,8-DXP occurs predominantly via the action of peroxyl and hydroxyl radicals (Gieseg et al., 2009).

Clinical utility of 7,8NP and neopterin

In contrast to 7,8NPs anti-oxidant properties several studies have shown that neopterin can act as a pro-oxidant, enhancing oxidant production thereby promoting cell death, potentially leading to plaque rupture (Sugioka et al., 2010). This has led to a direct association of neopterin with plaque instability in cardiovascular disease subjects (Zouridakis et al., 2004). Furthermore, there is increasing evidence of neopterins clinical efficacy as a prognostic marker of cardiovascular events (Avanzas et al., 2005; Avanzas & Kaski, 2009; Fuchs et al., 2009; Nazer et al., 2011b).

With IFN-γ being the primary stimulant for 7,8NP production a link between immunocompetent cells may be established through monitoring of 7,8NP (Adachi et al., 2007). For this reason, measurement of 7,8NP and to a greater extent its oxidised product neopterin are routinely used as markers of immune system activation in patients suffering

from infections, autoimmune diseases, malignancies, allograft rejection, cardiac failure, renal failure and cardiovascular disease (Adachi et al., 2007; Berdowska & Zwirska-Korczala, 2001).

Stable ratios of 7,8NP to neopterin for arterial (2:1) and venous blood (3:1) have been well established in vivo further highlighting the utility of both molecules as biomarkers of inflammatory cell activation (Fuchs et al., 1989; Weiss et al., 1992). Neopterin levels measured in healthy subjects have been reported at 6.7 ± 1.5 nM in blood (Murr., Schroecksnadel, Schonitzer, Fuchs, & Schennach, 2005). Whereas healthy levels of 7,8NP vary around ≈5.8 nM (Flavall, Crone, Moore, & Gieseg, 2008) which is likely a reflection of 7,8NPs instability relative to neopterin. However, what makes the two molecules valuable biomarkers of cardiovascular disease is that significantly elevated levels have been extensively measured in patients during cardiovascular events, reflecting the T_h1 activity and inflammatory aspects of the disease (Avanzas & Kaski, 2009).

Higher baseline levels were recently found in females who experienced coronary events, during follow up, after being admitted for chronic stable angina (CSA) (Garcia-Moll, D. Cole, E. Zouridakis, & J. Kaski, 2000). Endorsing these results, two subsequent studies demonstrated that neopterin levels, in hypertensive patients with typical angina, were an independent predictor of major adverse coronary events during a 1-year follow-up period. Moreover, with increasing neopterin levels a significant gradual increase in the number of adverse events was seen during follow-up. Patients in the highest neopterin group (> 7 nmol/L) had a three-fold higher risk of developing adverse cardiovascular events (Avanzas et al., 2004; Avanzas et al., 2005). These studies, among numerous others, add to the cumulative evidence in recent years indicating that neopterin, a marker of macrophage activation, may be a useful tool in the assessment of cardiovascular risk.

As neopterin is already known as a valid biomarker of inflammatory events it may be used in comparison to sFlt-1 to determine its diagnostic benefit. Since a correlation between cardiovascular events and neopterin has already been established (Avanzas et al., 2004; Avanzas et al., 2005; Garcia-Moll, Coccolo, Cole, & Kaski, 2000; X. Garcia-Moll, D. Cole, E. Zouridakis, & J. Kaski, 2000; Nazer et al., 2011b; Ray et al., 2007), analysis of neopterin levels in conjunction with sFlt-1 levels may provide further power to biomarker risk assessment with respect to CVD. In support of this, recent studies have compared other markers of inflammation

such as C-reactive protein (CRP), eluding to the possible use of a combination of conventional markers for risk stratification (Zethelius et al., 2008).

1.5 Objectives of study

Multiple biological pathways have been implicated in the aetiology of CVD including, but not limited to, inflammation, hypoxia and oxidative stress. Identifying markers of these pathway outcomes or processes may facilitate risk prediction and development of treatment regimens (Stoner et al., 2013). However CVD is now known to involve multiple complex mechanisms, such that there is no single definitive biomarker of cardiovascular risk. However, the function of many CVD biomarkers overlap. Furthermore, some of these markers are better suited to identifying the particular pathogenesis of specific cardiovascular events. Therefore, two potential outcomes of CVD biomarker use can be derived; biomarkers can be selected to identify a specific stage of CVD or alternatively simultaneous measurement of multiple biomarkers can give a more detailed overview of the specific nature of cardiovascular events.

In order for biomarkers to be used in conjunction, for risk prediction and diagnosis, appropriate analysis must be made to determine whether biomarkers measured together give compounding evidence of cardiovascular risk and furthermore whether measurements can provide predictive results. Biomarker levels typically vary much more between individuals than within one individual over time. As a result, longitudinal studies across a high subject group are useful in controlling for this biomarker variability across a population (Gonzalez et al., 2008).

This study focussed predominantly on of sFlt-1, neopterin and 7,8 NPs potential for use alone and in conjunction with other biomarkers of CVD.

With the aim to identify a potential prognostic use for sFlt-1, neopterin and 7,8-NP, plasma samples from 514 patients, who were stable after experiencing a CVD event, were assayed. These patients' medical admissions were followed up for a median period of 8 years. Plasma from 27 patients was also taken prior to carotid endarterectomy procedures and analysed to determine the levels of sFlt-1 and other biomarkers produced in late stage CVD.

As well as determining the prognostic utility of s-Flt-1, this study also aimed to assess the pathophysiology of CVD in terms of sFlt-1, neopterin and 7,8-NP production, via analysis of atherosclerotic plaque, which may give insight into the association between inflammation and hypoxic up-regulation of sFlt-1.

2

Materials and Methods

2.1 Reagents, kits, media and buffers

Reagents

All reagents were prepared to the standard of analytical grade or better. All solutions were prepared with de-ionised water, which was purified using a milli-Q ultrafiltration system, referred to as nano-pure water.

7,8-Dihydroneopterin triphosphate (7,8NP)	Schricks Laboratory, Switzerland
Acetic acid (glacial)	Scharlau Chemie S.A., Spain
Acetonitrile (ACN)	J.T. Baker, NJ, USA
Ammonium phosphate dibasic ($AmPO_4$)	Sigma-Aldrich Co. LLC, NZ
Ascorbic acid	Sigma Chemical Co., MO, USA
Dimethyl sulfoxide (DMSO)	BDH Lab Supplies, England
Ethanol	BDH Lab Supplies, England
Hydrochloric acid (HCL)	BDH Lab Supplies, England
Iodine (I)	BDL Lab Supplies, England
Lactate	Sigma-Aldrich Co. LLC, NZ
Leukine® (GM-CSF)	Sigma-Aldrich Co. LLC, NZ
Methanol (MeOH)	Merck, Darmstadt, Germany
Neopterin (NP)	Schircks Laboratory, Switzerland
Orthophosphoric acid	Sigma Chemical Co., MO, USA
Potassium Iodide (KI)	May & Baker Ltd, England
Phorbol 12-myristate 13-acetate (PMA)	Sigma Chemical Co., MO, USA
Interferon Gamma (IFN-γ)	Roche diagnostics, Manheim, Germany

Kits

Lactate assay kit	Roche diagnostics, Indianapolis, Indiana, USA
sFlt-1 ELISA kit	R&D Systems, Minneapolis, Minnesota
12 well adherent cell culture plate	Cell star®,
Cell culture multi well plate, 12 well,	Greiner Bio-one, Kremsmünster, Austria

Media

Cell/plaque culture media:

Penicillin (1000U)/streptomycin (1000 µg/ml) solution	Invitrogen, Life technologies, NZ
RPMI (Roswell Park Memorial Institute) 1640	Sigma-Aldrich Co. LLC, NZ
10% Human serum	Canterbury University, Christchurch, NZ

Buffers & solutions

Ammonium Phosphate HPLC buffer:

NH_4PO_4 (dibasic), 2.64g, was added to 900 ml of nanopure grade water were combined in a 1000ml beaker and mixed on a magnetic stirrer. Once all of the ammonium phosphate had dissolved the pH of the solution was adjusted to 2.5 with concentrated phosphoric acid added dropwise with a Pasteur pipette. The solution was then made up to 1000ml with nanopure water and mixed well. In order to remove contaminants the 1000ml of buffer was then vacuum filtered through a 0.45 µm membrane filter (Phenomenex), into a 1000ml Schott bottle, using a Millipore filter system.

Acidic iodide solution:

Solid iodine, 2.7g, and 5.4g potassium iodide were added to 35 ml of water. Concentrated HCl, 4.37mL, was then added to make up to a final volume of 50 ml (5.4% I_2 / 10.8% KI in 1M HCl).

This solution forms a triodide ($I_{3(aq)}^-$) equilibrium:

$I_{3(aq)}^- \leftrightarrow I_{(aq)}^- + I_{2(aq)}$

Ascorbic acid solution:

Ascorbic acid, 1.057g, was dissolved in in 10 ml of water to give a 0.6M solution. Note that ascorbic acid in solution does not keep for more than a day as is oxidised easily, especially in the presence of light. Therefore it was prepared fresh and used within an hour of preparation whilst being keep covered with aluminium foil.

IFN-γ solution:

IFN-γ was diluted in PBS with 2.5% sucrose (sterile-filtered), as per manufacturer's instructions, to give a solution of 10,000 U/ml. This stock solution was aliquoted into 500 µl aliquots and stored at -20ºC until used. A new vial was used after one vial was defrosted 2 times as IFN- γ activity was lost after 2 freeze-thaw cycles.

PMA solution:

PMA (99% pure) was dissolved in DMSO to produce 5mM, 20µl stock aliquots. Before use the 20µl stock was mixed with 980µl of de-ionised water to make a 100µM solution, then 50µl of this solution was then added to 5950µl of de-ionised water to make a final concentration of 200nM. This final solution was never kept for more than a day.

2.2 Plaque culture technique

Endarterectomy plaque and plasma collection:

Plaque and plasma were collected from the Christchurch General Hospital, under the supervision of Prof. Justin Roake, from patients undergoing a carotid endarterectomy procedure. Fresh plaques were kept on ice between transfers from the hospital to the University of Canterbury School Of Biological Sciences. Plaque obtained was either cultured within the hour of removal from the patient or otherwise frozen at -80°C. The plasma collected was centrifuged at 2000 rpm (MultifugeSR, Biostratergy, New Zealand) for 12 minutes in order to pellet the red blood cells. The supernatant was then transferred to two labelled 1.7 ml centrifuge tubes and stored at -80˚C.

Sterile conditions:

All plaque and cell culturing was carried out under sterile aseptic conditions under a class II biological safety hood. (Clyde-Apex BH 200). All equipment was either sterile–bought

plastic ware (Falcon, Bector Dickinson & Co.; Nunc, Nalge Nunc International; Greiner, Greiner Bio-one, Neuburg, Germany) or was sterilised via autoclaving (15 min, 121˚C, 15 psi). All media and solutions added to cells and plaque was sterilised via autoclaving. The cells and plaque were kept at 37˚C in a humidified atmosphere calibrated to 5% carbon dioxide: 95% air (Sanyo Electric Co. Ltd, Japan). All items were also sprayed with 70% ethanol (30% distilled water) before insertion into the class II safety hood.

Collection of human serum for use in Culture media:

Human plasma was collected, under ethics approval CTY/98/07/069 granted by the Upper South (B) Regional Ethics Committee, from anonymous haemochromatosis patient blood. This blood was collected into 450 ml vacuum-sealed bags, for the University of Canterbury, by the New Zealand Blood Bank (Riccarton Branch, Christchurch).
Blood was kept at room temperature for two hours to allow for clotting to occur. The blood was then transferred to 4˚C overnight to allow for separation of the human serum from the clot.

The following day separated serum was transferred to 50 ml centrifuge tubes using a 20 ml syringe. The tubes were then centrifuged at 1000 g for 15 minutes (MultifugeSR, Biostratergy, New Zealand) in order to pellet the remaining red blood cells.
The clear serum was then transferred to new 50 ml centrifuge tubes whilst taking care not to transfer any of the pelleted cells. If red blood cells remained then the centrifuge procedure was repeated.

The serum was then transferred to a -80˚C freezer for long term storage. The serum was generally used within a 3 month period.

Preparation of cell and plaque culture medium:

Powdered RPMI was dissolved in nano-pure water with sodium bicarbonate ($NaHCO_3$) according to manufacturer's instructions. The pH was then adjusted to 7.4 by the addition of 11.4 M hydrochloric acid (HCl). The solution was then filtered through a 0.22µm Millex®-GP_{50} filter and peristaltic pump (CP-600, life technologies, Maryland, USA) before transfer into sterile 500 ml bottles. 5.6 ml of the combined 10000 U/ml penicillin and 10000 µg/ml streptomycin was then added. The final solution was then kept at 4˚C until it was required for plaque or cell culture.

Before use in plaque or cell culture 45 ml aliquots of the RPMI 1640 penicillin/streptomycin mixture were transferred to 50 ml sterile centrifuge tubes. 5 ml of defrosted human serum was then added before storage at 4˚C. The 50 ml cell culture solutions were always used within 1 week of preparation.

Plaque culture procedure:

Under sterile conditions the freshly excised atherosclerotic plaques were initially photographed before being sliced into 2 mm sections using a sterile surgical blade. Sections were then put into, previously weighed, sterile 2 ml centrifuge tubes. These tubes containing the sections were then weighed to determine the plaque weight.

Each plaque section was then transferred to a well on a 12 well adherent cell culture plate (Cell culture multi well plate, 12 well, Cell star®, Greiner Bio-one, Kremsmünster, Austria). After transfer to the cell culture well 2 ml of the plaque culture RPMI 1640 media was added. The lid of the cell culture plate was labelled, according to the order in which the plaque sections were cut from the whole plaque, before being incubated at 37˚C in a humidified atmosphere calibrated to 5% carbon dioxide and 95% air (Sanyo Electric Co. Ltd, Japan) for 24 hours.

2.3 Human monocyte derived macrophage (HMDM) culture

Lymphocyte isolation:

Human plasma was collected, under ethics approval CTY/98/07/069 granted by the Upper South (B) Regional Ethics Committee, from anonymous haemochromatosis patient blood. This blood was collected into 450 ml vacuum-sealed bags, for the University of Canterbury, by the New Zealand Blood Bank (Riccarton Branch, Christchurch).

Blood was initially inverted 10 times to ensure an adequate distribution of red blood cells existed within the bag. After inversion the bags were sprayed with ethanol and separated into 50 ml falcon tubes. The 50 ml falcon tubes were subsequently centrifuged, at 1000 g in room temperature for 30 minutes, to pellet erythrocytes and form a buffy coat (Fig 2.1).

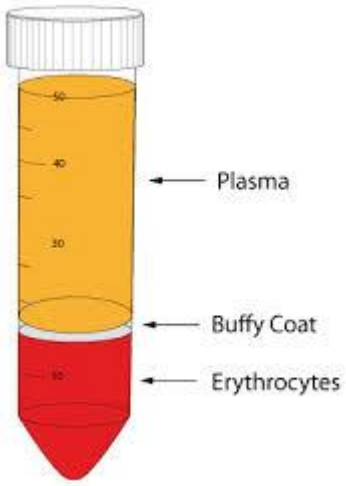

Fig. 2.1 Post-centrifuged blood. After centrifuging at 1000 g for 30 minutes the erythrocytes form a pellet. The buffy coat is the fraction of an anti-coagulated blood that contains most of the white blood cells and platelets.

The serum plasma was removed via syringe down to the 30ml mark of the falcon tube. Approximately 15-17.5 ml of buffy coat was then transferred, via mixing cannula in combination with a 20 ml syringe, into a new 50 ml falcon tube (erythrocytes may also be transferred but will be removed in subsequent processing).

The newly transferred buffy coat was then mixed with 17.5 ml of PBS and gently inverted. Using a mixing cannula, attached to a 20ml syringe, 15 ml of Lymphprep® solution was carefully added beneath the buffycoat/PBS mixture (a new cannula is needed for each tube so not to contaminate the Lymphprep®).

The 50 ml buffy coat/PBS/Lymphprep® tubes were once again centrifuged at 1000 g at 18˚C for 20 minutes. This process pellets the remaining red blood cells and forms a floating monocyte/lymphocyte layer approximately halfway down the tube. This monocyte layer was then transferred, using a mixing cannula attached to a 20 ml syringe, to new 50 ml flacon tubes.

Each tube was filled to 45 ml with PBS, re-suspending the cells, before centrifuging for 15 minutes at 500 g. This PBS and centrifuge step was then repeated another two times.
After the final centrifuge step, cells were re-suspended in 30 ml RPMI and counted. The cells were counted by adding 20 µl of cell suspension to 180 µl of trypan blue before transfer to a haemocytometer. This ensured that the suspension was at a minimum concentration of 5×10^6 cells/ml.

HMDM seeding and feeding:

After counting, cells were transferred to Cell star® 12 well adherent cell culture plates before incubation at 37°C, in a humidified atmosphere calibrated to 5% carbon dioxide and 95% air, for 40 hours. This allows for T-cell death and platelet adhesion to occur.
After incubation, cells were transferred to 50 ml falcon tubes (making sure to pipette thoroughly to remove any monocytes resting on the plate bottom) and spun at 500 g in room temperature for 15 minutes.

The supernatant was then removed and the cell pellet was re-suspended, prior to counting once again with trypan blue, whilst adjusting to ensure concentrations of 5×10^6 cells/ml RPMI with 10% heat inactivated human serum (HIHS). 1 µL of 25 µg/ml GM-CSF (Leukine® made up in nanopure water) per 1 ml of cell suspension was also added. For example: 25×10^6 cells/ml = 720×10^6 total cells. This is enough to make 150 ml at 5×10^6 cells/ml. In this case 10 ml of the concentrated cells would be added to three different tubes. 35 ml would then be added along with 5 ml of HIHS and 50 µl of GM-SCF solution to give three tubes each containing 50.05 ml with a concentration of 25×10^6 cells/ml.

1 ml of the 25×10^6 cells/ml suspension was then added to each well on Cell star® 12 well adherent cell culture plates and incubated at 37°C, in a humidified atmosphere calibrated to 5% carbon dioxide and 95% air. The cells media was changed approximately every 3 days leaving approximately 200 µl of the old media in the wells allowing adhered cells to remain.

2.4 IFN-γ stimulation of macrophages and live plaque

After the plaque sections had been incubated for 24 hours (Macrophages 11 days after seeding) the media was removed using a 1ml pipette. This media was transferred to two 1.7 ml tubes, labelled with the appropriate incubation time stamp, before transfer to storage at -80°C.

New media (2 ml or 1 ml for macrophages) was then added to each well before incubation under the same conditions for another 24 hours. After this second 24-hour period media was again stored at -80°C. This time only 1900 µl (900 µl for macrophages) of media was added to each well, along with 100 µl (50 µl for macrophages) of the 10000 U/ml IFN-γ

stock solution (which had been previously defrosted), to give a final concentration of 500U/ml in each well.

Plaque sections and macrophages were then incubated under the same conditions for a further 24 hours. Media was taken after this 24-hour incubation and the addition of IFN-γ to the media was repeated once more along with one final 24-hour incubation period. After the last incubation period the final media was collected and stored, for future analysis, along with the other 24-hour periodical samples at -80˚C.

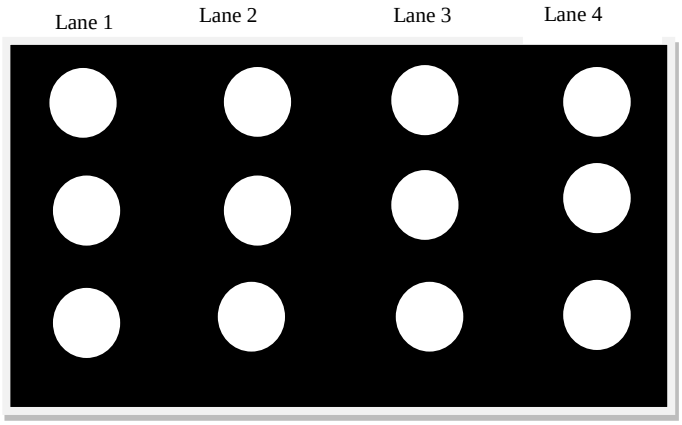

Lane	0	1 (24)	2 (48)	3 (72)	4 (96)
IFN-γ	None	None	500U/ml	500U/ml	Final collection

Fig. 2.2 IFN-γ Procedure for macrophages and Atherosclerotic plaque

2.5 PMA stimulation of live plaque

After the plaque sections had been incubated for 24 hours the media was removed using a 1 ml pipette. This media was transferred to two 1.7 ml tubes, labelled with the appropriate incubation time stamp (24 hours), before transfer to storage at -80˚C. 1.6 ml of new media was then added to each well, along with 400 µl of the 1000 nM PMA solution, to give a final concentration of 200 nM PMA per well, before incubation under the same conditions for another 24 hours. The same media change, 200 nM PMA addition and 24 hour incubation period was repeated twice more. After the last incubation period the final media was collected and stored, for future analysis, along with the other 24-hour periodical samples at -80˚C.

Alternative procedure:

The same procedure was carried out on other plaque sections however the final media change contained 100 µl of 10000 U/ml IFN-γ and 1900 µl of cell culture media, rather than the previously added 200 nM PMA.

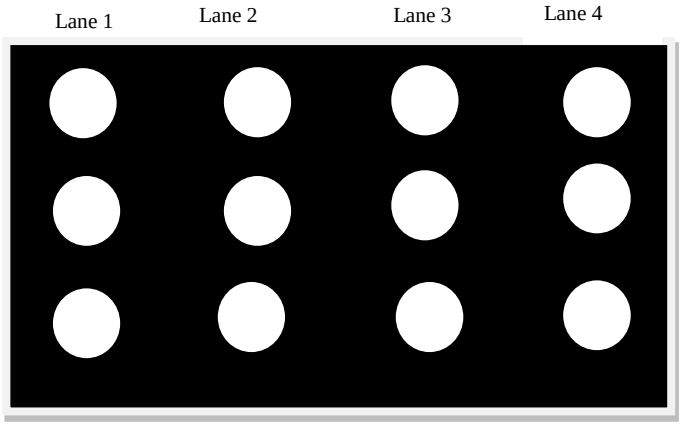

Lane	0	1 (24)	2 (48)	3 (72)	4 (96)
PMA	None	200nM	200nM	200nM	Final collection

Fig. 2.3 PMA procedure for atherosclerotic plaque

2.6 Lactic acid assay

The lactic acid content of plaque and cell cultures was measured using a method derived from the Roche Diagnostics Lactic Acid Assay Kit (Roche Diagnostics, Indianapolis, Indiana, USA). The kit primarily employs an enzyme, lactate oxidase (LOD), for the conversion of lactic acid to pyruvate and hydrogen peroxide. Peroxidase (POD) was then used to catalyse the reaction between hydrogen peroxide and a hydrogen donor. In the presence of 4-aminoantipyrine (AAP) this produced a purple chromogen, with intensity proportional to the concentration of lactic acid present in the media.

Live cells in culture utilize supplementary glucose to produce lactic acid. Therefore, this measurement of lactic acid gave an indication of active metabolism by cells. The kit can detect between 0.22 and 15.5 mM lactic acid.

Two working reagents are provided in the kit. Reagent 1 (R1) contains the hydrogen donor, ascorbate oxidase, buffers and preservatives. Reagent 2 (R2) contains AAP, lactate oxidase, horse peroxidase, buffers and preservatives.

In order for the kit to be used in 250 µl 96 well plates (96 well, Greiner Bio-one, Kremsmünster, Austria) volumes of both the sample and the reagents had to be reduced from those in the standard lactic acid assay method.

One blank of R1 with nanopure de-ionised water and another containing RPMI R1 and R2 were injected into the first two wells of a 96 well plate. A working standard curve was then established using lactate diluted in de-ionised water to seven standards between 0.22 and 15.5 mM (limits of detection). These standards were then injected, in duplicate, into a 96 well plate along with one blank of R1 with de-ionised water and another containing RPMI R1 and R2

The standard method required that 840 µl of R1 and 168 µl of R2 be added to 20 µl of sample (or standard). However, these volumes would not fit in the wells. Therefore, one fifth of each solution was used. 20 µl of sample (or standard) was added to 80 µl of R1 in a 1.5 ml centrifuge before it was vortexed for 30 seconds. 20 µl of this mixture, containing 4 µl of sample and 16 µl of R1, was then pipetted into the desired wells.
The remaining 152 µl of R1 was then added to the wells. Once all samples and R1 had been added to the wells 33.6 µl of R2 was added to each well. The plate was then covered and left to incubate and mix on a plate rocker for 30 minutes.
The absorbance at 660 nm of each sample and standard well was then determined using a plate reader.

The lactic acid levels found in the cell culture blank were subtracted from those found in the plaque culture and cell culture samples to give the levels of lactate produced by the cells and plaque alone.

2.7 sFlt-1 assay

The sFlt-1 content was measured in plaque media, cell cultures and plasma using a method derived from the R&D systems sFlt-1 ELISA kit (R&D Systems, Minneapolis, Minnesota). The assay employes a monoclonal antibody, specific for sFlt-1, which is pre-coated onto a 96 micro well plate. Any sFlt-1 is bound to the immobilized antibody. An

enzyme-linked polyclonal antibody specific to sFlt-1 is then added which also binds the sFlt-1. A corresponding substrate to the enzyme is then added which prompts the development of a colour change in the wells. The colour developed is proportional to the amount of sFlt-1 in solution.

Using the sFlt-1 standard provided 8 sFlt-1 standard concentrations were prepared ranging from 30 pg/ml to 2000 pg/ml using the supplied calibrator diluent (RD6-10). Calibrator diluent was also used as a blank. Quality control standards were also prepared from heat-treated human plasma spiked to 100 pg/ml.

Defrosted plaque media and plasma samples were thoroughly vortexed and centrifuged for 15 minutes at 1000 g.

Whilst wearing a face mask to avoid contamination 100 µl of assay diluent (RD-68) was added to each well. This was followed by the addition of 100 µl of standard, control, or sample per well. The plate was then covered with an adhesive strip and left to incubate at room temperature for two hours on a plate rocker.

Using an auto-washer and the wash buffer provided each well was washed a total of four times. After the last wash any remaining wash buffer was aspirated from the wells.
200 µl of sFlt-1 conjugate was then added to each well before the plate was again covered and left to incubate on the plate rocker for another two hours. After the incubation period the washing and aspiration procedure was repeated.

A 200 µl aliquot of substrate solution was then added before a final incubation in the dark for 30 minutes.

Finally 50 µl of stop solution was added to each well, prompting a colour change from blue to yellow. The optical density of each well was determined within 30 minutes of stop solution addition using a microplate plate reader set to 450 nm

Alternative sample preparation:

Levels of sFlt-1 in endarterectomy plasma samples were determined to be far greater than the limit of detection for the ELISA kit. These samples were therefore diluted (1:20) with

calibrator diluent. Subsequently, levels determined from the standard curve were multiplied by 20.

2.8 Neopterin and dihydroneopterin HPLC method

High performance liquid chromatography (HPLC), an analytical technique used to separate specific components of a complex mixture based on their chemical and physical properties, was used to analyse pterin levels in both plasma and culture samples. The HPLC system used (Shimadzu Corporation, Japan) utilized a LC20AD pump in conjunction with an on-line de-gasser, SIL-20AC temperature controlled autosampler, CTO-20 column oven and a RF10AXL fluorescence detector.

Peaks generated by the column separation were integrated using LC solutions software (Shimadzu Corporation, Japan). The method used was based on that used by Shricks Laboratory (Shricks Laboratory, Switzerland) for assessing the quality of neopterin and 7,8NP standards.

HPLC setup

A mixture of 20% methanol and 80% water was initially pumped through the HPLC at 1 ml/minute for 15 minutes in order to wash the lines. After the 15 minute wash, line A was purged with water for three minutes before it was purged with pre-prepared $AmPO_4$ (20 mM, pH 2.5). $AmPO_4$/10% ACN was then left to pump at 1 ml/minute for 5 minutes or until the pressure stabilized. The Neopterin SCX column was then connected and left to pump at 1 ml/minute. A Luna strong cation exchange (SCX) 250×4.6 mm column (Phenomenex, USA) was employed as the stationary phase, to retain and separate the injected samples. Making sure that the column oven was set to 30°C, the RF10AXL fluorescence detector, set at 353 nm excitation and 438 nm emission wavelengths, was switched on before the pressure was left to stabilize.

Neopterin standard curve preparation

In this definitive quantitative assay neopterin calibrators (standards) were fitted to a regression model in order to determine the quantitative value of neopterin in unknown samples. The neopterin linear regression (standard) curve, consisting of serially diluted concentrations of a 100 µM stock solution with nanopure de-ionised water (Schircks Laboratory, Switzerland),

ranged between 10 nM and 100 nM. 10 µl of these standards were then injected, in duplicate, into the HPLC running at 1ml/min $AmPO_4$/10% ACN. These standards were expressed computationally, by the LC solutions software as peaks. The area under these peaks was proportional to the amount of neopterin present in the solution. Therefore a standard curve was generated by plotting area on the Y-axis and neopterin concentration on the X-axis. From this curve unknown concentrations of neopterin were derived (Fig 13).

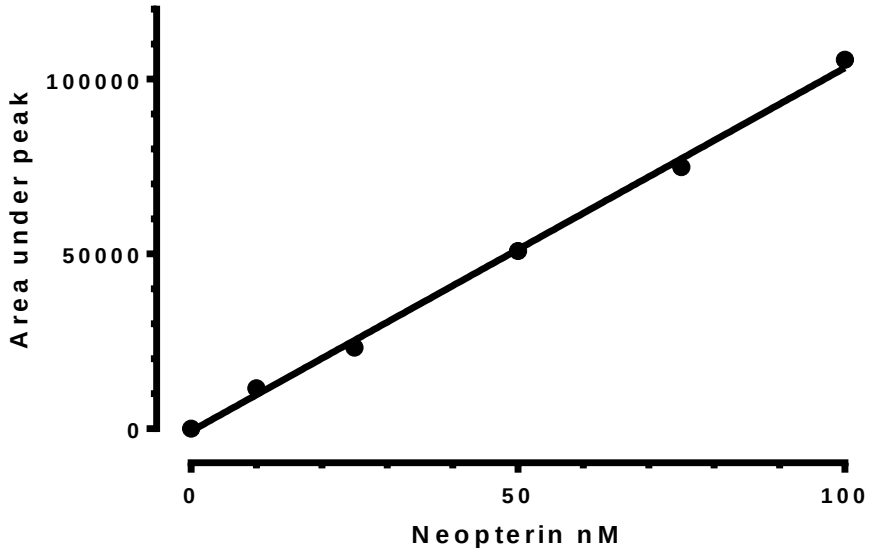

Fig 2.4. neopterin linear regression (standard) curve

Acidic iodide oxidizing potential testing:

In order to make sure that the acidic iodide stock solution could convert 7,8-NP ≥98% to neopterin it had to be tested before use. Using a highly sensitive microbalance 2 mg of pure 7,8-NP (Schricks Laboratory, Switzerland) was weighed out into a cap cut from the top of a 1.7 µl centrifuge tube. The cap was then transferred to a 20 ml, aluminium foil covered, bottle with 10 ml of the 20 mM, pH-2.5 $NH_4PO_4$and sonicated until dissolved. The concentration of 7,8NP was then calculated using the molecular weight of 7,8NP (MW=253). The 7,8NP containing sample was oxidised using 40 µl of the acidic iodide for 15 minutes in the dark, before 20 µl of ascorbic acid was added to reduce the remaining acidic iodide. 10 µl of this sample was then injected, in duplicate, into the HPLC running at 1ml/min $AmPO_4$/10% ACN. The concentration derived was then compared to the concentration of 7,8NP added to determine the oxidizing efficiency.

Plasma and cell culture sample preparation and injection:

Neopterin:

100 µl of defrosted plasma or culture was initially transferred to 1.5 ml centrifuge tubes with 100 µl of 100% ACN. The tubes were then vortexed thoroughly for five seconds before being centrifuged at 20,300 g for 5 minutes at 4˚C. 100 µl of the resulting supernatant was then loaded into HPLC vials. 10 µl of each loaded sample was then injected into the HPLC for analysis.

Total pterin:

100 µl of defrosted plasma or culture was initially transferred to 1.5 ml centrifuge tubes with 100 µl of 100% ACN. The tubes were then vortexed thoroughly for five seconds before being centrifuged at 20,300 g for 5 minutes at 4˚C. 40 µl of pre-tested acidic iodide solution was then added to the supernatant. It was then left to incubate in the dark at room temperature for 15 minutes. Following incubation 40 µl (20 µl for cell culture) of ascorbic acid was added to the samples, to reduce the iodine, prompting a colour change from brown to clear. The samples were subsequently centrifuged at 20,300 g for 5 minutes at 4˚C before 100 µl of the resulting supernatant was loaded into HPLC vials. 10 µl of each loaded sample was then injected into the HPLC for analysis.

2.9 Statistical methods

All statistics on data from the CDCS cohort were calculated using the IBM SPSS statistics 19 software. (SPSS Inc., Armonk, New York). All statistics on data from the endarterectomy cohort were calculated using Graph Pad Prism 6 software (GraphPad Software Inc., La Jolla, California).

Patient population

CVD patients (n=514), who were admitted to Christchurch Hospital following a cardiovascular event between July 2002 and August 2007, were enrolled in the study to evaluate potential markers of mortality following a cardiovascular event. Patients were recruited into the study according to the following inclusion criteria; ischemic discomfort plus one or more of electrocardiogram changes (ST segment depression or elevation of at least 0.5 mm, T-wave inversion of at least 3 mm in at least three leads, or left bundle branch block), elevated levels of cardiac markers, a history of coronary disease, or were aged at least 65 years in patients with diabetes or vascular disease. Patients were excluded from the study if they had

a severe comorbidity that limited their life expectancy to less than 3 years, or were aged <18 years. Clinical events were investigated upon re-admittance to hospital where all cause death (ACD), CVD death and total cardiovascular events (TCVE) were the major study end points.

Of the 514 patient cohort, 365 were male and 149 were female. The clinical parameters assessed largely focussed on the biomarkers sFlt-1, neopterin and 7,8NP. These biomarkers were compared to BNP, measured previously in the same cohort by Endolab of the Christchurch Heart Institute, along with age at baseline, gender, alcohol consumption, diastolic blood pressure, diastolic, tobacco usage, statin usage, type two diabetes status and bodyweight (Refer to table 3.1.1 in Results).

sFlt-1 data, prior to forming statistical models, was compared to data obtained in a similar study by Matsumoto *et al.* (2013) in order to determine the relative statistical power of the dataset. Statistical power was calculated to determine the significance of the data in terms of sample size and the ability of the data to test the null hypothesis.

General linear model analysis

Multiple univariate general linear models were used to assess the hypothesis that variables commonly associated with CVD exhibit a significant relationship to the biomarkers sFlt-1, neopterin, 7,8NP and total neopterin. A type III sum of squares method (equivalent to Yates' weighted-squares-of-means technique) was employed to deal with the unbalanced models.

Cox regression proportional hazards model and Kaplan-Meier analysis

Variables were split into above and below median values before Kaplan-Meier analyses were performed to evaluate the incidence of mortality and CVD during the follow up period. To evaluate significant difference at different time points in the survival curves, each curve was subjected to Log-rank, Breslow and Tarone-Ware analysis. Cox proportional hazard regression analyses were performed to evaluate the relationships between age at baseline, the biomarkers sFlt-1, neopterin, 7,8 NP, and BNP with respect to TCVE and ACD. All tests were two-sided, and p values <0.05 represented statistically significant differences.

Endarterectomy statistics

Blood samples from the endarterectomy cohort were obtained immediately prior to the carotid endarterectomy procedure at Christchurch Hospital, by Prof Justin Roake and associates of the Vascular Surgery Department, after which extracted plasma was analysed for sFlt-1, neopterin, 7,8 NP and total neopterin. In the 27 patient cohort, 19 were male and 8 were female. The clinical parameters assessed largely focussed on the biomarkers sFlt-1, neopterin and 7,8 NP (Refer to tables 6.1 and 6.2 in Appendix).

A Prism™ Standard 2 tailed T-test with Tukey post-hoc was used to analyse the data obtained from the analysis of Endarterectomy patient plasma.

SPSS™ Bivariate analysis of the plasma data was used to obtain correlative statistics on sFlt-1, neopterin, 7,8 NP and total neopterin.

Prism™ 2 way ANOVA was used to analyse the variance between subgroups in the cell culture and plaque samples

3

Results

3.1 Cardiovascular disease cohort study (CDCS)

Acute coronary syndrome patient plasma was used to assess the clinical utility of sFlt-1 in comparison with neopterin and 7,8NP, total neopterin levels. The plasma was collected from patients in a stable condition following an acute coronary syndrome event (Table 3.1.1). Each patient's clinical outcome was followed using hospital and National Health Information Service databases over a median period of 5 years.

Variable	sFlt-1 Min	sFlt-1 Max	Pterin Min	Pterin Max	sFlt-1 Mean	Pterin Mean	N Male	N Female
Age (Years)	34.0	93.0	39.0	91.0	68.8±0.5	68.48±1.1	365	149
Height (cm)	147.0	192.0	147.0	192.0	186.3±0.4	168.7±0.8	365	149
Weight (Kg)	40.0	150.0	46.0	130.0	77.7±0.7	78.0±1.5	365	149
Alcohol intake (per week)	0.3	60.0	0.3	58.0	9.9±1.0	9.0±1.1	365	149
Systolic BP	80.0	230.0	80.0	230.0	128.1±1.0	131.9±2.2	365	149
Diastolic BP	48.0	119.0	52.0	110.0	74±0.5	77.12±1.1	365	149
sFlt-1 (pg/ml)	11.0	581.0	11.0	265.0	117.3±2.7	89.5±2.7	365	149
Neopterin (nM)	0.0	210.8	0.0	210.8	22.9±1.8	22.9±1.8	92	46
7,8 NP (nM)	1.56	591.0	1.56	591.0	66.2±7.8	66.2±7.8	92	46
Total neopterin (nM)	16.58	624.6	16.58	624.6	94.4±9.1	94.4±9.1	92	46
Statin usage	-	-	-	-	-	-	315	109
Tobacco usage	-	-	-	-	-	-	189	54
Diabetes II	-	-	-	-	-	-	60	22

Table 3.1.1 General summary of CDCS patients. Clinical parameters were assessed at baseline for patients of the CDCS cohort. The data presented shows mean±SEM.

The descriptive statistics of the CDCS cohort indicates that levels of sFlt-1 (in 514 patients) ranged from 11 pg/ml to 581 pg/ml, with a mean of 117.3±2.7 pg/ml and a standard deviation of 62 pg/ml. Levels of sFlt-1 did not differ significantly between males (117.5±3.3 pg/ml) or females (116.5±4.8 pg/ml). Levels of total neopterin, in 138 of the CDCS patients, ranged between 16.58 nM and 624.6 nM, with a mean of 94.4±9.1 nM and a standard deviation of 107.08 nM. Unlike sFlt-1 total neopterin was significantly higher in females (134.2±23.9 nM) than males (74.6±5.7 nM). Neopterin levels (22.9±1.8 nM) contributed less to the overall total neopterin count than 7,8NP levels (66.2±7.8 nM). Of the two pterins only 7,8 NP levels were significantly different between males (53.2±5.2 nM) and females (93.1±20.9 nM). Mean neopterin levels were 26±4.7 nM and 21.3±1.6 nM for females and males respectively.

3.1.1 Statistical Power of CDCS in comparison with Matsumoto et al., 2013.

Statistical power is the strength/magnitude of the study. The more power the less likely the chances of making an error in accepting the null hypothesis, otherwise referred to as a type two error. In this case the sFlt-1 data, obtained from the CDCS cohort plasma by ELISA assay, was compared to the data obtained in a similar experiment by Matsumoto *et al.* (2013). This tells us, that although different values were obtained by Matsumoto *et al.* (2013), the value of the data generated in this thesis is significant.

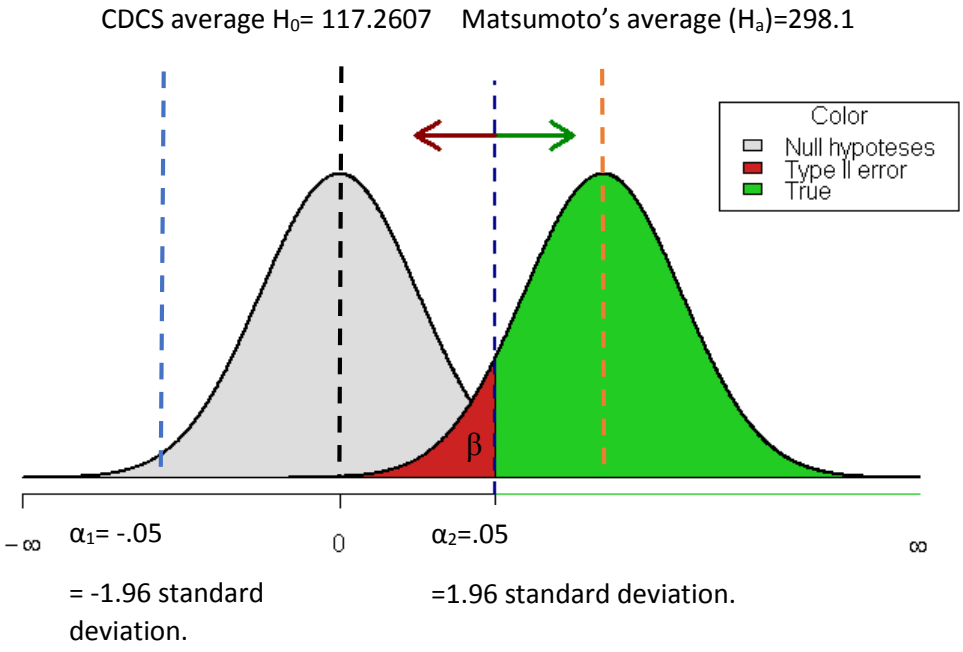

Fig 3.1.1. Distribution Schematic. Indicating distribution of the data on CDCS cohort (Grey) and Matsumoto Cohort (Green) sFlt-1 levels.

Calculation of statistical power for CDCS:

N = 514, σ = 61.9, H_0 = 117.2607

$-1.96 = \frac{(\alpha 1 - 117.2607)}{61.9/\sqrt{514}}$ $\quad$ $1.96 = \frac{(\alpha 2 - 117.2607)}{61.9/\sqrt{514}}$

$\alpha_1 = (-1.96\left(\frac{61.9}{\sqrt{514}}\right)) + 117.2607$ $\quad$ $\alpha_2 = \left(1.96\left(\frac{61.9}{\sqrt{514}}\right)\right) + 117.2607$

α_1 = 111.9093278 $\quad$ α_2 = 122.6120722

Probability of (111.9093278<α<1226127022) In terms of pg/ml

Conversion to percentage probability:

$\frac{111.9093278 - 298.1}{61.9/\sqrt{514}} < \alpha < \frac{122.6120722 - 298.1}{61.9/\sqrt{514}}$

-68.19441848< α <-64.2744185

Power (β) = 0.94251729 = 94% Probability of correctly rejecting the null hypothesis when it is false.

As can be observed from the calculation above, the dataset has a 94.25% likelihood of correctly rejecting the null hypothesis (that sFlt-1 is not an independent predictor of all-cause mortality in patients post CVD event).

3.1.2 Relationship between CVD variables and biomarkers

Multiple univariate general linear models were used to assess the hypothesis that variables commonly associated with CVD exhibit a significant relationship to the biomarkers sFlt-1, neopterin, 7,8NP and total neopterin.

Dependent Variable: sFLT1

Source	Type III Sum of Squares	Mean	df	Mean Square	F	Sig.
Corrected Model	144996.476		6	24166.079	6.958	.000
Intercept	53123.711		1	53123.711	15.297	.000
BNP	25584.641	36.80±2.90	1	25584.641	7.367	.007
Drinks/Week	58847.323	9.50±1.50	1	58847.323	16.945	.000
Diastolic BP	46227.330	73.23±0.85	1	46227.330	13.311	.000
Heart rate	15606.492	465.66±0.79	1	15606.492	4.494	.035
BMI	3746.073	28.09±0.30	1	3746.073	1.079	.300
Gender	2715.418		1	2715.418	.782	.377
Error	1121756.388		323	3472.930		
Total	6007959.000		330			
Corrected Total	1266752.864		329			

Table 3.1.2. Commonly associated variables expressed in a general linear model with sFlt-1 as the dependent variable. Data is expressed as mean ± SEM. Covariates were assessed for their association to sFlt-1 expressed as a linear model. All measures were taken post-recovery from an initial CV event. A type III sum of squares method (equivalent to Yates' weighted-squares-of-means technique) was employed to deal with the unbalanced models.

Aside from gender and BMI all covariates BNP, drinks/week, diastolic blood pressure and heart rate were shown to be significantly associated ($P<0.05$) to the linear regression model of sFlt-1 (Table. 3.1.2).

Dependent variable: Total neopterin

Source	Type III Sum of Squares	Mean	df	Mean Square	F	Sig.
Corrected Model	75844.152[a]		6	12640.692	2.021	.074
Intercept	7215.664		1	7215.664	1.154	.286
BNP	1796.485	31.63±2.90	1	1796.485	.287	.594
Drinks/Week	62012.016	9.03±1.12	1	62012.016	9.916	.002
Diastolic BP	428.536	77.12±1.12	1	428.536	.069	.794
HR	3692.188	66.27±0.97	1	3692.188	.590	.445
BMI	.760	27.35±0.40	1	.760	.000	.991
Gender	26708.697		1	26708.697	4.271	.042
Error	437747.885		70	6253.541		
Total	981549.961		77			
Corrected Total	513592.037		76			

Table 3.1.3. Commonly associated variables expressed in a general linear model with both neopterin and 7,8NP combined as the dependent variable. Data is expressed as mean± SEM. Covariates were assessed for their association to total neopterin expressed as a linear model.

Unlike the general linear model of sFlt-1, aside from gender and alcohol consumption, none of the covariates were significantly associated with total neopterin (Table 3.1.3).

From this model there is no evidence provided to support the hypothesis that levels of BNP, diastolic blood pressure, heart rate or BMI are associated with total neopterin levels in patients after ACS. On the other hand alcohol consumption, like with sFlt-1, was a significant ($P<0.05$) covariate and may therefore be associated with pathways responsible for total neopterin and sFlt-1 regulation.

Dependent Variable: Neopterin

Source	Type III Sum of Squares	Mean	df	Mean Square	F	Sig.
Corrected Model	2615.558[a]		6	435.926	2.127	.061
Intercept	842.859		1	842.859	4.112	.046
BNP	1086.871	31.63±2.90	1	1086.871	5.302	.024
Drinks/Week	351.248	9.03±1.12	1	351.248	1.714	.195
Diastolic BP	7.666	77.12±1.12	1	7.666	.037	.847
Heart rate	12.127	66.27±0.97	1	12.127	.059	.809
BMI	1003.512	27.35±0.40	1	1003.512	4.896	.030
Gender	14.016		1	14.016	.068	.794
Error	14758.277		72	204.976		
Total	53387.304		79			
Corrected Total	17373.835		78			

Table 3.1.4. Commonly associated variables expressed in a general linear model with neopterin as the dependent variable. Data is expressed as mean± SEM. Covariates were assessed for their association to neopterin expressed as a linear model.

BNP, and BMI were significantly associated (P<0.05) with neopterin, indicating that these variables are potentially associated to levels of neopterin post CVD event. However, no other covariates in the model exhibited any significant association (P<0.05) (Table 3.1.4). Notably, the same significant relationship was not observed, between neopterin and alcohol consumption, that was observed between alcohol consumption and both sFlt-1 and total neopterin. On the other hand, neopterin, like sFlt-1 was significantly associated with BNP.

Dependent Variable: 7,8 NP

Source	Type III Sum of Squares	Mean	df	Mean Square	F	Sig.
Corrected Model	69518.554[a]		6	11586.426	1.957	.084
Intercept	3037.864		1	3037.864	.513	.476
BNP	55.537	31.63±2.90	1	55.537	.009	.923
Drinks/Week	51904.133	9.03±1.12	1	51904.133	8.766	.004
Diastolic BP	498.291	77.12±1.12	1	498.291	.084	.773
HR	3900.932	66.27±0.97	1	3900.932	.659	.420
BMI	771.396	27.35±0.40	1	771.396	.130	.719
Gender	25052.786		1	25052.786	4.231	.043
Error	408555.772		69	5921.098		
Total	724441.464		76			
Corrected Total	478074.326		75			

Table 3.1.5. Commonly associated variables expressed in a general linear model with 7,8 NP as the dependent variable. Data is expressed as mean± SEM. Covariates were assessed for their association to 7,8NP expressed as a linear model.

Much like total neopterin, both alcohol consumption and gender were shown to be significantly associated to 7,8NP ($P<0.05$). All other included covariates were not significantly associated to 7,8NP as was also observed in the general model of total neopterin ($P>0.05$) (Table 3.1.5).

3.1.3 Direct correlations between Biomarkers and significant variables

A multiple comparison bivariate analysis was used to assess the relationship between significant variables in the general linear models and the biomarkers. In the same analysis the direct relationship between the biomarkers was assessed.

		sFLT1	Drinks Per Week	Neopterin	Total Neopterin	7,8NP	BNP
sFLT1	Pearson Correlation	1	.178**	.042	-.088	-.098	.098*
	Sig. (2-tailed)		.001	.618	.304	.260	.027
	N	514	362	144	138	135	514
Drinks per Week	Pearson Correlation	.178**	1	.098	.287**	.267*	-.081
	Sig. (2-tailed)	.001		.364	.007	.013	.125
	N	362	362	88	86	85	362
Neopterin	Pearson Correlation	.042	.098	1	.372**	.141	.070
	Sig. (2-tailed)	.618	.364		.000	.102	.405
	N	144	88	144	136	135	144
Total neopterin	Pearson Correlation	-.088	.287**	.372**	1	.972**	-.012
	Sig. (2-tailed)	.304	.007	.000		.000	.889
	N	138	86	136	138	135	138
7,8NP	Pearson Correlation	-.098	.267*	.141	.972**	1	-.024
	Sig. (2-tailed)	.260	.013	.102	.000		.782
	N	135	85	135	135	135	135
BNP	Pearson Correlation	.098*	-.081	.070	-.012	-.024	1
	Sig. (2-tailed)	.027	.125	.405	.889	.782	
	N	514	362	144	138	135	514

Table 3.1.6. Correlations observed between significant factors. Analysis of correlations between biomarkers sFlt-1, neopterin, 7,8NP, Total neopterin, BNP and the commonly associated factor drinks per week. **: the correlation is significant at the P<0.01 level. *: the correlation is significant at the P<0.05 level.

From the direct correlations shown in Table 3.1.6 a strong positive correlation (P<0.01) can be observed for alcohol consumed per week with sFlt-1 and total neopterin. A slightly weaker positive correlation can also be observed between levels of 7,8NP and alcohol

consumption. However, no correlation could be derived from alcohol consumed per week with neopterin or BNP.

sFlt-1 was also shown to exhibit no significant correlation to neopterin 7,8NP or total neopterin levels. However a significant correlation was observed between sFlt-1 and both alcohol consumption and BNP.

3.1.4 Survival analysis of CDCS patients

In order to determine the predictive and prognostic capabilities of the biomarkers Kaplan-Meier and Cox proportional regression analyses were performed to evaluate the incidence of death and TCVE (Total cardiovascular events) in the follow up period post-cardiovascular event. Using information derived from the general linear models and direct correlation statistics, significant variables were identified to be included in the Cox proportional regression models. Of the 138 patients analysed for total neopterin, neopterin and 7,8 NP, from the 514 patient CDCS cohort, 32 patients died, 22 of which died from CVD and 88 patients developed TCVE. Of the 514 patients analysed for sFlt-1, 148 patients died, 97 of which died from CVD, and 358 patients developed TCVE.

Total neopterin survival analysis

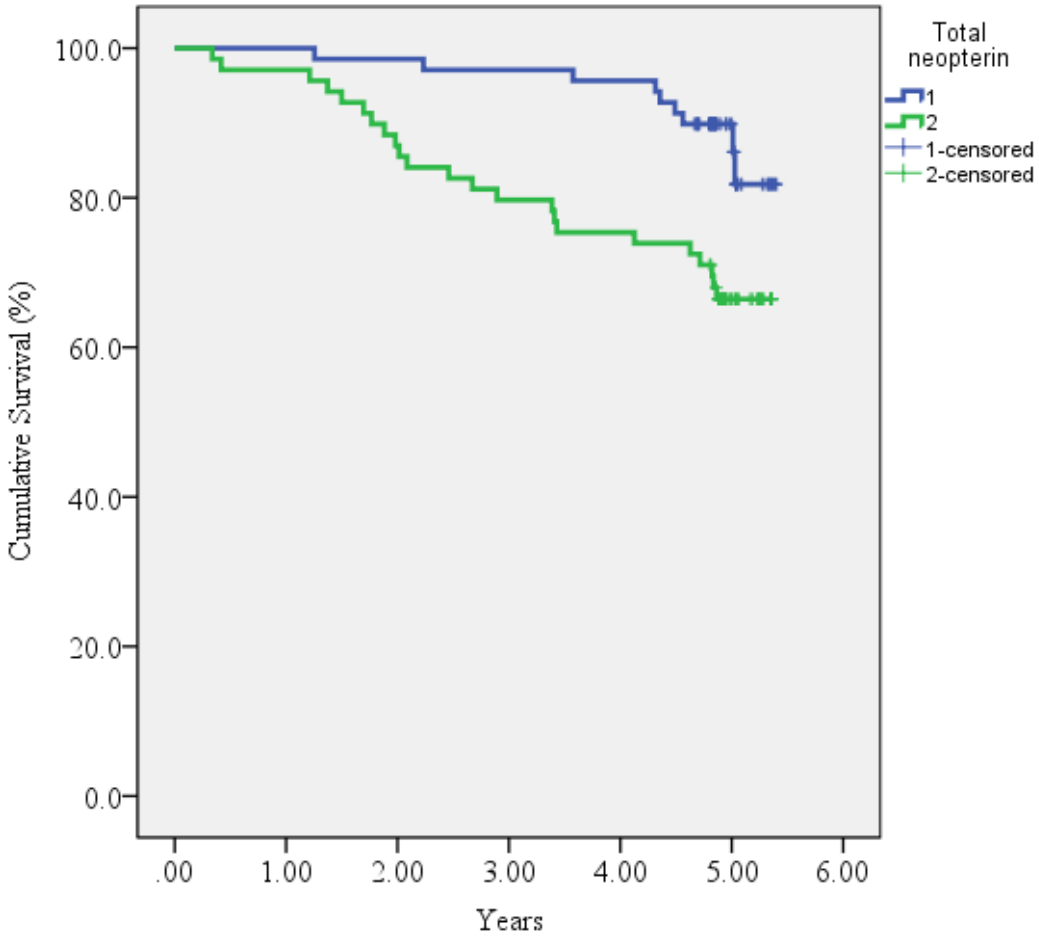

Fig 3.1.2. Total neopterin ACD Kaplan-Meier analysis. Cumulative survival of ACD in CDCS patients with above median (2, green) and below (1, blue) total neopterin levels over a 5.4 year period. 1 and 2 censored represents patients who were lost to follow-up.

	Chi-Square	df	Sig.
Log Rank	7.717	1	.005
Breslow	9.565	1	.002
Tarone-Ware	8.896	1	.003

Table 3.1.7. Test for equality of survival distributions for the different levels of total neopterin. Log Rank analysis indicates difference in equality of survival functions when all time points are weighted the same. Breslow analysis indicates difference in equality of survival functions when all time points are weighted by the number of cases at risk at each time point. Tarone-Ware analysis indicates difference in equality of survival functions when all time points are weighted by the square root of the number of cases at risk at each time point.

	Coefficient	SE	Sig.	Hazard Ratio	95.0% CI for Hazard Ratio	
					Lower	Upper
Total neopterin	1.972	.695	.005	7.187	1.839	28.080
BNP	.637	.655	.331	1.891	.524	6.829
Age at baseline	.295	.102	.004	1.343	1.100	1.641
Drinks Per Week	1.179	.576	.041	3.250	1.052	10.041

Table 3.1.8. Cox proportional hazards model for ACD vs total neopterin, BNP, age at baseline and drinks per week. A model of time to ACD based on the value of the covariates BNP, age at baseline, drinks per week and Total neopterin. Median separation points being 94.4 nM, 34.1 pg/ml, 9.0 drinks and 68.8 years for Total neopterin, BNP, drinks per week and age at baseline respectively.

When patients were divided into two groups, according to the median value for total neopterin (94.4 nM), a significant association was exhibited between patients with an above median level of total neopterin and ACD (all cause death), with reduced survival observable in patients with above median levels (Fig. 3.1.2). Furthermore, overall tests for the equality of survival scores at different time points showed that all time points were significant ($p < 0.05$), establishing that there is a statistically significant difference between patient's survival with above and below median levels of total neopterin across the 5.4 year follow up period (Table. 3.1.7).

Further analysis of its prognostic use, in determining ACD using a Cox proportional analysis, revealed that higher than median total neopterin, higher alcohol consumption and a higher than median age were all associated with adverse outcomes. With the assumption that

the covariates have an effect on the hazard function, total neopterin, age at baseline and alcohol consumption were all shown to be significant. As a result the hazard ratios of 7.187, 1.343 and 3.250, for total neopterin, age at baseline and alcohol consumption respectively, can be deemed as significant with respect to matching the Cox proportional hazard model (Table 3.1.8). This result, along with the Kaplan-Meier analysis, indicates that 7,8NP is an independent predictor of survival in patients post-CVD event. However, the commonly used ventricular wall stress biomarker BNP, which is a well-established prognostic marker in CVD, was not significant.

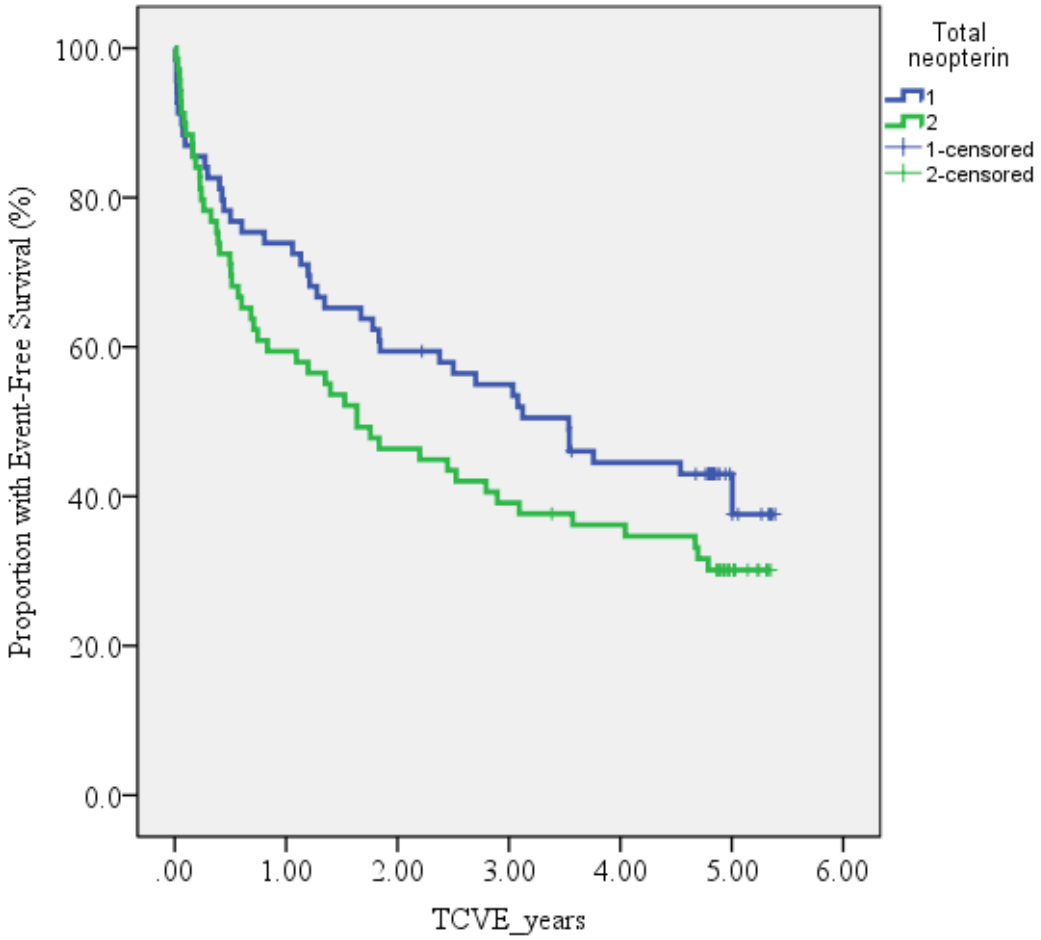

Fig 3.1.3. Total neopterin TCVE Kaplan-Meier analysis. TCVE in CDCS patients with above (2, green) and below (1, blue) median total neopterin (94.4728 nM) levels over a 5.4 year period. 1 and 2 censored represents patients who were lost to follow-up.

	Chi-Square	df	Sig.
Log Rank	2.189	1	.139
Breslow	2.185	1	.139
Tarone-Ware	2.301	1	.129

Table 3.1.9. Test for equality of TCVE distributions for the different levels of total neopterin

	Coefficient	SE	Sig.	Hazard Ratio	95.0% CI for Hazard Ratio	
					Lower	Upper
Total neopterin	.242	.309	.432	1.274	.696	2.333
BNP	.095	.330	.773	1.100	.576	2.099
Age at baseline	.125	.056	.025	1.133	1.016	1.263
Drinks per week	.463	.299	.121	1.589	.885	2.854

Table 3.1.10. Cox proportional hazards model for TCVE vs total neopterin, BNP, age at baseline and drinks per week. A model of time to TCVE based on the value of the covariates BNP, Age at baseline, drinks per week and total neopterin. Median separation points being 94.4 nM, 34.1 pg/ml 9.0 drinks and 68.8 years for Total neopterin, BNP, drinks per week and age at baseline respectively.

In contrast, to total neopterins prognostic utility in determining ACD, its potential predictive capabilities for determining TCVE were not supported by this dataset.

Like the Kaplan-Meier analysis for ACD, TCVE were shown to occur early in the follow up period as well as being more frequent over the 5.4 year follow up period for patients with higher than median levels of total neopterin (Fig 3.1.3). However, overall tests of TCVE at different time points showed that at all time points the difference, between above and below median levels of total neopterin, was not- significant ($p>0.05$) (Table 3.1.9).

A univariate Cox proportional regression analysis of the dataset showed that, of the four variables BNP, total neopterin, age at baseline and drinks per week, only age at baseline was significantly associated with TCVE ($p<0.05$). Therefore, in the same model, total neopterin, alcohol consumption and BNP are not indicated as predictive markers with respect to TCVE in patients post CVD event (Table 3.1.10). This result, along with the insignificant Kaplan-Meier analysis, suggests that, although total neopterin and alcohol consumption may be significant prognostic markers of ACD, they are not significantly associated with the incidence of TCVE.

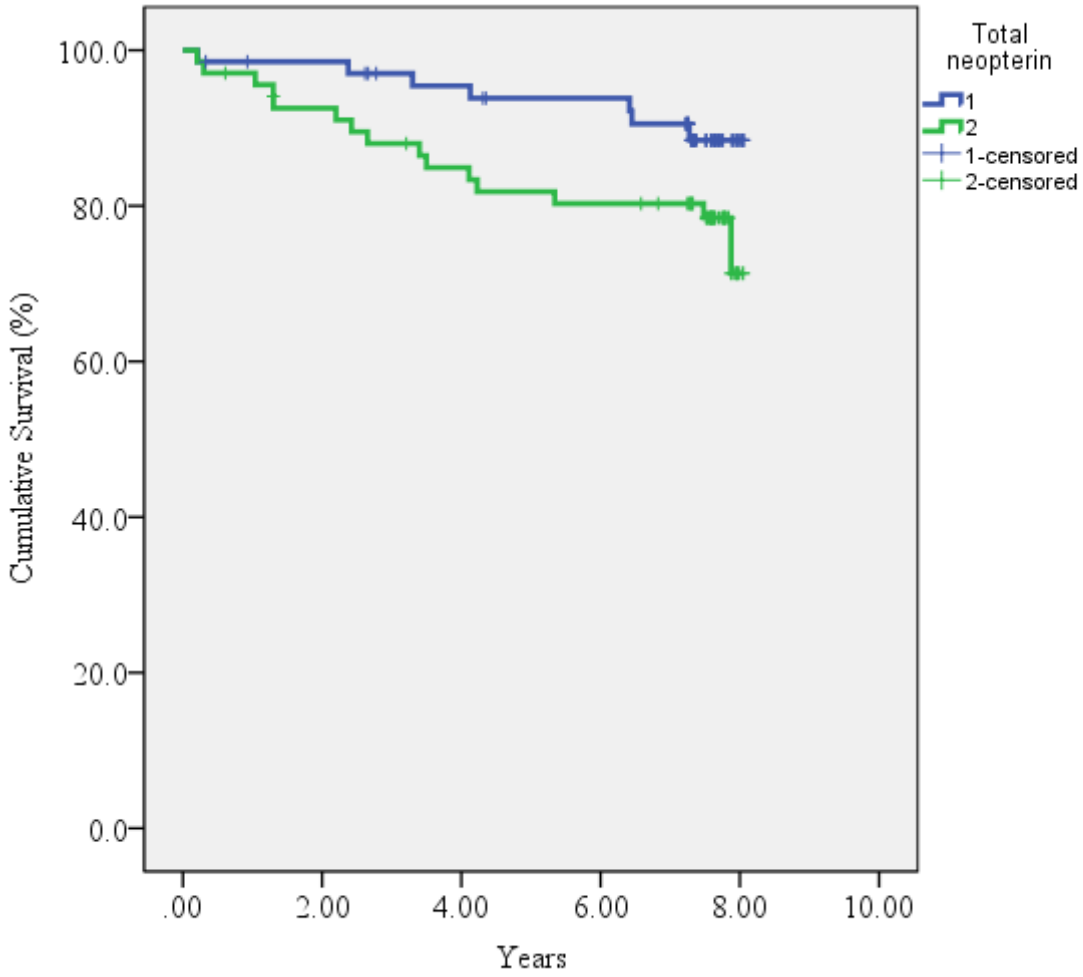

Fig 3.1.4. Total neopterin CVD death Kaplan-Meier analysis. CVD death in CDCS patients with above (2, green) and below (1, blue) median total neopterin (94.4728 nM) levels over a mean 5.4 year period. 1 and 2 censored represents patients who were lost to follow-up.

	Chi-Square	df	Sig.
Log Rank	3.204	1	.073
Breslow	3.012	1	.083
Tarone-Ware	3.040	1	.081

Table 3.1.11. Test for equality of CVD death distributions for the different levels of total neopterin.

	Coefficient	SE	Sig.	Hazard Ratio	95.0% CI for Hazard Ratio	
					Lower	Upper
Total neopterin	1.110	.556	.046	3.034	1.020	9.027
BNP	.458	.570	.422	1.580	.517	4.833
Age at baseline	.190	.096	.048	1.210	1.002	1.461
Drinks per week	-.172	.523	.741	.842	.302	2.344

Table 3.1.12. Cox proportional hazards model for CVD death vs total neopterin, BNP, age at baseline and alcohol consumption. A model of time to CVD death based on the value of the covariates BNP, Age at baseline, drinks per week and total neopterin. Median separation points being 94.4 nM, 34.1 pg/ml 9.0 drinks and 68.8 years for total neopterin, BNP, drinks per week and age at baseline respectively.

Although a difference in CVD death, between patients with above and below median levels of total neopterin, was observed, over the 5.4 year follow up period, this difference was not significant (Fig 3.1.4.). Overall analysis of the survival curves indicates that, at any point in the survival analysis, the difference observed between the two groups was not significant ($p>0.05$) and therefore doesn't suggest a positive relationship between higher levels of total neopterin and CVD death (Table 3.1.11).

Like the Cox proportional analysis of TCVE neither BNP nor drinks per week were significantly associated with CVD death. Although patients expressing higher than median levels of total neopterin were not indicated as significantly more at risk of CVD death by the Kaplan-Meier analysis, the Cox proportional regression provides a different outlook. In the same cox proportional regression analysis total neopterin and age at baseline are indicated as significant ($P<0.05$), with patients in the above median total neopterin group having a 3-fold higher risk of CVD death. Unlike total neopterin both BNP and alcohol consumption exhibited no significant relationship to CVD death in the 5.4 year follow up period (Table 3.1.12). Therefore, the significant association observed, between ACD and total neopterin, may be due to a relationship between total neopterin and CVD death.

Neopterin survival analysis

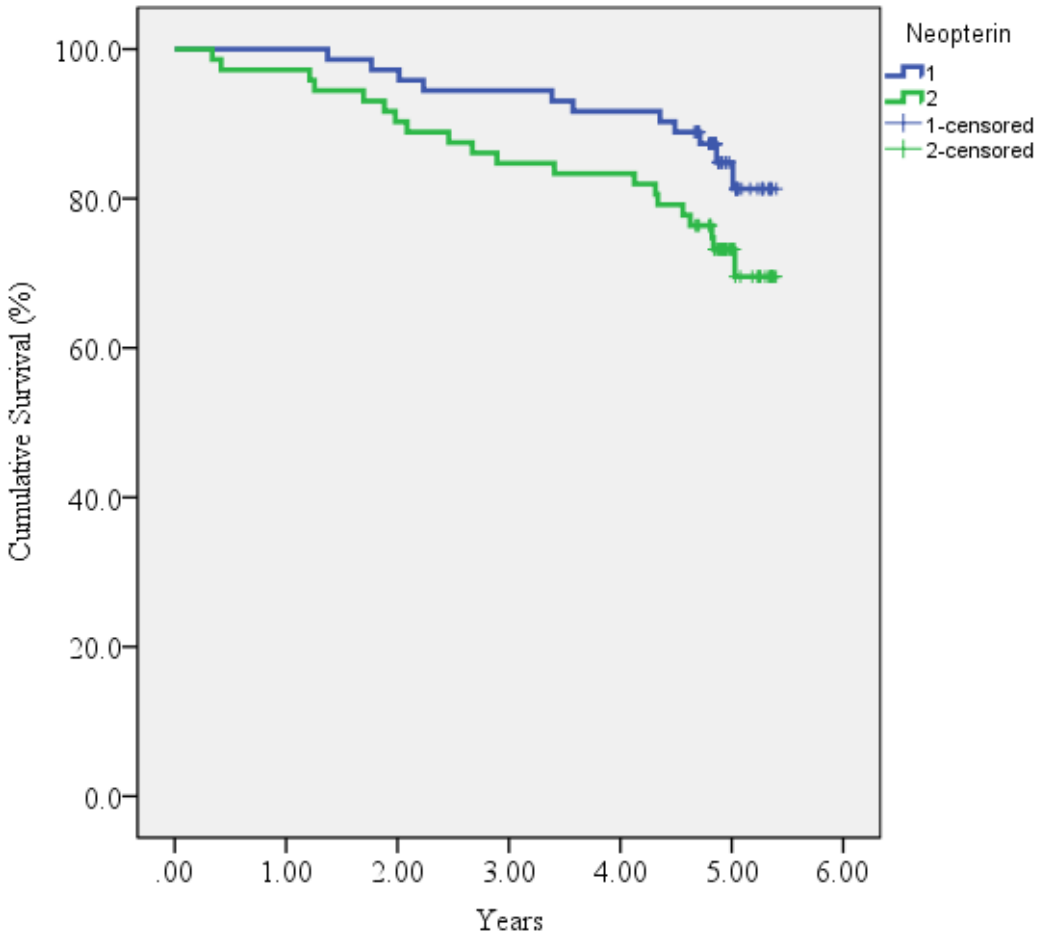

Fig 3.1.5. Neopterin ACD Kaplan-Meier analysis. Cumulative survival of CDCS patients with above (2, green) and below (1, blue) median neopterin (22.8555 nM) levels over a 5.4 year period. 1 and 2 censored represents patients who were lost to follow-up.

	Chi-Square	df	Sig.
Log Rank	3.228	1	.072
Breslow	3.707	1	.054
Tarone-Ware	3.521	1	.061

Table 3.1.13. Test for equality of survival distributions for the different levels of neopterin.

	Coefficient	SE	Sig.	Hazard ratio	95.0% CI for Hazard Ratio	
					Lower	Upper
BNP	.609	.670	.363	1.839	.494	6.839
Age at baseline	.285	.108	.008	1.330	1.077	1.642
Drinks per week	1.019	.550	.064	2.772	.943	8.148
Neopterin	1.725	.697	.013	5.614	1.431	22.017

Table 3.1.14. Cox proportional hazards model for ACD vs neopterin, BNP, age at baseline and drinks per week. A model of time to ACD based on the value of the covariates BNP, Age at baseline, drinks per week and neopterin. Median separation points being 22.9 nM, 9.0 drinks, 34.1 pg/ml and 68.8 years for neopterin, drinks per week, BNP and age at baseline respectively.

From the Kaplan-Meier analysis (Fig. 3.1.5), for neopterin vs ACD, no significant difference can be identified at any time point, between levels above and below the median, for neopterin in patients after recovery from a CVD event (Table 3.1.13).

Neopterin, expressed as a covariate alongside age at baseline, alcohol consumption and BNP, in a univariate Cox proportional regression model, however shows that neopterin is a significant predictor of death, with patients in the above average neopterin group experiencing a 5.6 fold greater risk of ACD post CVD event. However, unlike neopterin, the model identifies BNP and drinks per week as non-significant ($P>0.05$) predictors of ACD (Table 3.1.14).

Therefore, neopterins prognostic utility is supported. As analysis shows a significant difference in ACD for above and below median levels and significant prognostic ability in combination with the cofactor age at baseline.

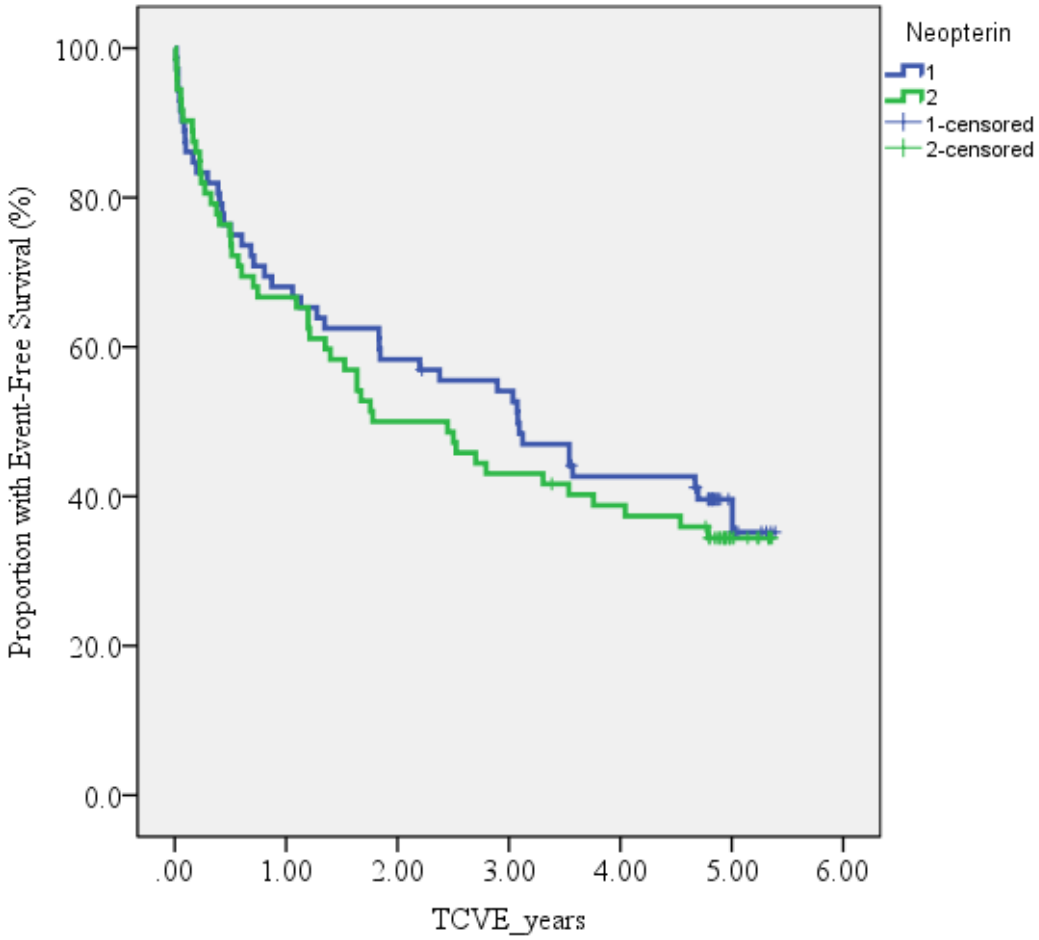

Fig 3.1.6. Neopterin TCVE Kaplan-Meier analysis. TCVE in CDCS patients with above (>22.9 nM, 2, green) and below (<22.9 nM, 1, blue) median neopterin (22.86 nM) levels over a 5.4 year period. 1 and 2 censored represents patients who were lost to follow-up

	Chi-Square	df	Sig.
Log Rank	.338	1	.561
Breslow	.391	1	.532
Tarone-Ware	.400	1	.527

Table 3.1.15. Test for equality of TCVE distributions for the different levels of neopterin.

	Coefficient	SE	Sig.	Hazard ratio	95.0% CI for Hazard Ratio	
					Lower	Upper
BNP	.162	.325	.618	1.176	.622	2.225
Drinks per week	.525	.302	.082	1.690	.936	3.052
Age at baseline	.125	.056	.025	1.134	1.016	1.265
Neopterin	.169	.312	.588	1.184	.643	2.181

Table 3.1.16. Cox proportional hazards model for TCVE vs neopterin, drinks per week, BNP and age at baseline. A model of time to TCVE based on the value of the covariates BNP, Age at baseline, Drinks per week and Neopterin. Median separation points being 22.9 nM, 9.0 drinks, 34.1 pg/ml and 68.8 years for neopterin, drinks per week, BNP and age at baseline respectively.

Neopterins incapacity to predict TCVE is highlighted in the Kaplan-Meier analysis above (Fig. 3.1.6.). Cardiovascular events, occurring in patients with above and below median levels of neopterin, largely follow the same trend with an initial period of frequent CV events over the first two years, followed by a less frequent occurrence in the below median group over the next 3 years. No significant association was identified between levels of neopterin and TCVE at any period over 5.4 years (Table 3.1.15).

The biomarker utility of neopterin in predicting TCVE is further discredited by analysis of neopterin alongside BNP, drinks per week and age at baseline in a univariate cox proportional hazards model (Table 3.1.16). Much like the model of ACD, age at baseline significantly predicts TCVE. Neopterin however, does not show significant utility in predicting TCVE, alongside drinks per week and BNP in patients after recovery from a cardiovascular event.

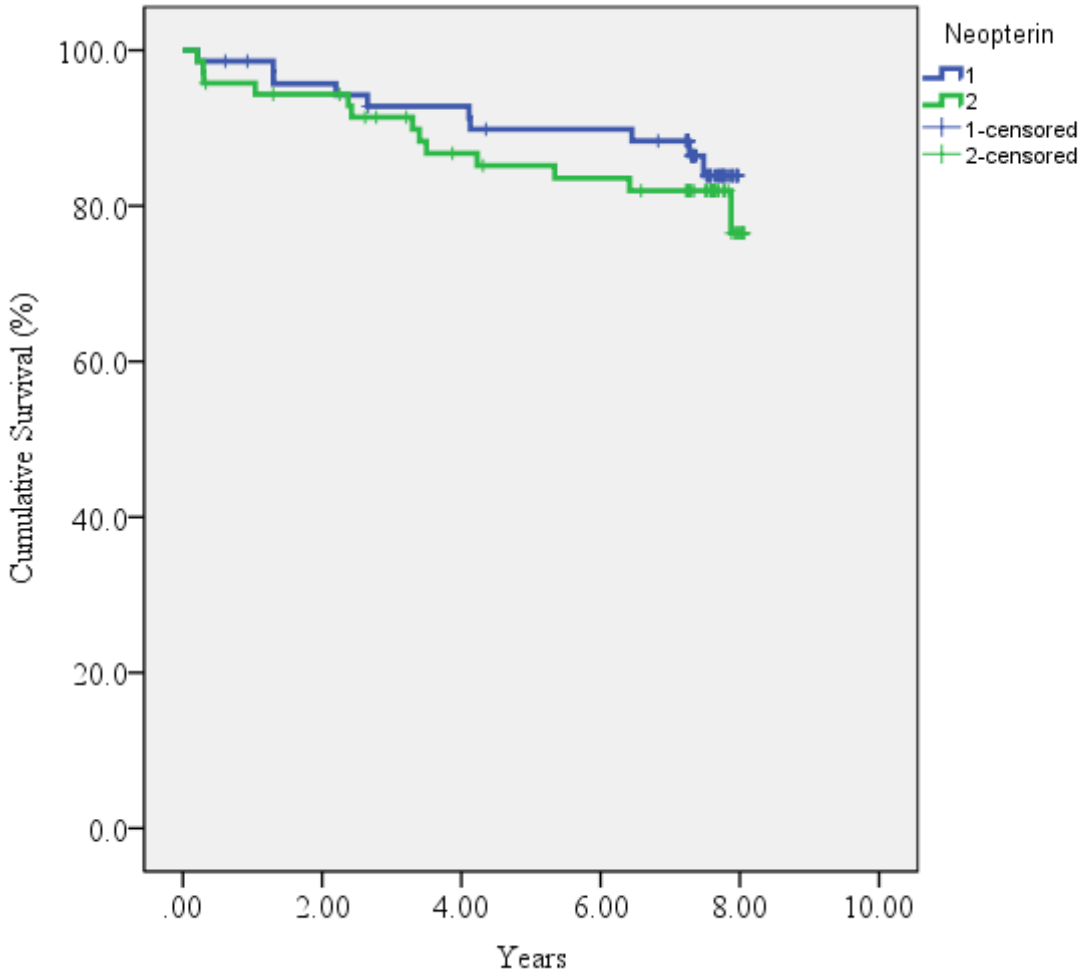

Fig 3.1.7. Neopterin CVD death Kaplan-Meier analysis. CVD death in CDCS patients with above (>22.9 nM, 2, green) and below (<22.9 nM, 1, blue) median neopterin (22.8555 nM) levels over a mean 5.4 year period. 1 and 2 censored represents patients who were lost to follow-up.

	Chi-Square	df	Sig.
Log Rank	.472	1	.492
Breslow	.541	1	.462
Tarone-Ware	.491	1	.484

Table 3.1.17. Test for equality of CVD death distributions for the different levels of neopterin.

	Coefficient	SE	Sig.	Hazard ratio	95.0% CI for Hazard Ratio	
					Lower	Upper
BNP	.700	.574	.223	2.013	.653	6.204
Drinks per week	-.262	.513	.609	.769	.281	2.103
Age at baseline	.153	.095	.106	1.165	.968	1.404
Neopterin	.203	.518	.695	1.225	.444	3.384

Table 3.1.18. Cox proportional hazards model for CVD death vs neopterin, BNP, drinks per week and age at baseline. A model of time to CVD death based on the value of the covariates BNP, Age at baseline, drinks per week and neopterin. Median separation points being 22.9 nM, 9.0 drinks, 34.1 pg/ml and 68.8 years for neopterin, drinks per week, BNP and age at baseline respectively.

Higher levels of neopterin did not result in any observable difference in the incidence of CVD death. As can be observed in the Kaplan Meier analysis incidence of CVD death remains relatively equal, in patients with above and below median levels of neopterin, throughout the 5.4 year follow up period (Fig 3.1.7).

Overall analysis of the survival curves indicates that, at any point in the survival analysis, the difference observed between the two groups was not significant ($p>0.05$) and therefore doesn't suggest a positive relationship between higher levels of neopterin and CVD death (Table 3.1.17).

The lack of an observable relationship between neopterin and CVD death is further identified by the Cox proportional analysis. No significant increase in prevalence of CVD death was observed in any of the variables included in the analysis (Table 3.1.18). The dataset therefore does not support the use of neopterin alongside age at baseline, alcohol consumption and BNP as a predictive marker of CVD death in patients post-recovery from a CVD event.

7,8NP survival analysis

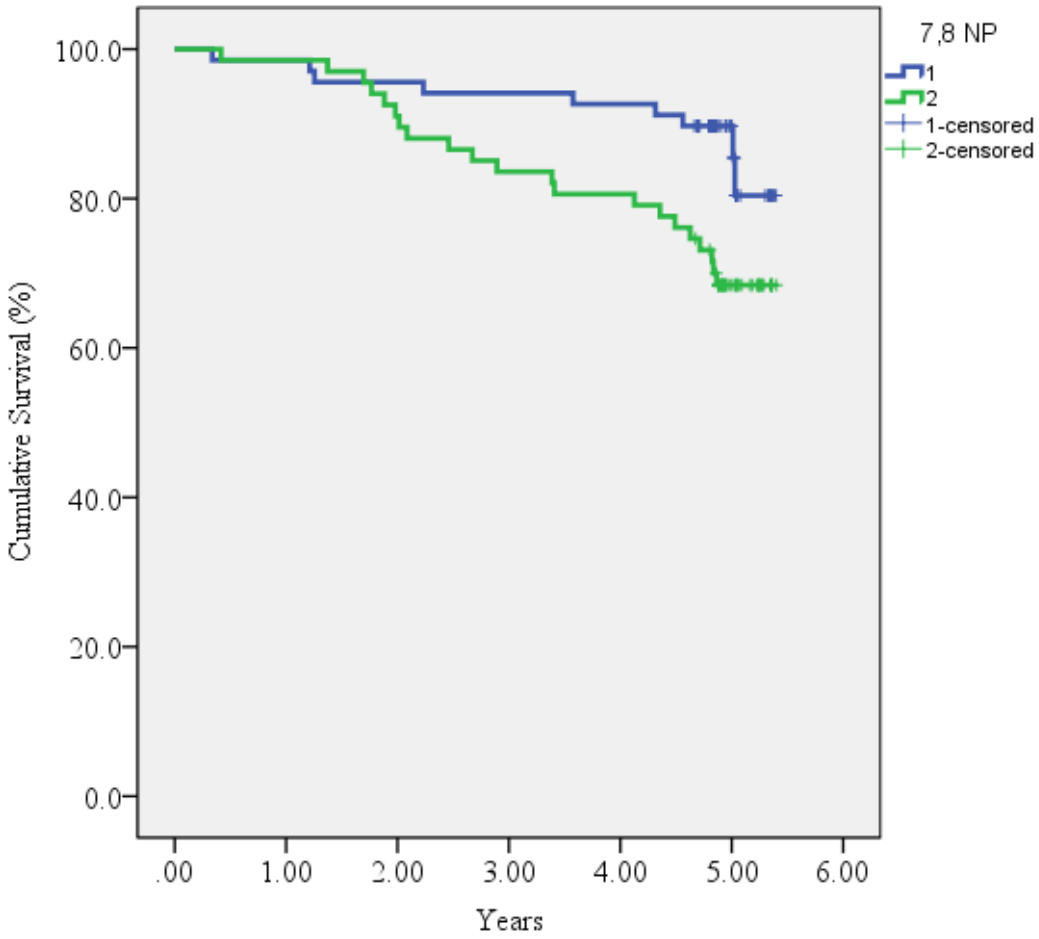

Fig 3.1.8. 7,8 NP ACD Kaplan-Meier analysis. Cumulative survival of CDCS patients with above (2, green) and below (1, blue) median 7,8 NP (66.2224 nM) levels over a 5.4 year period. 1 and 2 censored represents patients who were lost to follow-up.

	Chi-Square	df	Sig.
Log Rank	5.343	1	.021
Breslow	6.335	1	.012
Tarone-Ware	6.071	1	.014

Table 3.1.19. Test for equality of survival distributions for the different levels of 7,8 NP.

	Coefficient	SE	Sig.	Hazard ratio	95.0% CI for Hazard Ratio	
					Lower	Upper
BNP	.889	.636	.162	2.434	.700	8.458
Drinks per week	.970	.560	.083	2.638	.880	7.906
Age at baseline	.251	.103	.015	1.285	1.050	1.573
7,8NP	1.361	.619	.028	3.899	1.159	13.124

Table 3.1.20. Cox proportional hazards model for ACD vs 7,8 NP, drinks per week, BNP and age at baseline. A model of time to ACD based on the value of the covariates BNP, drinks per week, Age at baseline and 7,8NP. Median separation points being 66.2 nM, 9.0 drinks, 34.1 pg/ml and 68.8 years for 7,8NP, drinks per week, BNP and age at baseline respectively.

Over the 5.4 year follow up period patients, with 7,8NP levels above the median value of 66.2 nM, experienced a significantly higher rate of mortality. As identified, by the Kaplan-Meier analysis, patients in the higher plasma 7,8NP group were significantly more likely to die within the follow up period (Fig. 3.1.8) highlighting its potential prognostic utility in patients after recovery from a CV event. This is further supported by the Log-rank, Breslow and Tarone-Ware analyses, providing evidence that differences, between above and below median levels of 7,8 NP, in the incidence of ACD, are significant ($p<0.05$) across the 5.4 year period (Table. 3.1.19).

Of the four covariates BNP, age at baseline, alcohol consumption and 7,8NP only 7,8NP and age at baseline were significantly associated with ACD (Table 3.1.20), with hazard ratios of 3.899 and 1.285 respectively. Therefore 7,8NP shows prognostic promise, for its capability to predict ACD, in patients post-CV event in conjunction with the covariate age at baseline. On the other hand, BNP and alcohol consumption did not significantly fit the Cox proportional regression model ($P>0.05$).

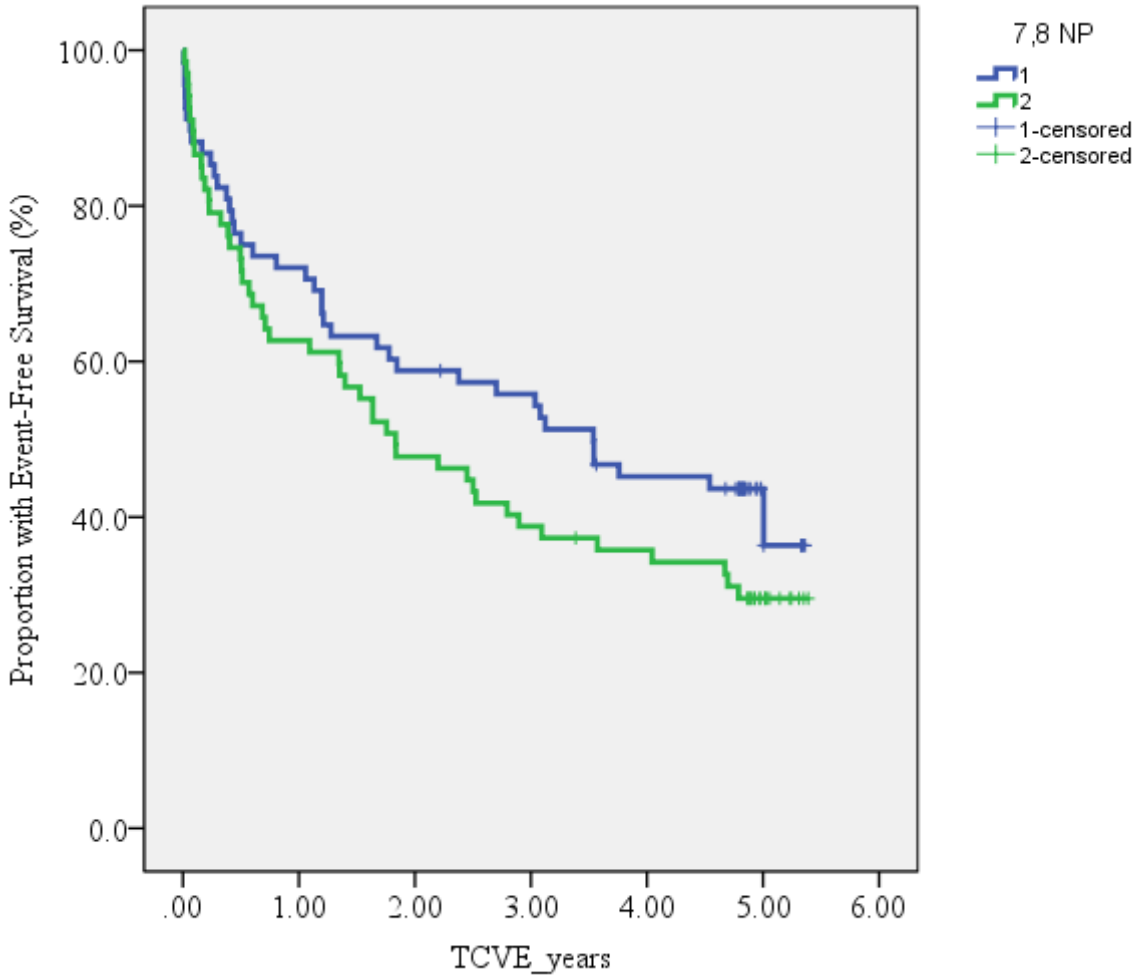

Fig 3.1.9. 7,8 NP TCVE Kaplan-Meier analysis. TCVE in CDCS patients with above (2, green) and below (1, blue) median 7,8 NP (66.2 nM) levels over a 5.4 year period. 1 and 2 censored represents patients who were lost to follow-up.

	Chi-Square	df	Sig.
Log Rank	2.027	1	.155
Breslow	1.692	1	.193
Tarone-Ware	1.951	1	.162

Table 3.1.21. Test for equality of TCVE distributions for the different levels of 7,8 NP.

	Coefficient	SE	Sig.	Hazard ratio	95.0% CI for Hazard Ratio	
					Lower	Upper
BNP	.190	.328	.563	1.209	.636	2.297
Drinks per week	.485	.298	.103	1.625	.907	2.912
Age at baseline	.110	.055	.047	1.116	1.001	1.244
7,8 NP	.188	.302	.533	1.207	.667	2.184

Table 3.1.22. Cox proportional hazards model for TCVE vs 7,8 NP, drinks per week, BNP and age at baseline. A model of time to TCVE based on the value of the covariates BNP, drinks per week, Age at baseline and 7,8NP. Median separation points being 66.2 nM, 9.0 drinks, 34.1 pg/ml and 68.8 years for 7,8NP, drinks per week, BNP and age at baseline respectively.

Although a difference in TCVE was observed, between patients with above and below median levels in a Kaplan-Meier analysis, 7,8NP was not shown to be significantly associated with TCVE (Fig. 3.1.9.). Across the 5.4 year period no significant association was made between TCVE and 7,8NP as highlighted by the log rank, Breslow and Tarone-Ware analyses (Table 3.1.21). Therefore, its predictive capabilities in determining incidence of CV events are not supported.

When associated with BNP, alcohol consumption and age at baseline in the same Cox proportional regression model only age at baseline was shown to be significant ($P<0.05$) with a hazard ratio of 1.116. Both of the markers of interest, BNP and 7,8NP and the alcohol consumption covariate, were not shown to significantly fit the model. Therefore, in the same model, 7,8NP, alcohol consumption and BNP are not indicated as predictive markers with respect to TCVE in patients post recovery from a CVD event (Table 3.1.22). This result, along with the insignificant Kaplan-Meier analysis, suggests that although 7,8NP, like total neopterin, may be a significant prognostic marker of ACD, it is not significantly associated with incidence of TCVE alone or in combination with BNP and alcohol consumption.

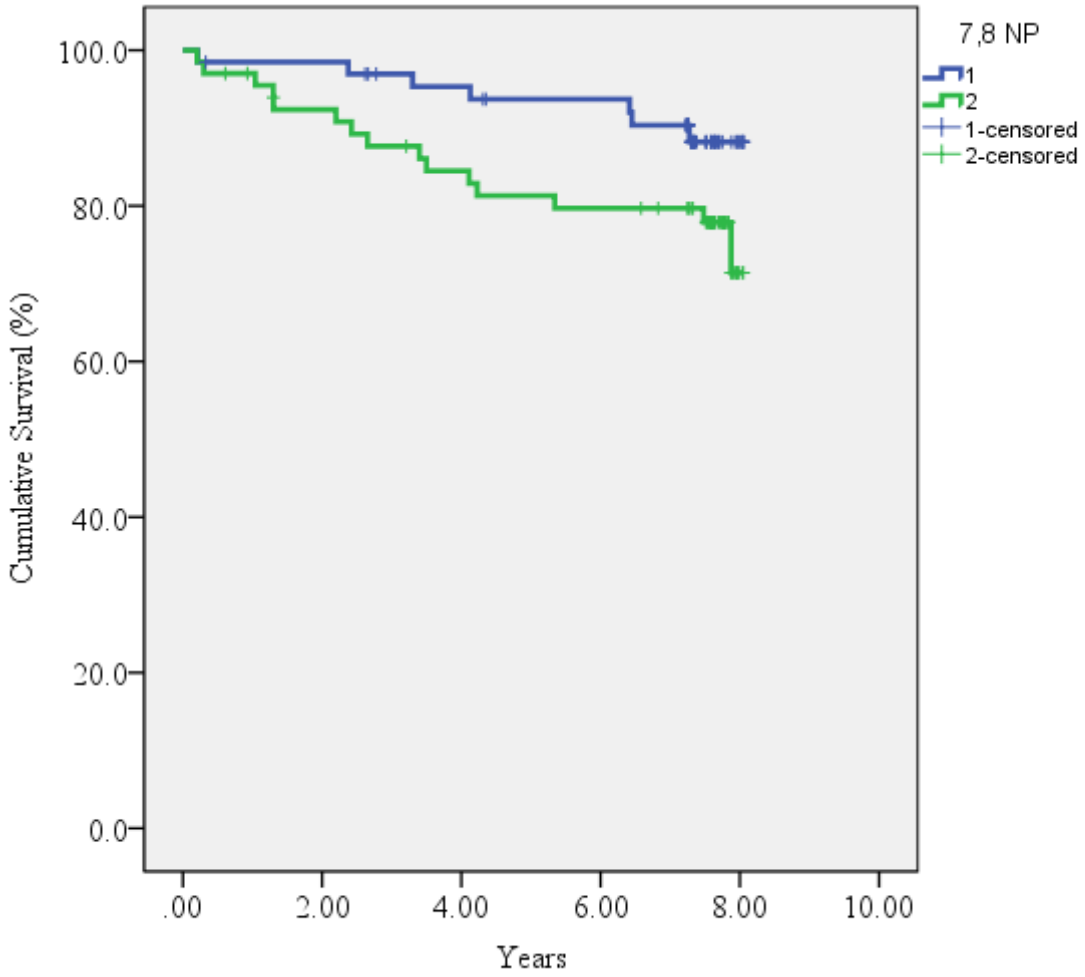

Fig 3.1.10. 7,8 NP CVD death Kaplan-Meier analysis. CVD death in CDCS patients with above (2, green) and below (1, blue) median 7,8 NP (66.2224 nM) levels over a mean 5.4 year period. 1 and 2 censored represents patients who were lost to follow-up.

	Chi-Square	df	Sig.
Log Rank	3.192	1	.074
Breslow	3.090	1	.079
Tarone-Ware	3.088	1	.079

Table 3.1.23. Test for equality of CVD death distributions for the different levels of 7,8 NP.

	Coefficient	SE	Sig.	Hazard ratio	95.0% CI for Hazard Ratio	
					Lower	Upper
BNP	.684	.556	.219	1.981	.666	5.889
Drinks per week	-.213	.520	.683	.808	.292	2.241
Age at baseline	.167	.095	.078	1.182	.981	1.423
Dihydroneopterin	1.162	.540	.032	3.197	1.108	9.220

Table 3.1.24. Cox proportional hazards model for CVD death vs 7,8 NP, drinks per week, BNP and age at baseline. A model of time to CVD death based on the value of the covariates BNP, drinks per week, Age at baseline and 7,8NP. Median separation points being 66.2 nM, 9.0 drinks, 34.1 pg/ml and 68.8 years for 7,8NP, drinks per week, BNP and age at baseline respectively.

Similar results were observed in the survival analysis of 7,8NPs relationship to CVD death that were observed in total neopterins relationship to CVD death. Although a difference in CVD death, between patients with above and below median levels of total neopterin, was observed, over the 5.4 year follow up period (Fig 3.1.10), this difference was not found to be significant at any point in the analysis ($P>0.05$) (Table 3.1.23). Therefore, its predictive capability in determining incidence of CVD death was not supported by this dataset.

No significant predictive capabilities were identified for BNP or alcohol consumption in determining incidence of CVD death ($P>0.05$). Age at baseline and 7,8NP however, did indicate significant predictive capabilities. From the Cox proportional regression model it can be observed that patients with an above median level of 7,8NP have a 3.2 fold greater chance of death from CVD over the 5.4 year follow up period. Furthermore this hazard ratio, as well as the hazard ratio for age at baseline, was significant ($P<0.05$) (Table 3.1.24). Therefore the capabilities of 7,8NP alongside age at baseline, in predicting CVD death, are supported by this dataset.

sFlt-1 survival analysis

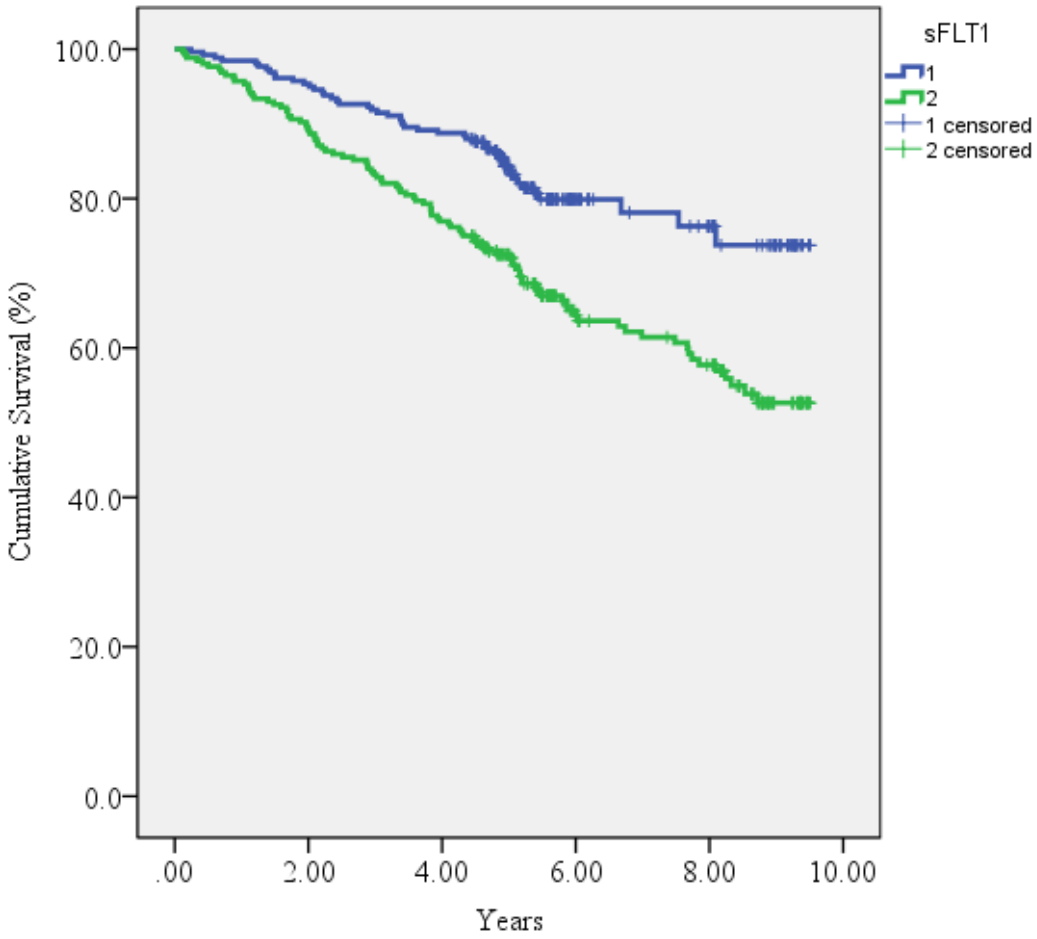

Fig 3.1.11. sFlt-1 ACD Kaplan-Meier analysis. Cumulative survival of CDCS patients with above (green) and below (blue) median sFlt-1 (117.2607 pg/ml) levels over a 4000 day (10 year) period. 1 and 2 censored represents patients who were lost to follow-up.

	Chi-Square	df	Sig.
Log Rank	15.738	1	.000
Breslow	14.949	1	.000
Tarone-Ware	15.414	1	.000

Table 3.1.25. Test for equality of survival distributions for the different levels of sFlt-1.

	Coefficient	SE	Sig.	Hazard ratio	95.0% CI for Hazard Ratio	
					Lower	Upper
BNP	.400	.231	.084	1.492	.948	2.348
Drinks per week	.224	.208	.282	1.251	.832	1.883
Age at baseline	.325	.046	.000	1.384	1.265	1.515
sFlt-1	.688	.229	.003	1.990	1.270	3.120

Table 3.1.26. Cox proportional hazards model for ACD vs sFlt-1, drinks per week, BNP and age at baseline. A model of time to ACD based on the value of the covariates BNP, drinks per week, Age at baseline and sFlt-1. Median separation points being 117.26 pg/ml, 9.0 drinks, 34.1 pg/ml and 68.8 years for sFlt-1, drinks per week, BNP and age at baseline respectively.

It is observable from the Kaplan-Meier analysis of ACD that patients with above median levels of sFlt-1 have a drastic increase in ACD compared to patients with below median sFlt-1 levels (Fig 3.1.11). Across the 10 year period a highly significant association was made between ACD and sFlt-1, at all time points in the analysis, as highlighted by the log rank, Breslow and Tarone-Ware analyses ($P<0.01$) (Table. 3.1.25). sFlt-1's prognostic capacity in determining all cause death post-recovery from a CVD event, is therefore highly supported by this dataset.

The prognostic capacity of sFlt-1 is further supported by its significant prognostic utility in conjunction age at baseline (Fig 3.1.25). Age at baseline and sFlt-1 were all shown to be significantly associated with ACD ($P<0.01$) with hazard ratios of 1.38 and 2.00 respectively indicating that patients with above median levels of sFlt-1 were twice as likely to die over the 10 year follow up period (Table 3.1.26). The same cannot be said for BNP and drinks per week, which were shown to be insignificant ($P>0.05$), with respect to the Cox proportional regression for ACD. Therefore, the use of sFlt-1, alone or alongside age at baseline, for determining potential risk of ACD post-recovery from a CVD event is highly supported by this dataset.

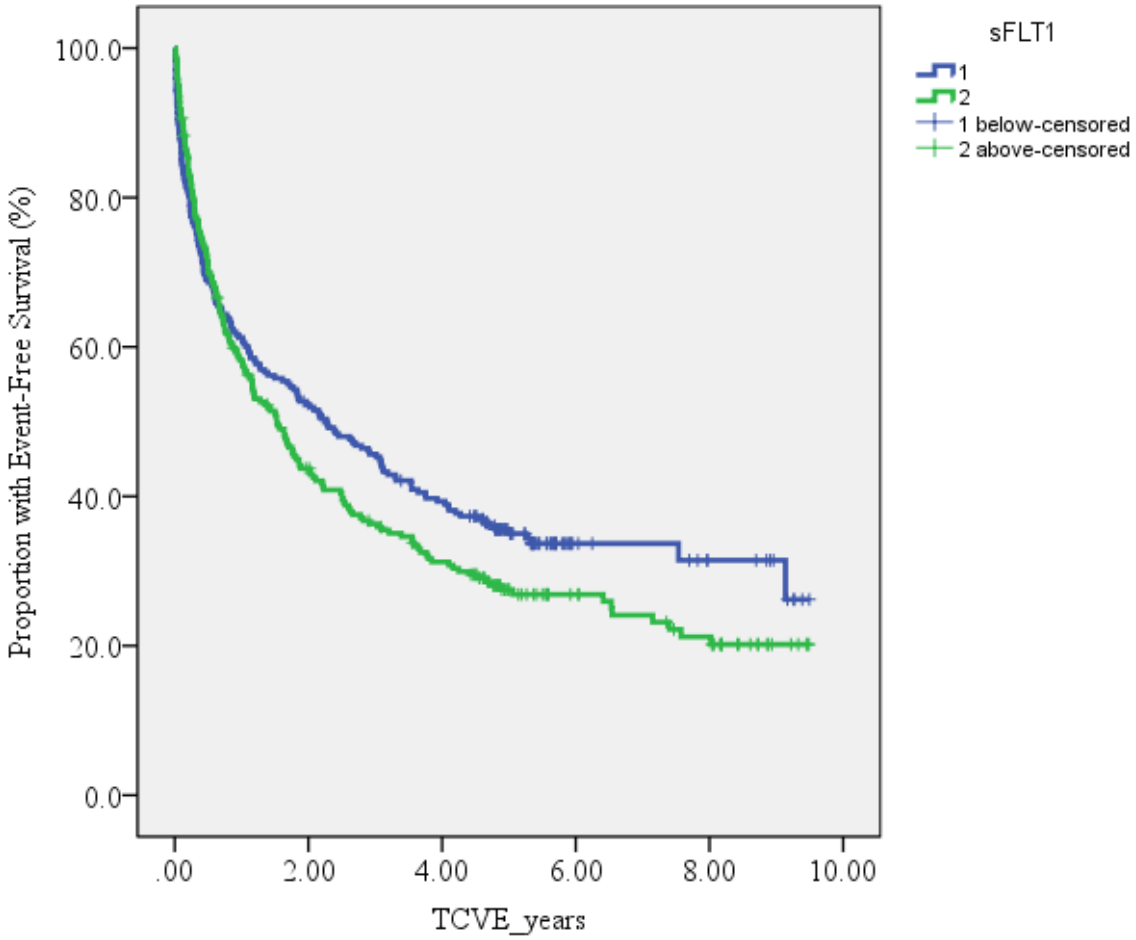

Fig 3.1.12. sFlt-1 TCVE Kaplan-Meier analysis. TCVE in CDCS patients with above (green) and below (blue) median sFlt-1 (117.2607 pg/ml) levels over a 10 year period. 1 and 2 censored represents patients who were lost to follow-up.

	Chi-Square	df	Sig.
Log Rank	2.523	1	.112
Breslow	.670	1	.413
Tarone-Ware	1.470	1	.225

Table 3.1.27. Test for equality of TCVE distributions for the different levels of sFlt-1.

	Coefficient	SE	Sig.	Hazard ratio	95.0% CI for Hazard Ratio	
					Lower	Upper
BNP	.163	.141	.247	1.177	.893	1.552
Drinks per week	.150	.130	.250	1.161	.900	1.498
Age at baseline	.107	.025	.000	1.113	1.059	1.170
sFlt-1	.230	.131	.078	1.259	.975	1.627

Table 3.1.28. Cox proportional hazards model for TCVE vs sFlt-1, drinks per week, BNP and age at baseline. A model of time to TCVE based on the value of the covariates BNP, drinks per week, Age at baseline and sFlt-1. Median separation points being 117.26 pg/ml, 9.0 drinks, 34.1 pg/ml and 68.8 years for sFlt-1, drinks per week, BNP and age at baseline respectively.

Over the initial 3 year follow up period approximately 60 percent of patients with both above and below median levels of sFlt-1 experienced CV events at almost the same rate. However, after this initial 3 year period, patients with a higher than median level of sFlt-1 experienced a higher incidence of CV events (Fig 3.1.12). Although patients expressing higher levels of sFlt-1 did eventually experience more CV events this was not shown to be significant in comparison to below median levels across the 10 year follow up period (Table 3.1.27).

When sFlt-1s utility in determining TCVE was analysed in a Cox proportional regression model, alongside BNP, alcohol consumption and age at baseline, its predictive utility trended towards significance ($p=0.078$) and BNP and alcohol consumption, were shown to be insignificant ($P>0.05$) (Table 3.1.28). Age at baseline however was shown to be a highly significant factor in predicting TCVE risk over the 10 year follow up ($P<0.01$).

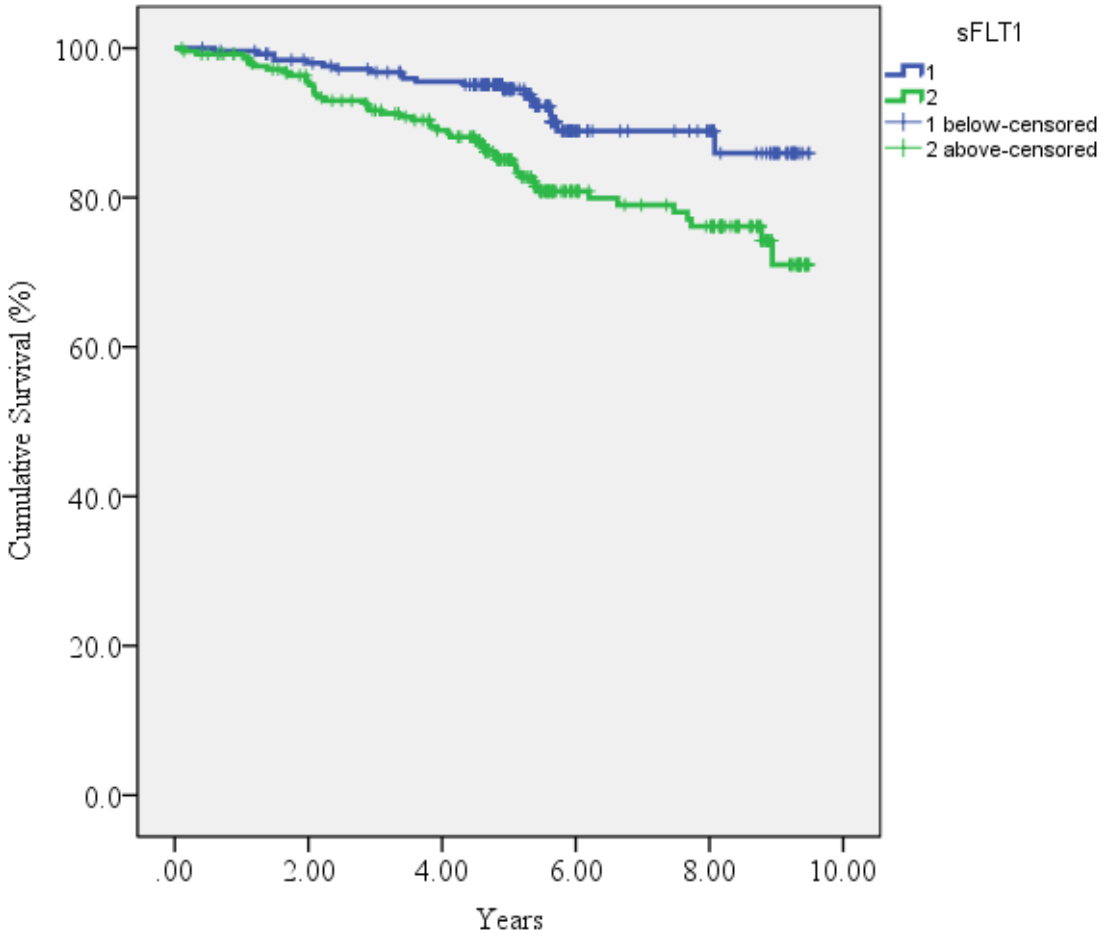

Fig 3.1.13. sFlt-1 CVD death Kaplan-Meier analysis. CVD death in CDCS patients with above (green) and below (blue) median sFlt-1 (117.2607 pg/ml) levels over a 10 year period. 1 and 2 censored represents patients who dropped out for reasons unrelated to the study or were lost track of.

	Chi-Square	df	Sig.
Log Rank	10.948	1	.001
Breslow	11.704	1	.001
Tarone-Ware	11.573	1	.001

Table 3.1.29. Test for equality of CVD death distributions for the different levels of sFlt-1.

	Coefficient	SE	Sig.	Hazard ratio	95.0% CI for Hazard ratio	
					Lower	Upper
BNP	.743	.320	.020	2.102	1.121	3.939
Drinks per week	.267	.275	.332	1.305	.762	2.236
Age at baseline	1.838	.373	.000	6.286	3.024	13.065
sFlt-1	.607	.308	.049	1.835	1.003	3.356

Table 3.1.30. Cox proportional hazards model for CVD death vs sFlt-1, BNP, drinks per week and age at baseline. A model of time to TCVE based on the value of the covariates BNP, drinks per week, Age at baseline and sFlt-1. Median separation points being 117.26 pg/ml, 9.0 drinks, 34.1 pg/ml and 68.8 years for sFlt-1, drinks per week, BNP and age at baseline respectively.

Incidence of CVD death was found significantly more in patients with above, compared to below, median levels of sFlt-1 (Fig 3.1.13.). The highly significant association between above median levels of sFlt-1 and ACD can therefore be attributed to CVD death. This result is further highlighted by the Log rank, Breslow and Tarone-Ware analyses of the Kaplan-Meier trend. All three analyses show that sFlt-1 is significantly associated to CVD death at any time over the 10 year follow up period (Table 3.1.29).

sFlt-1 was also shown, in the Cox proportional regression model, to have significant predictive utility in determining the risk of CVD death. Furthermore all of the other included covariates, with the exception of alcohol consumption, showed significant utility for determining the risk of CVD death (Table 3.1.30). Overall the results of The Kaplan Meier analysis and Cox proportional regression model provide compounding support for the predictive utility of sFlt-1. Indicating that when analysed alone, and in combination with the other significant covariates, sFlt-1 has a strong association with CVD death in patients post recovery from a CVD event.

3.2 Carotid endarterectomy cohort

Carotid endarterectomy plasma and plaque were analysed to determine the levels of pterins and sFlt-1, in patients with known atherosclerotic lesions, and to assess the capability of the plaque itself to produce these biomarkers. Plaque and blood samples from the endarterectomy cohort were obtained immediately prior to the carotid endarterectomy procedure at Christchurch Hospital, by Prof Justin Roake and associates of the Vascular Surgery Department (Refer to table 6.1 in Appendix for patient's plaque summary and 6.2 for individual patient plasma summary). Extracted plasma was analysed for sFlt-1, neopterin, 7,8NP and total neopterin. Atherosclerotic plaques were removed and immediately cultured, prior to assessment, or stored at -80 ˚C (refer to Methods section 2.2). Control patient plasma was donated by the Christchurch Heart Institute (Control patient plasma summarised in table 6.3 in appendix).

Variable	Min	Max	Mean	Mean Male	Mean Female	N Male	N Female
Neopterin (nM)	6.18	57.03	25.76±2.18	25.17±2.95	27.09±2.74	8	18
7,8NP (nM)	7.10	46.02	24.54±2.11	25.24±2.84	22.95±2.60	8	18
Total neopterin (nM)	23.25	81.58	50.30±3.01	50.41±4.21	50.05±2.86	8	18
sFlt-1 (pg/ml)	2.00	20453.00	8932.11±1121.83	9154.05±1424.68	8405.00±1823.17	8	19

Table 3.2.1. General Summary of endarterectomy patient's plasma. The data presented shows mean±SEM.

3.2.1 Plasma analysis

The plasma from the endarterectomy cohort was compared to age and gender matched control samples. The process was primarily carried out to confirm whether patients with carotid atherosclerotic plaque carried higher concentrations of the biomarkers than healthy individuals. Also, using this method, levels observed between genders or age groups were compared to identify whether elevated levels could be a result of these factors.

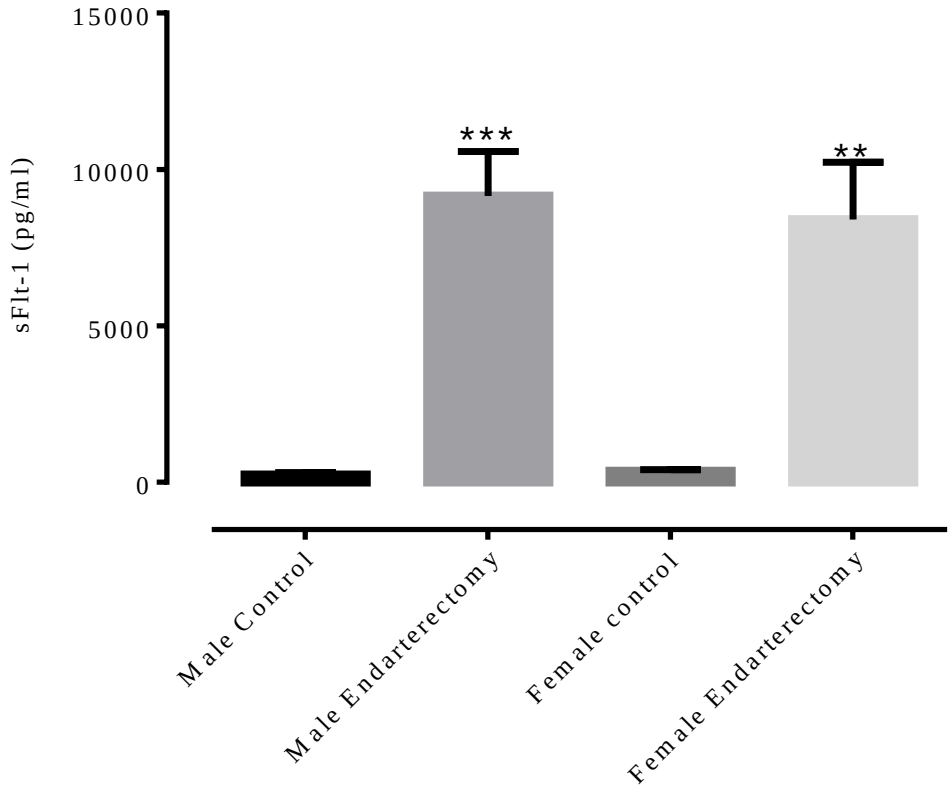

Fig 3.2.1. sFLT-1 measured in endarterectomy plasma versus age and gender matched control plasma. Error bars exhibit mean+SEM. Male N=19 (***=p<0.001), Female N=8 (**=p<0.01). Tukey post-hoc indicates levels of sFLT-1 are not significantly different across age groups or between gender groups (p>0.05).

Analysis of the endarterectomy patient plasma indicated a significant difference in sFlt-1 levels between healthy controls (n=24, Male=240±71 pg/ml, Female=355±52 pg/ml) and patients with advanced atherosclerotic lesions in the carotid artery (n=27, Male=1945±1425 pg/ml, Female=8404±1823 pg/ml) (Fig 3.2.1). No significant difference in sFlt-1 levels were observed between the genders or patients of different age groups (p>0.05), indicating that

higher levels of sFlt-1 in the atherosclerotic lesion patients occurred regardless of age and gender.

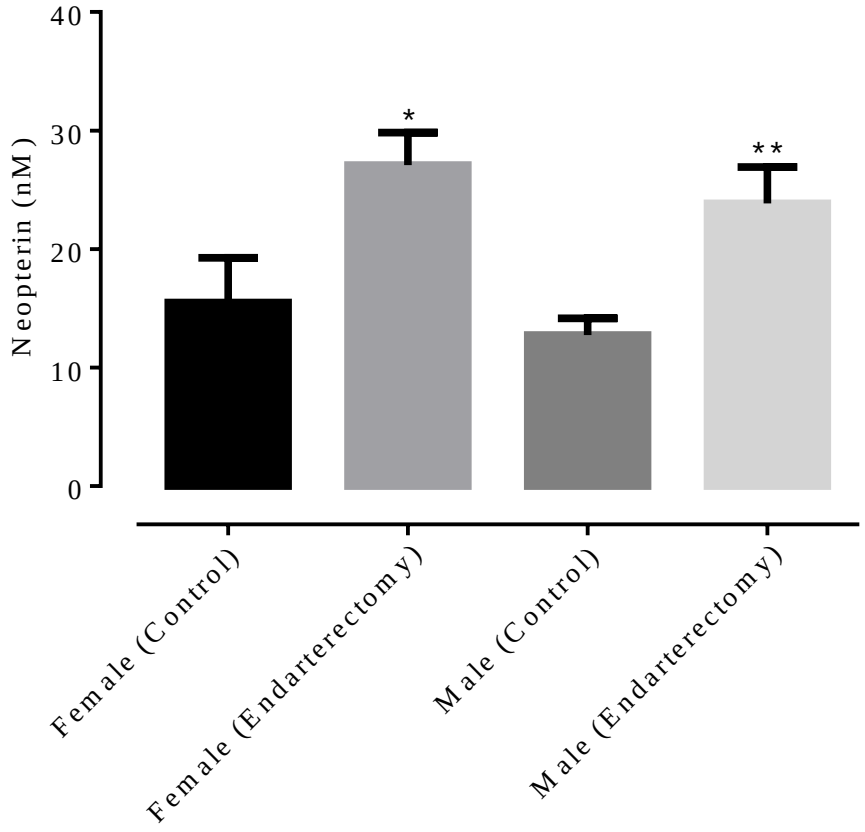

Fig 3.2.2. Neopterin measured in endarterectomy plasma vs age and gender matched control plasma. Error bars exhibit mean+SEM. Male N=18 (*= $p<0.05$), Female N=8 (**=$p<0.01$). Turkey post-hoc indicates levels of neopterin are not significantly different across age groups or between gender groups ($p>0.05$).

Levels of neopterin, measured in the endarterectomy patient cohort (n=26, Male=23.9±3.1 nM, Female=27.1±2.7nM) were significantly higher than those measured in age and gender matched controls (n=27, Male=12.8±1.4 nM, Female=15.5±3.8 nM) (Fig. 3.2.2), indicating that the elevated levels of neopterin were not attributed to either the gender or the age of the patients.

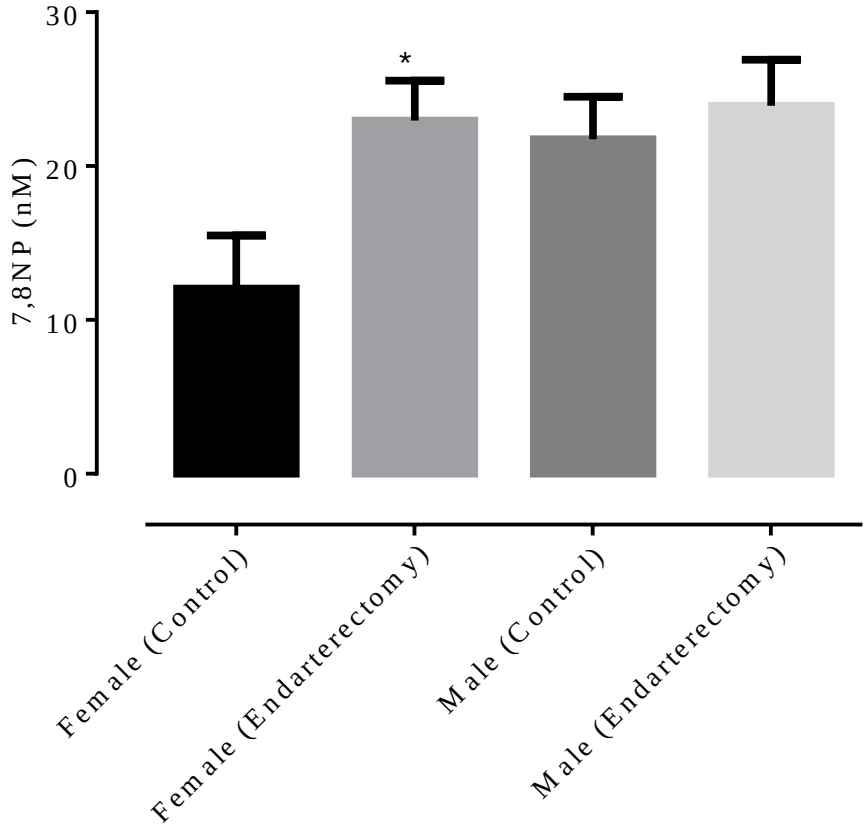

Fig 3.2.3. 7,8NP measured in endarterectomy plasma vs age and gender matched control plasma. Error bars display Mean+SEM. Male N=18 ($p>0.05$), Female N=8 (*=$p<0.05$). Tukey post-hoc analysis indicates a significant difference between the gender group controls ($P<0.05$).

Significantly higher Levels of 7,8NP were observed in females with advanced atherosclerotic lesions (23±2.6 nM) than in healthy control females (12±3.5 nM). Suggesting that females with advanced carotid atherosclerotic lesions experience higher levels of macrophage activation (Fig. 3.2.3).

Levels of 7,8NP measured in the male endarterectomy group (24±3.0 nM) were insignificant when compared to the male healthy control group (21.7±3.0 nM). Furthermore, there was a significant difference between the male and female healthy control levels, indicating that the male healthy controls had higher levels of 7,8 NP compared to females, regardless of whether they had a known carotid lesion or not.

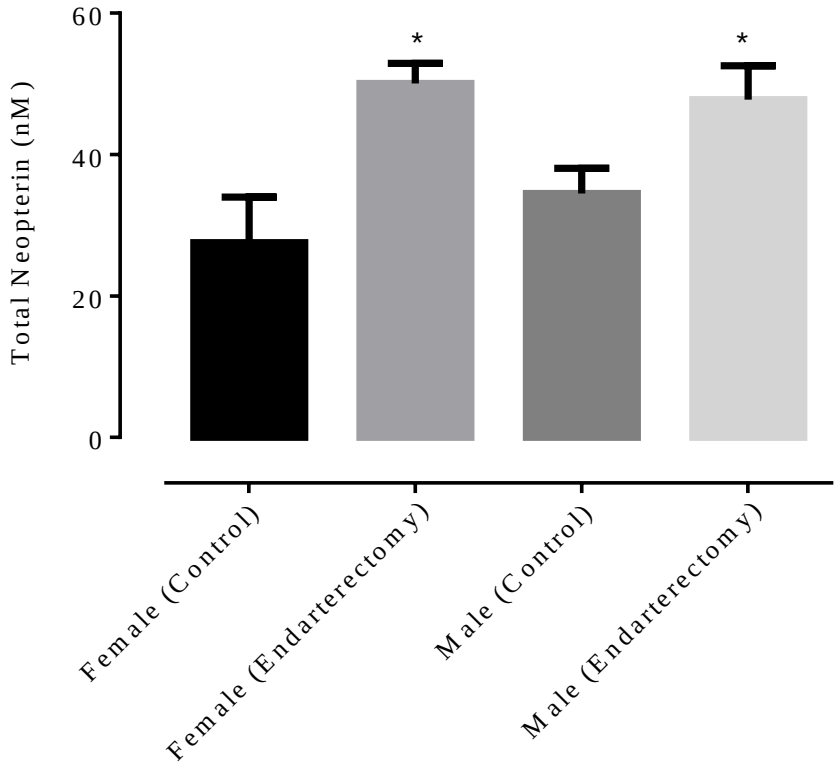

Fig 3.2.4. Total neopterin measured in endarterectomy plasma vs age and gender matched control plasma. Error bars display Mean+SEM. Male n=18 ($p<0.05$), Female n=8 ($p<0.05$). Tukey post-hoc analysis indicates no significant difference between the gender group controls ($p<0.05$).

Levels of total neopterin were significantly elevated for both males (48±3.0) and females (50±3.0 nM) in comparison to healthy age and gender matched controls (Female=27.5±6.5 nM, Males=34.5±3.5 nM) (Fig 3.2.4). The elevated levels of neopterin were not attributed to either the gender or the age of the patients, as the difference between the genders and age groups weren't significant ($p>0.05$).

3.2.2 Correlations

As levels of all the pterins and sFlt-1 were elevated, assesments were made to identify a possible correlation between the markers. In order to assess the possible association between levels of sFlt-1 and the pterins, in the plasma of the endarterectomy patients, a bivariate analysis was used.

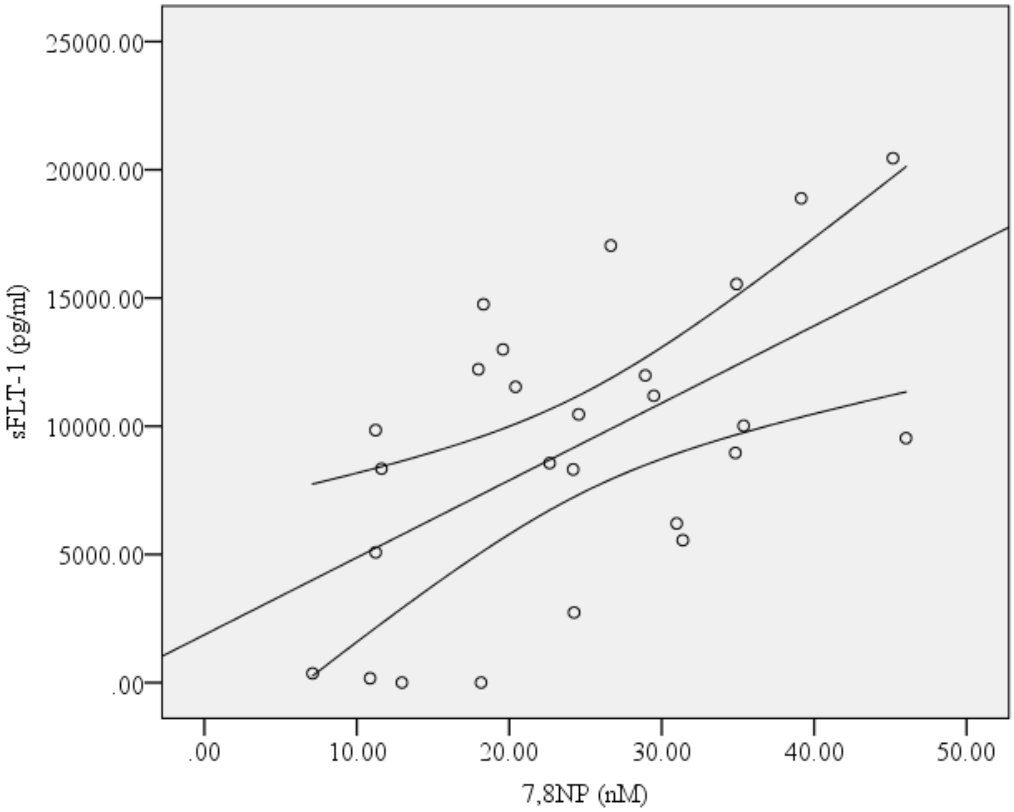

Fig 3.2.5. Bivariate analysis of sFlt-1 VS 7,8NP in endarterectomy patient plasma. n=27 sFlt-1, n=26 7,8NP, R^2=0.323, p=0.002, 95% Mean confidence intervals.

A statistically significant ($p<0.01$) positive correlation was observed between sFlt-1 and 7,8NP (Fig 3.2.5), indicating a potential association between the two markers. The correlation model accounts for 32.3% of the dataset (R^2=0.323), suggesting that much of the variation in the data isn't explained by the relationship.

The same positive relationship between sFlt-1 and 7,8NP was not observed in the healthy control group plasma ($p>0.436$, R^2=0.029).

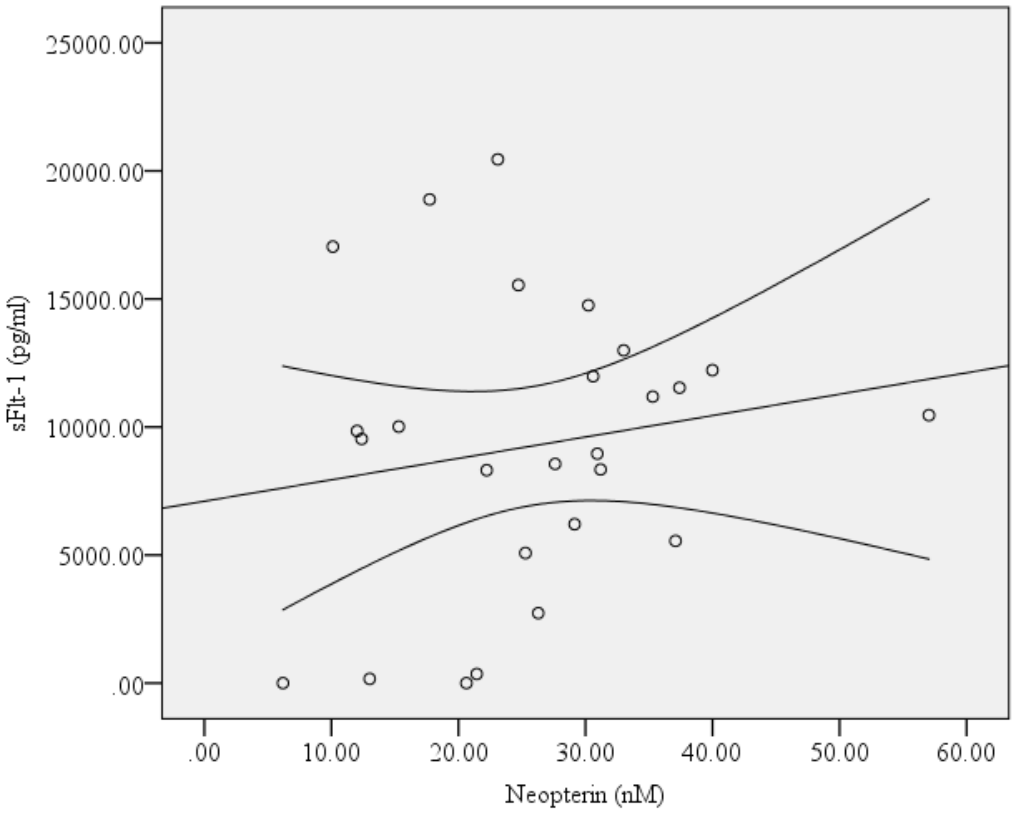

Fig 3.2.6. Bivariate analysis of sFlt-1 VS neopterin in endarterectomy patient plasma. n=27 sFlt-1, n=26 neopterin, R^2=0.027, p=0.424, 95% Mean confidence intervals.

Unlike 7,8NP, neopterin levels do not share any significant positive relationship (p>0.05) with levels of sFlt-1 in endarterectomy patient plasma (Fig 3.2.6).

As the model only accounts for 2.7% of the dataset variation, neopterin doesn't indicate a predictive capacity in determining sFlt-1 levels or vice versa. Even less of a relationship was observed, between levels of sFlt-1 and neopterin, in the healthy patient control group (p>0.05, $R^2=2.9\times10^{-4}$).

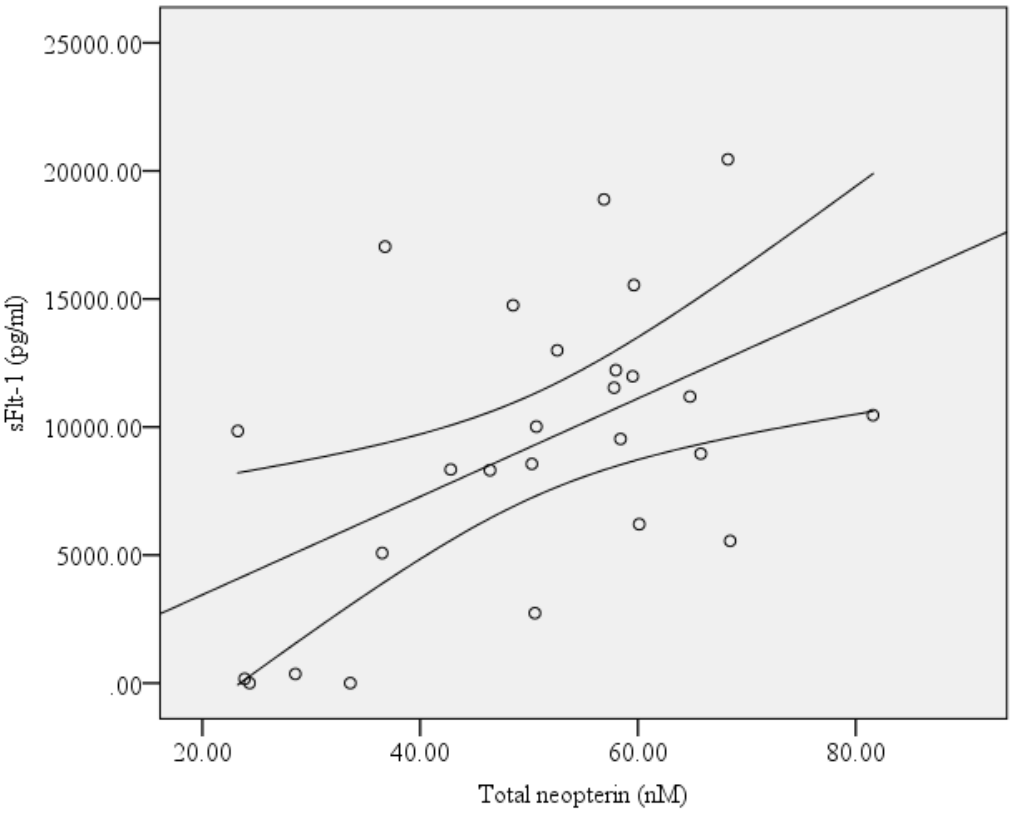

Fig 3.2.7. Bivariate analysis of sFlt-1 VS total neopterin in endarterectomy patient plasma. n=27 sFlt-1, n=26 total neopterin, R^2=0.267, p=0.007, 95% Mean confidence intervals.

A significant (p<0.01) relationship was observed, between levels of sFlt-1 and levels of total neopterin, in plasma from patients in the endarterectomy cohort (Fig 3.2.7). With the model accounting for 26.7% of the dataset (R^2=0.267), much of the variation is unexplained.

There was no significant correlation, between sFlt-1 and total neopterin in the healthy control cohort. Only 3.5% of the data was accounted for by the linear correlation model (R^2=0.035).

3.2.3 IFN-γ treated HMDM analysis (positive control)

In order to confirm the notion, that IFN-γ exerts a stimulatory effect on human macrophages, live cultured human macrophages were administered with IFN-γ. The direct effects of IFN-γ treatment were then assessed in terms of macrophage activation (pterin production) and macrophage health/metabolism (lactate production).

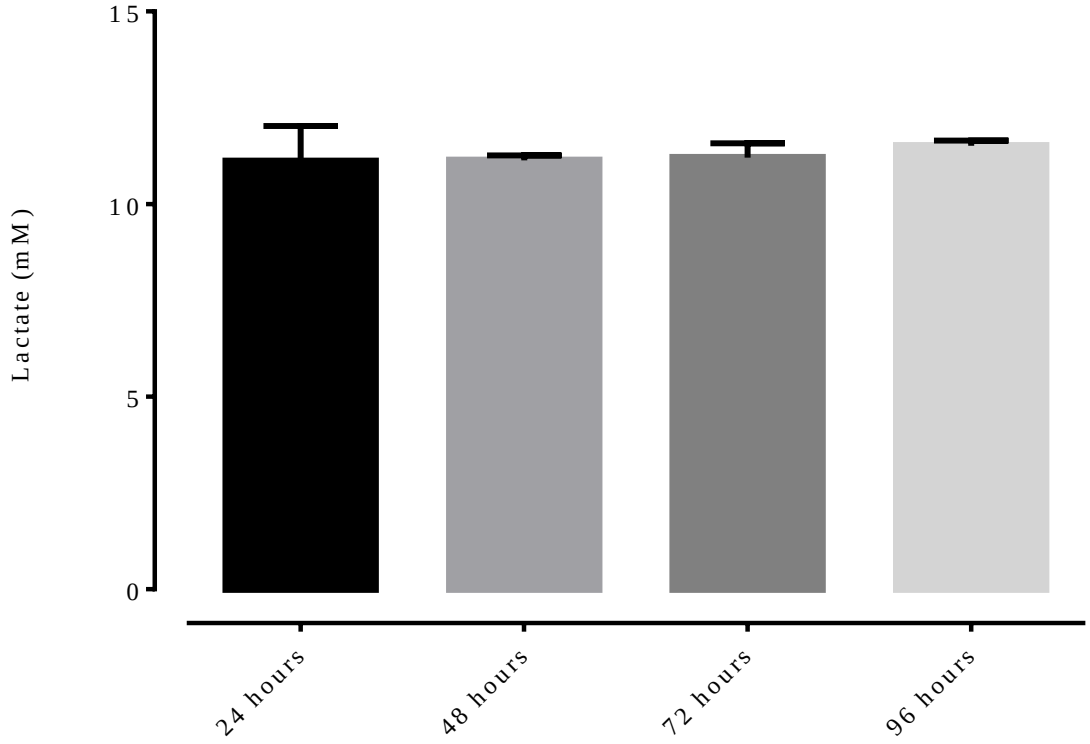

Fig 3.2.8. HMDM vulnerability testing (positive control). 24 hours: no IFN-γ, 48 hours: 105 units IFN-γ /ml, 72 hours: 248 units IFN-γ /ml, 96 hours: 478 units IFN-γ /ml. n= 25×10^6 cells/well (12 wells). Error bars= Mean ± SEM, ($p>0.05$).

Analysis of lactate produced by HMDMs, over the 96 hour period, indicates that neither varying levels of IFN-γ nor time in incubation has decreased the survival of the HMDMs (Fig 3.2.8). Levels of lactate remained stable over the 96 hour period, with no significant decrease ($p>0.05$) from 11.11 ± 1.35mM.

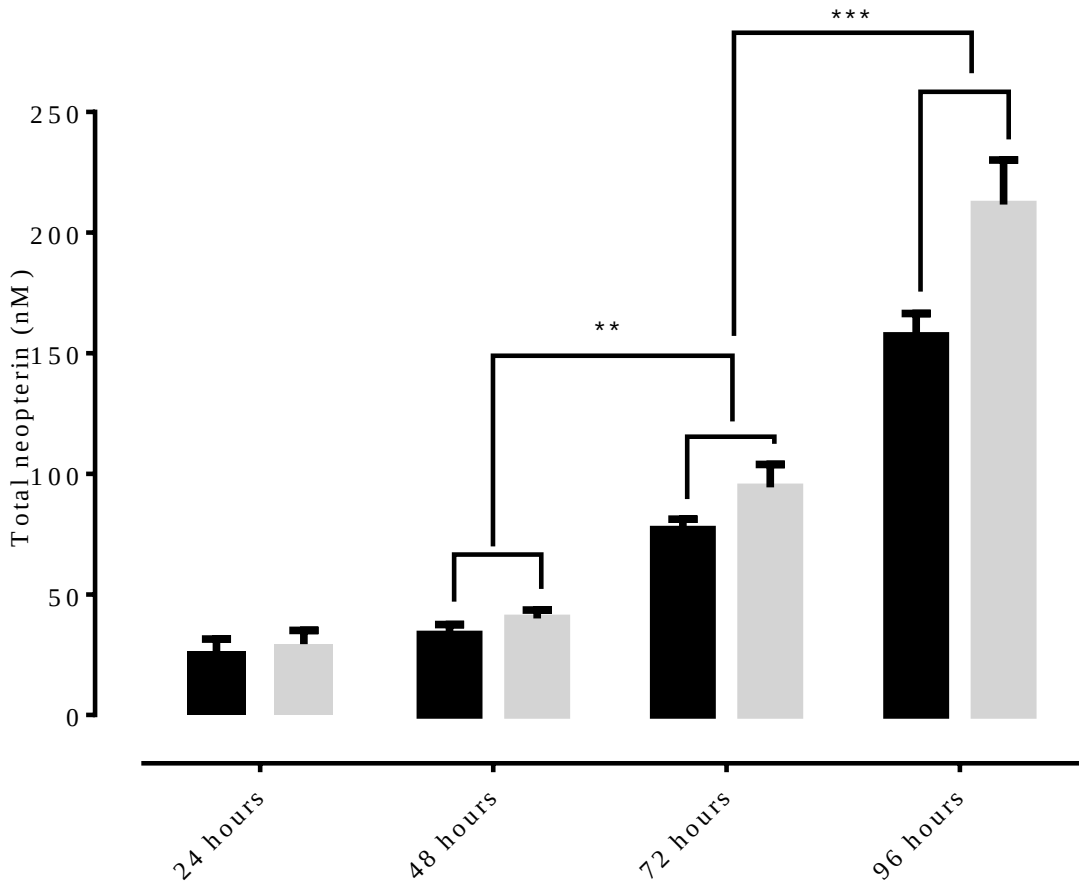

Fig 3.2.9. HMDMs Total neopterin and neopterin production with IFN-γ treatment. Neopterin produced: Black, total neopterin produced: Grey. 24 hours: no IFN-γ, 48 hours: 500 units IFN-γ /ml added, 72 hours: 500 units IFN-γ /ml added. 2 way ANOVA: **= $p<0.01$, ***= $p<0.001$. Error bars= Mean ± SEM.

Levels of total neopterin increased substantially over the 96 hour time course with increasing doses of IFN-γ (Fig 3.2.9). Total neopterin levels significantly increased between the 48 hour and 72 hour period. An increase of greater significance was then observed between the 72 hour and 96 hour periods.

Neopterin levels also increased substantially with increasing doses of IFN-γ over the 96 hour period (Fig 3.2.9). Neopterin levels significantly increased between the 48 hour and 72 hour periods. An increase of greater significance was then observed between the 72 hour and 96 hour periods.

Levels of 7,8NP (the difference between neopterin and total neopterin), on the other hand, did not significantly increase with doses of IFN-γ until 24 hours after the final dose was

administered. At 96 hours of incubation a significant ($p<0.001$) increase in 7,8 NP was observed from 4.12 ± 1.4 to 69.93 ± 1.4 nM.

3.2.4 Dead IFN-γ treated plaque analysis (negative control)

To assess whether plaque culture could actively produce pterin in the absence of live tissue IFN-γ was administered to dead plaque tissue (frozen at -80°C) cultured under the same plaque culture method as the live tissue (refer to Methods 2.4) (Refer to plaque 99 in Appendix Table 6.1)

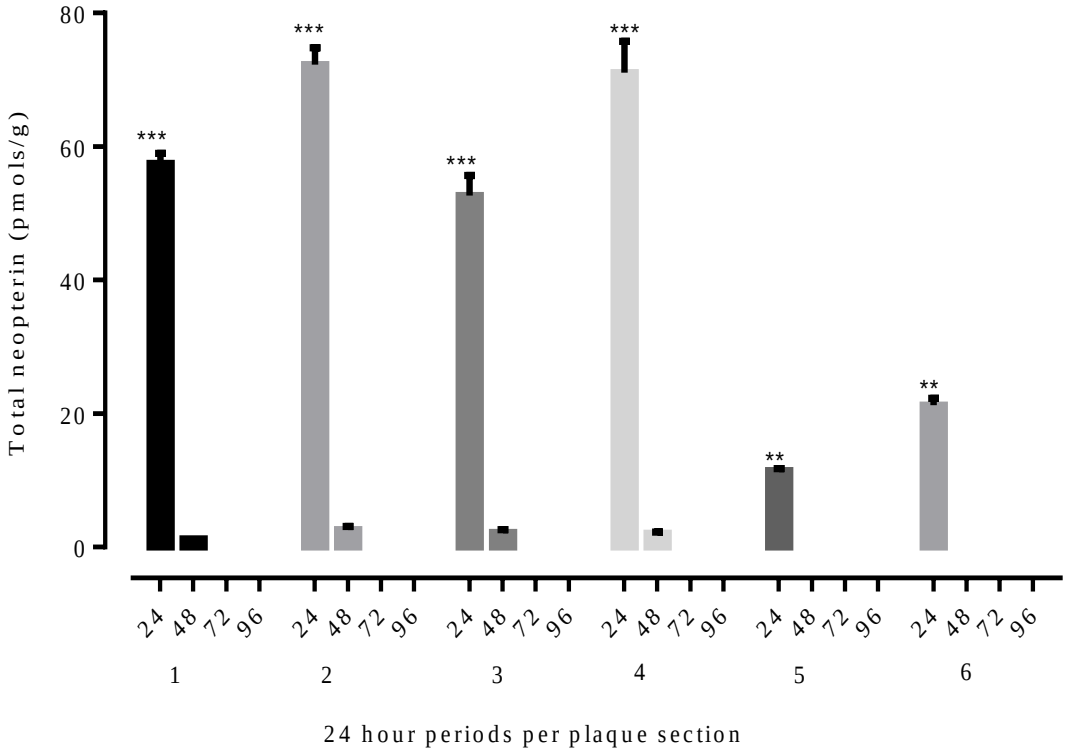

Fig 3.2.10. Dead plaques Total neopterin production with IFN-γ treatment. 2 way ANOVA: **= $p<0.01$, ***= $p<0.001$. Error bars= Mean ± SEM.

A significant decrease in total neopterin was observed in all plaque sections, following the initial 24 hour period of incubation, despite the addition of IFN-γ (Fig 3.2.10).

Plaque sections 1, 2, 3 and 4 experienced the most significant decrease ($p<0.001$) in total neopterin. Plaque sections 5 and 6 also experienced a significant ($p<0.01$) decrease in total neopterin, but not to the same extent as the other sections.

After 72 hours plaque sections 1, 2, 3, 4, 5 and 6 had all decreased to a level below the LOD for the method of measurement.

Levels of 7,8NP and neopterin also both decreased significantly in all plaque sections ($p<0.001$) to a level below the LOD after 72 hours of incubation.

3.2.5 Live untreated plaque analysis

Media from untreated live plaque culture was analysed to determine whether levels of pterin increased without IFN-γ treatment. Using this method the capability of the plaque to self-stimulate inflammatory cell populations, in the absence of IFN-γ, was assessed (Refer to plaque 95 in Appendix Table 6.1).

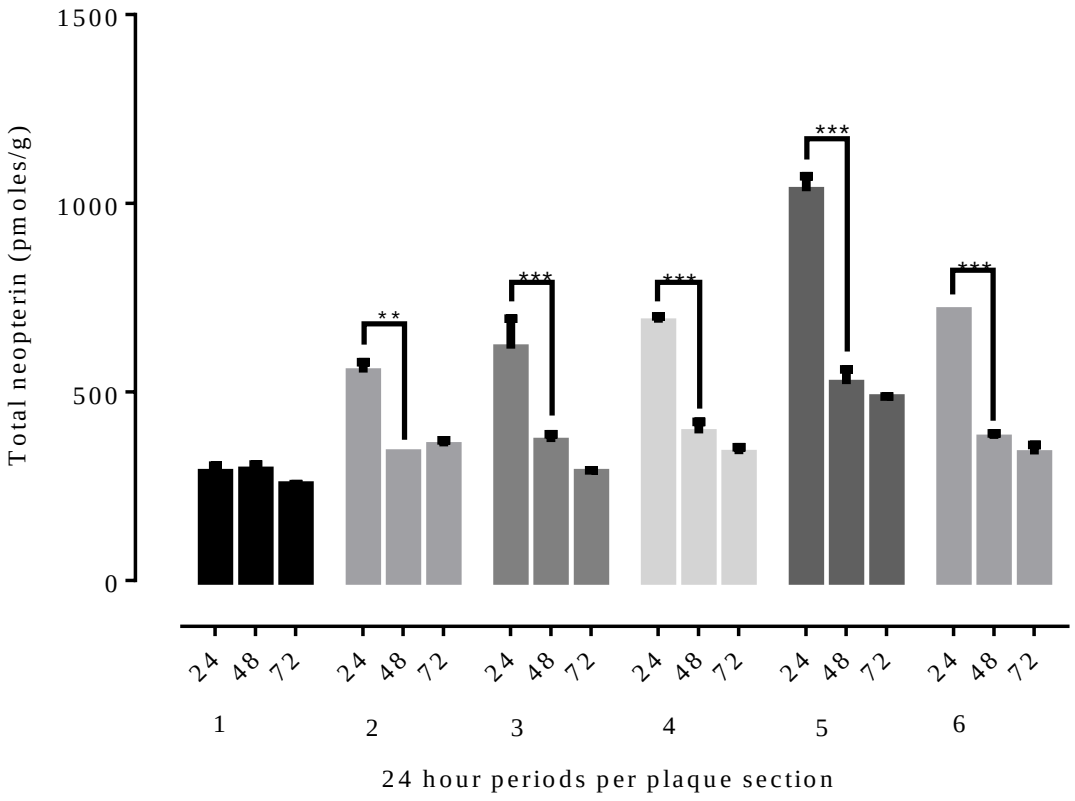

Fig 3.2.11. Total neopterin production per gram of untreated live plaque. 2 way ANOVA: **= $p<0.01$, ***= $p<0.001$. Error bars= Mean ± SEM.

Every plaque section analysed, with the exception of section 1, exhibited a significant decrease in total neopterin levels following the initial 24-hour incubation period (Fig 3.2.11). Following 48 hours of incubation no further significant decrease in total neopterin was observed for any of the plaque sections.

Levels of total neopterin, after the 24-hour incubation period, were significantly lower and significantly higher, in plaque sections 1 and 5 respectively, compared to the other plaque sections.

After 48 hours of incubation levels of total neopterin were not significantly different across the plaque sections, with the exception of plaque section 5, which still had significantly ($p<0.05$) higher levels of total neopterin after both 48 and 72 hours of incubation.

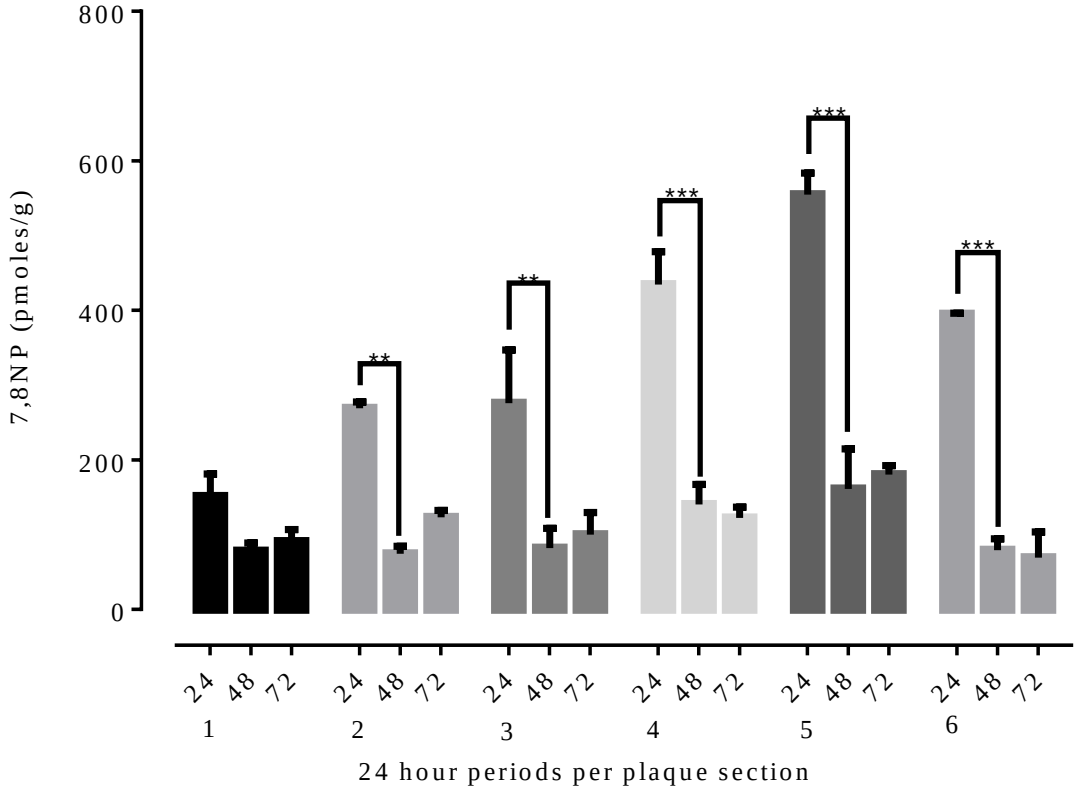

Fig 3.2.12. 7,8NP production per gram of untreated live plaque. 2 way ANOVA: *p=<0.05, **= p<0.01, ***= p<0.001. Error bars= Mean ± SEM.

Levels of 7,8 NP decreased significantly following the initial 24 hour incubation period in all plaque sections, with the exception of section 1, largely mirroring the initial decrease observed in total neopterin levels. Following the 48 hour incubation time levels of 7,8NP were observed to increase slightly. However, this increase wasn't significant ($p>0.05$) (Fig 3.2.12).

Levels of 7,8NP measured after the initial 24 hour incubation were significantly higher, in sections 4 and 5, compared to all other plaque sections. After 48 hours of incubation

however, levels of 7,8NP were not significantly different across any of the plaque sections ($p>0.05$).

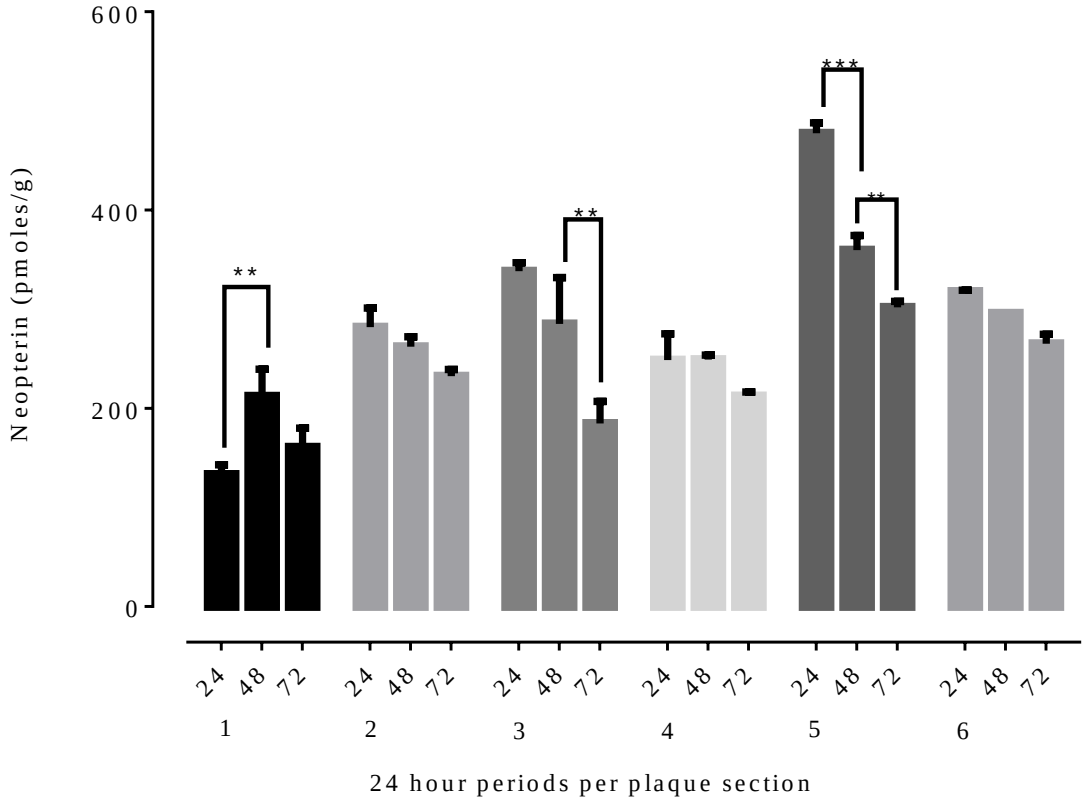

Fig 3.2.13. Neopterin production per gram of untreated live plaque. 2 way ANOVA: *= $p<0.05$, **= $p<0.01$, ***= $p<0.001$. Error bars= Mean ± SEM.

Levels of neopterin decreased or remained stable, after the initial 24-hour incubation period, in all plaque sections with the exception of plaque section 1 which significantly increased (Fig 3.2.13). Of the 6 plaque sections analysed only sections 3 and 5 decreased significantly.

In section 5 a significant decrease was observed following the 24 hour incubation period. A decrease, although less significant, was also observed between the 48 and 72 hour incubation periods. In plaque section 3 a significant decrease in neopterin was only observed between the 48 and 72 hour periods.

The significant difference in neopterin levels, between plaque sections, was observed to decrease over time. After the initial 24-hour incubation period levels of neopterin were

significantly lower in plaque section 1 ($p<0.01$) and significantly higher in plaque section 5 ($p<0.01$) compared to all other plaque sections.

Following the 48-hour incubation period, levels of neopterin were significantly higher in section 5 compared to sections 1, 2, and 4.

After 72-hours of incubation plaque sections 5 and 6 still had significantly higher levels of neopterin in comparison to the other sections 3 and 1.

3.2.6 Live IFN-γ treated plaque analysis

IFN-γ was administered to live plaque sections to determine whether inflammatory cell populations, within the plaque, could be stimulated to produce pterin and therefore contribute to elevated levels observed in the plasma. Furthermore, the effects of IFN-γ on the health of live plaque cells and levels of sFlt-1 were assessed via measurement of lactate and sFlt-1 in the plaque culture media (Refer to plaque 97 in Appendix Table 6.1).

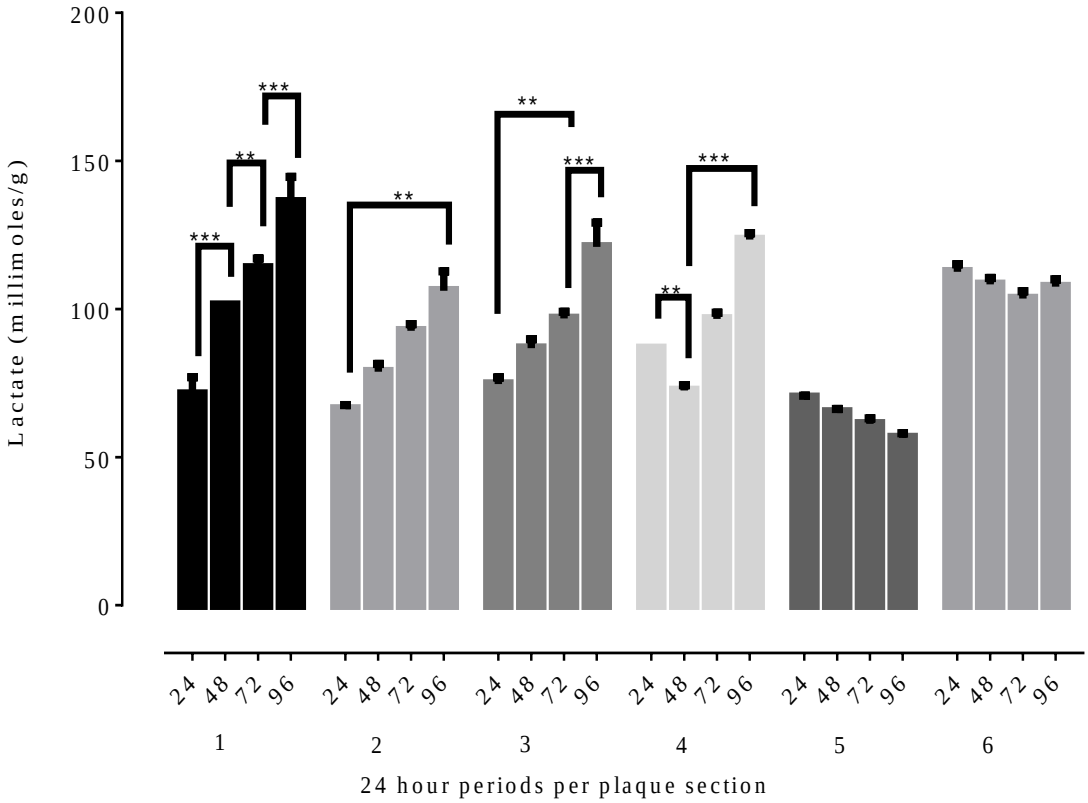

Fig 3.2.14. Lactate produced per gram of IFN-γ treated live plaque. 48 hours: 500 units IFN-γ /ml, 72 hours: 500 units IFN-γ /ml. 2 way ANOVA: *= $p<0.05$, **= $p<0.01$, ***= $p<0.001$. Error bars= Mean ± SEM.

Analysis of lactate produced by plaque sections, treated with 500 units of IFN-γ/ml, indicates that levels increased significantly or remained statistically stable over the course of the IFN-γ treatment (Fig 3.2.14).

Levels of lactate increased significantly in plaque sections 1, 2 and 3 between all incubation time points. Lactate levels, produced by section 4, were initially observed to decrease significantly between the first 24-48 hour periods of incubation, prior to IFN-γ administration. Levels were then observed to significantly increase across the 72 and 96 hour periods. No significant increase or decrease ($p>0.05$) in lactate was observed for sections 5 or 6.

Levels measured after the first 24 hour incubation period were not significant across most of the plaque sections, aside from plaque sections 4 and 6 which were significantly higher than other sections.

Sections 1, 2 and 3 all significantly increased after the initial 24 hour incubation. Lactate levels in section 1, however, remained significantly higher than other sections, at all time points, aside from section 6. Lactate levels, between the 24 and 48 hour incubation periods, decreased in section 4. However, at the 72 and 96 hour incubation periods, no significant difference was observed between lactate levels in section 4 and those observed in sections 2 or 3.

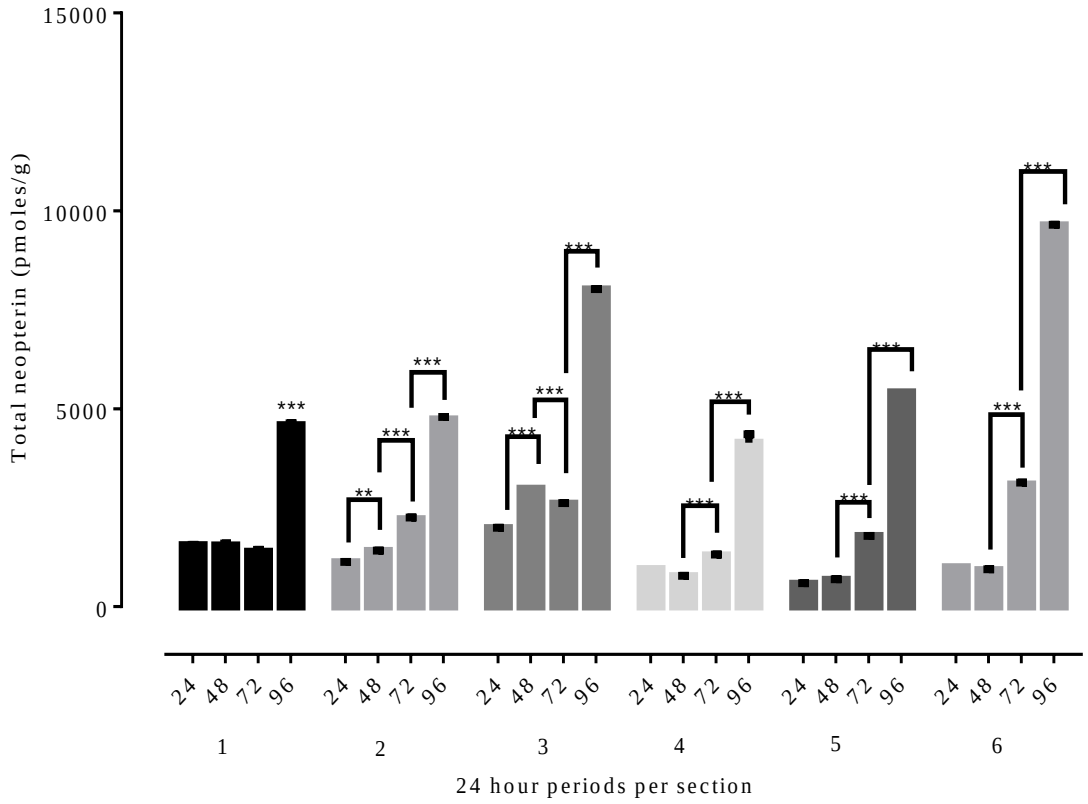

Fig 3.2.15. Total neopterin produced per gram of IFN-γ treated live plaque. 48 hours: 500 units IFN-γ /ml, 72 hours: 500 units IFN-γ /ml. 2 way ANOVA: *= p<0.05, **= p<0.01, ***= p<0.001. Error bars= Mean ± SEM.

A significant increase in total neopterin was observed for all plaque sections over the total 96 hour incubation period with the addition of IFN-γ (Fig 3.2.15.).

Total neopterin levels increased, only in sections 2 and 3, in the absence of IFN-γ over the first 48 hours of incubation. Upon addition of IFN-γ to the plaque culture media, after 48 hours of incubation, total neopterin levels were observed to significantly increase for plaque sections 2, 4, 5 and 6.

After the second IFN-γ dose was added, levels of total neopterin significantly increased for all plaque sections.

Total neopterin produced by the plaque sections varied. However, a similar trend in total neopterin up-regulation was observed, after IFN-γ treatment, with the exception of sections 1 and 3 which remained stable or decreased after the first dose.

After addition of the first IFN-γ dose neopterin levels produced were significantly higher in plaque sections 2, 3, and 6 compared to the other sections. At 96 hours levels of total neopterin produced by sections 3 and 6 were significantly higher than all other sections.

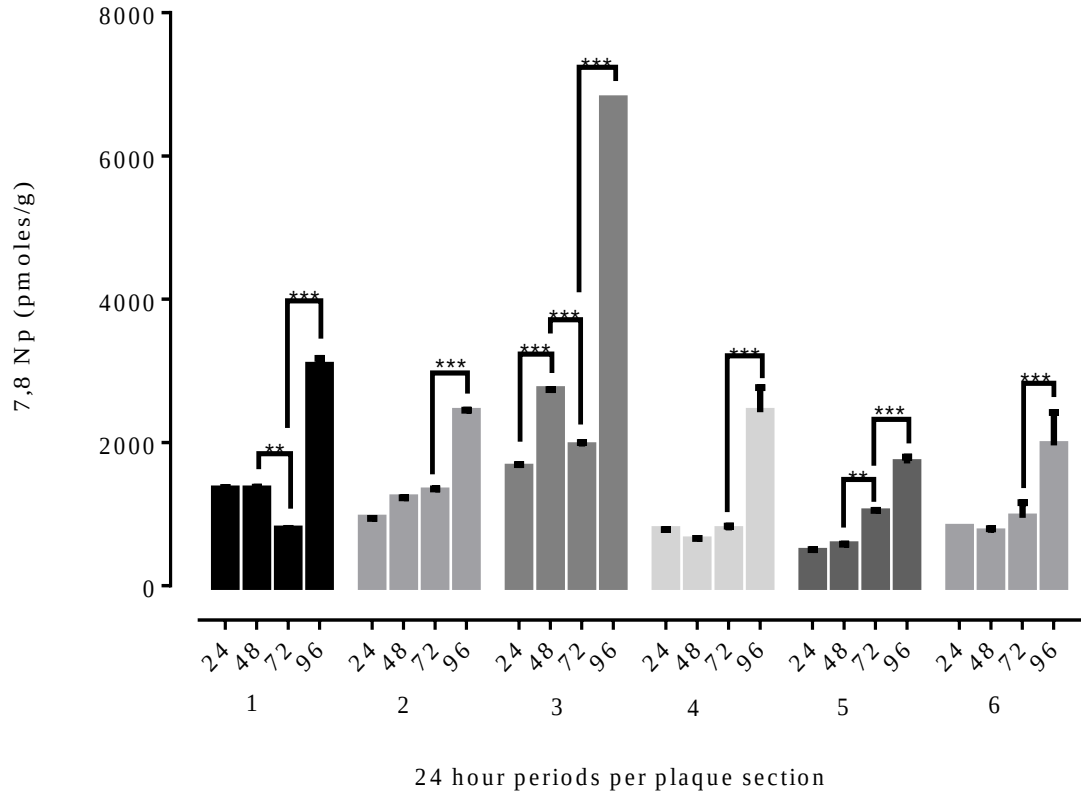

Fig 3.2.16. 7,8NP produced per gram of IFN-γ treated live plaque. 48 hours: 500 units IFN-γ /ml, 72 hours: 500 units IFN-γ /ml. 2 way ANOVA: *= $p<0.05$, **= $p<0.01$, ***= $p<0.001$. Error bars= Mean ± SEM.

A general increase in 7,8 NP was observed with the addition of IFN-γ to plaque sections (Fig 3.2.16.). Levels of 7,8 NP increased or remained stable after the first IFN-γ dose with the exception of sections 1 and 3 which significantly decreased.

After the second dose of IFN-γ 7,8NP was significantly upregulated in all plaque sections. These levels were significantly higher, after the first and second dose of IFN-γ, in plaque section 3 compared to all other plaque sections.

No significant difference, in 7,8 NP levels, were observed between any of the other plaque sections besides sections 1 and 4, which produced significantly lower levels, after 72 hours of incubation.

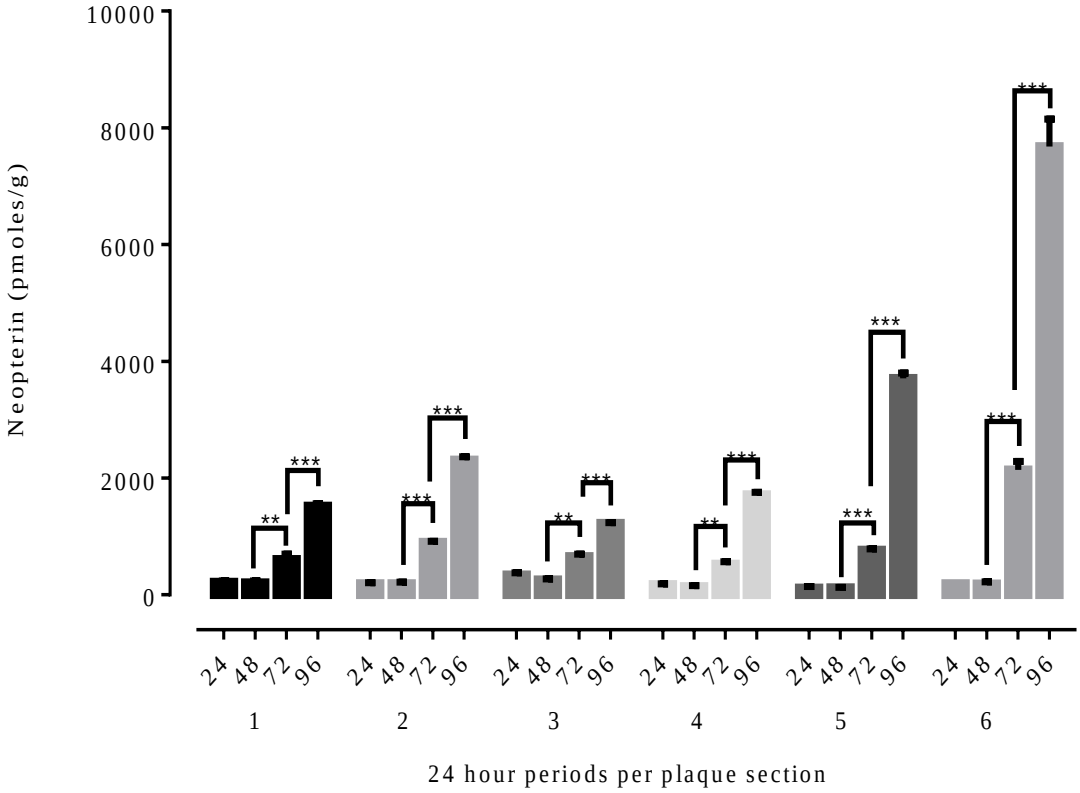

Fig 3.2.17. Neopterin produced per gram of IFN-γ treated live plaque. 48 hours: 500 units IFN-γ /ml, 72 hours: 500 units IFN-γ /ml. 2 way ANOVA: *= $p<0.05$, **= $p<0.01$, ***= $p<0.001$. Error bars= Mean ± SEM.

A significant increase in neopterin production was observed for all plaque sections after the first IFN-γ dose at 48 hours. On average a 4 fold increase in neopterin was observed after the first dose of IFN-γ. A significant increase in neopterin was then observed again for all plaque sections after the second dose of IFN-γ (Fig 3.2.17.).

No significant difference was observed, between levels of neopterin produced in the initial 24 and 48 hour incubation periods, before the administration of IFN-γ. 24 hours after the initial IFN-γ dose was administered levels of neopterin had increased significantly for all plaque sections but levels produced by section 6 were significantly higher than the other plaque sections.

After the second dose of IFN-γ, levels of neopterin produced were still significantly higher in section 6 compared to other plaque sections. Levels of neopterin were also significantly higher in sections 2 and 4 compared to sections 1, 3 and 4.

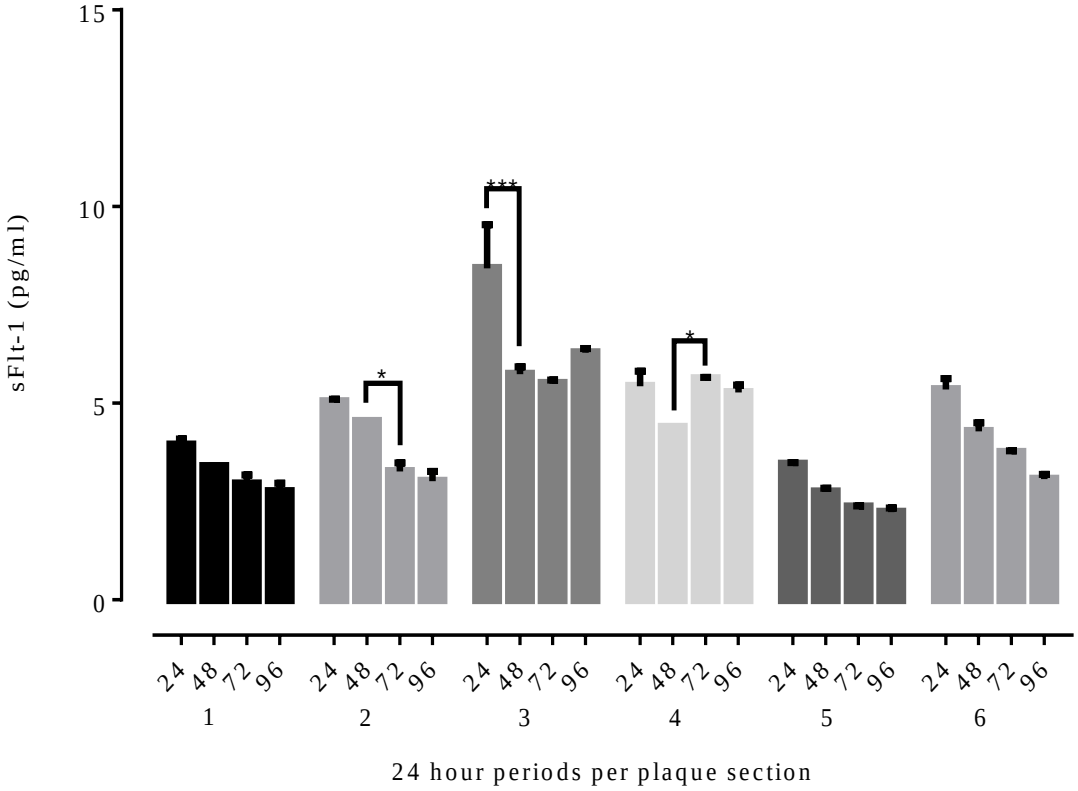

Fig 3.2.18. sFlt-1 produced per gram of IFN-γ treated live plaque. 48 hours: 500 units IFN-γ /ml, 72 hours: 500 units IFN-γ /ml. 2 way ANOVA: *= p<0.05, **= p<0.01, ***= p<0.001. Error bars= Mean ± SEM.

IFN-γ, generally, did not increase the level of sFlt-1 produced by the atherosclerotic plaque (Fig 3.2.18.). A decrease or insignificant change in sFlt-1 was observed for all plaque sections, with the exception of plaque section 4 which exhibited an increase in sFlt-1 after the first dose of IFN-γ. However, sFlt-1 levels in section 4 did not significantly change overall between the initial and final incubation periods.

Levels of sFlt-1 remained significantly higher in sections 3 and 4 compared to other sections after the addition of IFN-γ. sFlt-1 remained significantly lower in plaque section 5 compared to all other plaque sections after every incubation period.

3.2.7 Live PMA treated plaque analysis

In order to determine the capability of T-cell populations to stimulate inflammatory cells within the plaque, the sections were treated with PMA. The media was then analysed for pterin content to assess the extent of macrophage activation occurring as a result of T-cell stimulation. The levels produced indicate the potential of the plaque to contribute to arterial pterin levels as a result of inflammatory T-cell stimulation (Refer to plaque 103 in Appendix Table 6.1).

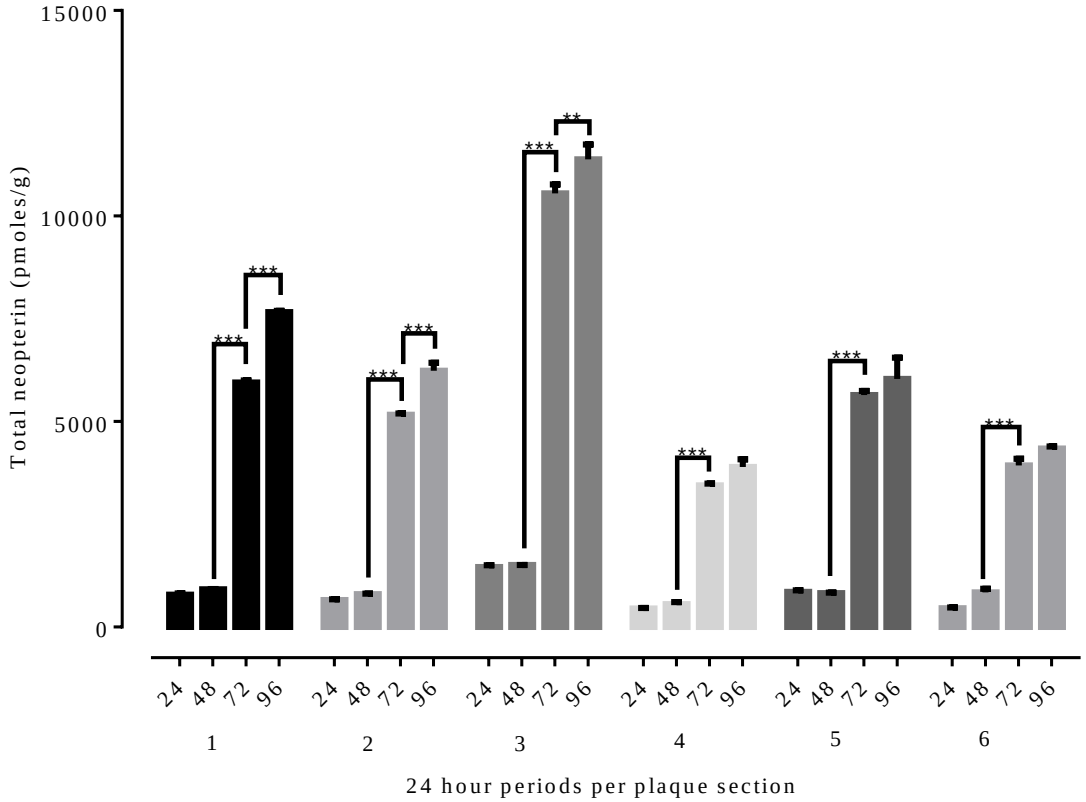

Fig 3.2.19. Total neopterin produced per gram of PMA treated live plaque. 200nM PMA media was added at 24, 48 and 72 hour incubation periods. 2 way ANOVA: *= $p<0.05$, **= $p<0.01$, ***= $p<0.001$. Error bars= Mean ± SEM.

No significant change in total neopterin was observed, after the first dose of PMA, in any of the plaque sections. Total neopterin production increased significantly in all plaque sections after the second dose of PMA, indicating a 24 hour lag period in total neopterin up-regulation after the initial PMA dose (Fig 3.2.19.).

After the third dose of PMA levels of total neopterin increased significantly in sections 1, 2 and 3 but remained statistically at the same level for sections 4, 5 and 6.

No significant difference in total neopterin levels, measured at the 24 and 48 hour incubation periods, were observed between the plaque sections with the exception of section 3 which produced significantly higher levels of total neopterin, at all incubation time points.

Measurements at 72 and 96 hours of incubation were significantly lower in sections 4 and 6 and significantly higher in sections 1 and 3 compared to other sections.

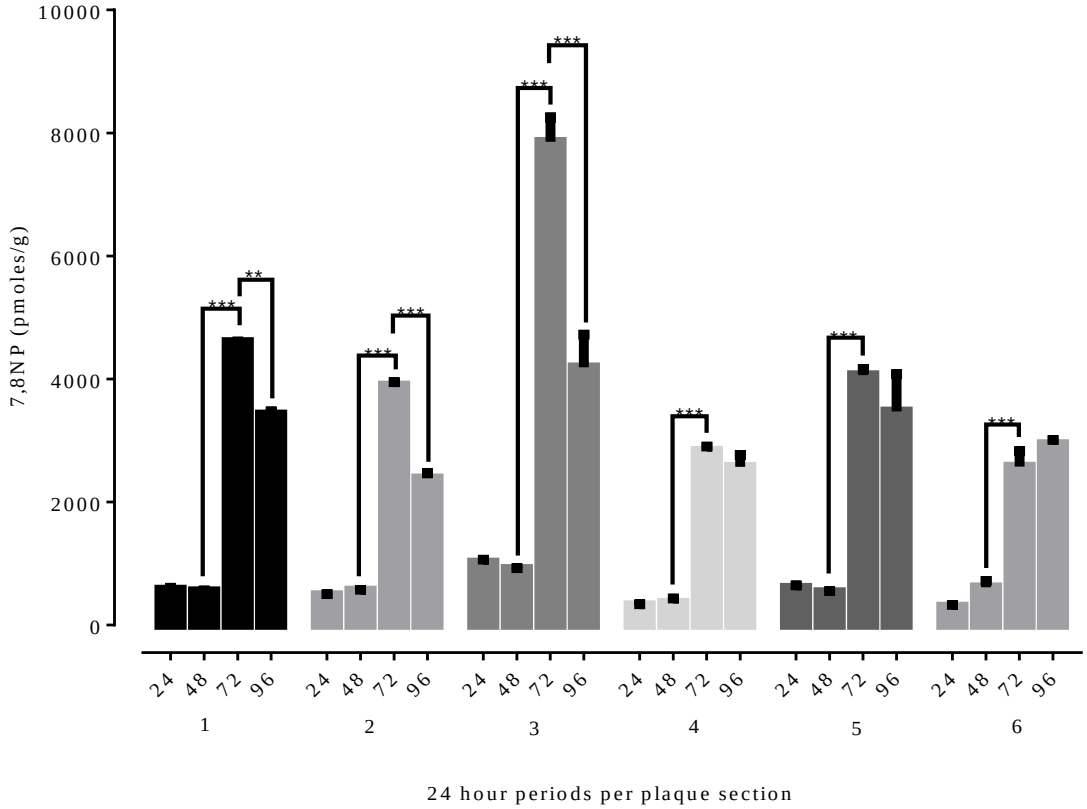

Fig 3.2.20. 7,8NP produced per gram of PMA treated live plaque. 200nM PMA media was added at 24, 48 and 72 hour incubation periods. 2 way ANOVA: *= $p<0.05$, **= $p<0.01$, ***= $p<0.001$. Error bars= Mean ± SEM.

The same 24 hour delay, observed in total neopterin up-regulation, was observed for 7,8 NP after the first dose of PMA. 24 hours after the second dose of PMA a significant increase in 7,8NP was observed for all plaque sections (Fig 3.2.20.).

Plaque sections 1, 2 and 3, which were observed to increase significantly in total neopterin levels after the 3rd dose of PMA, exhibited a significant decrease in the level of 7,8 NP produced. 7,8 NP measured in sections 4 and 5 also decreased, although insignificantly,

after the 3rd dose of PMA. Section 6 was the only section which produced a higher level of 7,8 NP, following the 3rd dose of PMA, although this increase was insignificant.

No significant difference was observed between any of the plaque sections over the first 48 hours of incubation. However, section 3 produced significantly higher levels of 7,8 NP, in comparison to all other plaque sections, after the second dose of PMA.

After the 3rd dose of PMA levels produced by section 3 had significantly decreased to a level not significantly different from that of sections 1 or 5.

Levels of 7,8 NP produced, after the 2nd and 3rd doses of PMA, by sections 4 and 6 were significantly lower than all other sections.

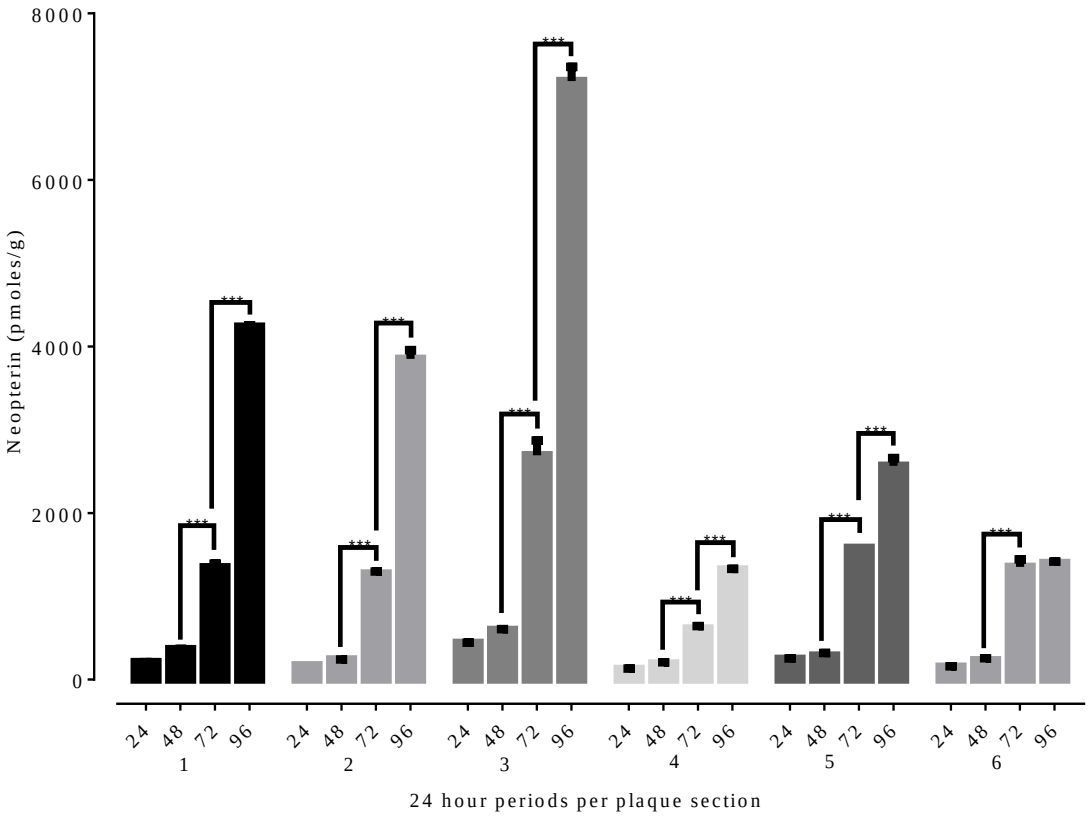

Fig 3.2.21. Neopterin produced per gram of PMA treated live plaque. 200nM PMA media was added at 24, 48 and 72 hour incubation periods. 2 way ANOVA: *= p<0.05, **= p<0.01, ***= p<0.001. Error bars= Mean ± SEM.

A general increase in neopterin was observed in all plaque sections following repeated doses of PMA. 24 hours after the 2nd dose of PMA neopterin levels significantly increased in all plaque sections (Fig 3.2.21).

After the 3rd PMA dose a further significant increase in neopterin production was observed with the exception of section 6, which didn't significantly change, between the 72 and 96-hour incubation periods.

Levels of neopterin produced by the plaque sections, as observed in the 7,8 NP and total neopterin analysis, did not significantly change, between the 24 and 48 hour incubation periods, in any of the plaque sections.

Section 3 had produced significantly higher levels of neopterin, 24 hours after the second dose of PMA, compared to the other plaque sections. Section 4, on the other hand, produced significantly lower levels of neopterin, 24 hours after the second dose, compared to all other plaque sections.

Levels of neopterin remained significantly higher in section 3, 24 hours after the 3rd, dose of PMA and were significantly lower in sections 4 and 6 compared to the other plaque sections.

3.2.8 Live IFN-γ and PMA treated plaque analysis

Plaque sections were treated, initially with PMA followed by IFN-γ, to assess whether IFN-γ could further promote the effects of macrophage activation occurring as a result of T-cell stimulation by PMA (Refer to plaque 106 in Appendix Table 6.1).

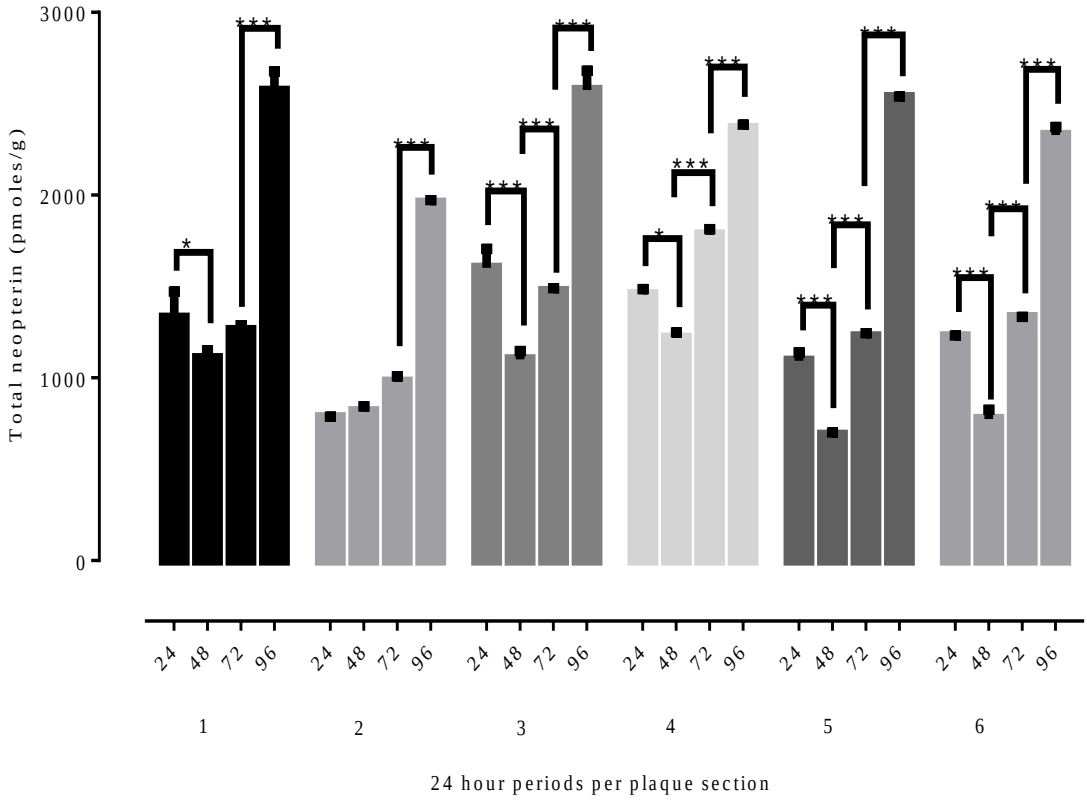

Fig 3.2.22. Total neopterin produced per gram of PMA and IFN-γ treated live plaque. 200nM PMA media was added at 24 and 48 hour incubation periods. IFN- γ was added at the 72 hour incubation period. Two-way ANOVA: *= $p<0.05$, **= $p<0.01$, ***= $p<0.001$. Error bars= Mean ± SEM.

PMA generally caused a delayed up-regulation of total neopterin whereas the effects of IFN-γ were more immediate. Levels of total neopterin significantly decreased between the 24 and 48-hour incubation periods, following administration of PMA, with the exception of plaque section 2 (Fig 3.2.22.).

After the second dose of PMA levels of total neopterin increased to a level not significantly different from the initial 24 hour reading before PMA was added. This increase occurred in all plaque sections aside from section 4, which produced significantly higher levels, after the second PMA dose.

After IFN-γ treatment, over the final 24 hour period, the level of total neopterin produced by all plaque sections increased significantly

Aside from the 48-hour incubation period levels of total neopterin, produced by section 2, were significantly lower than in any other section. After the second dose of PMA section four produced significantly higher levels of total neopterin compared to the other plaque sections.

There was no significant difference, in total neopterin production observed between the plaque sections 24 hours following treatment with IFN-γ, aside from section 2 which was significantly lower and section 4 which was lower but tended towards insignificance ($p<0.05$).

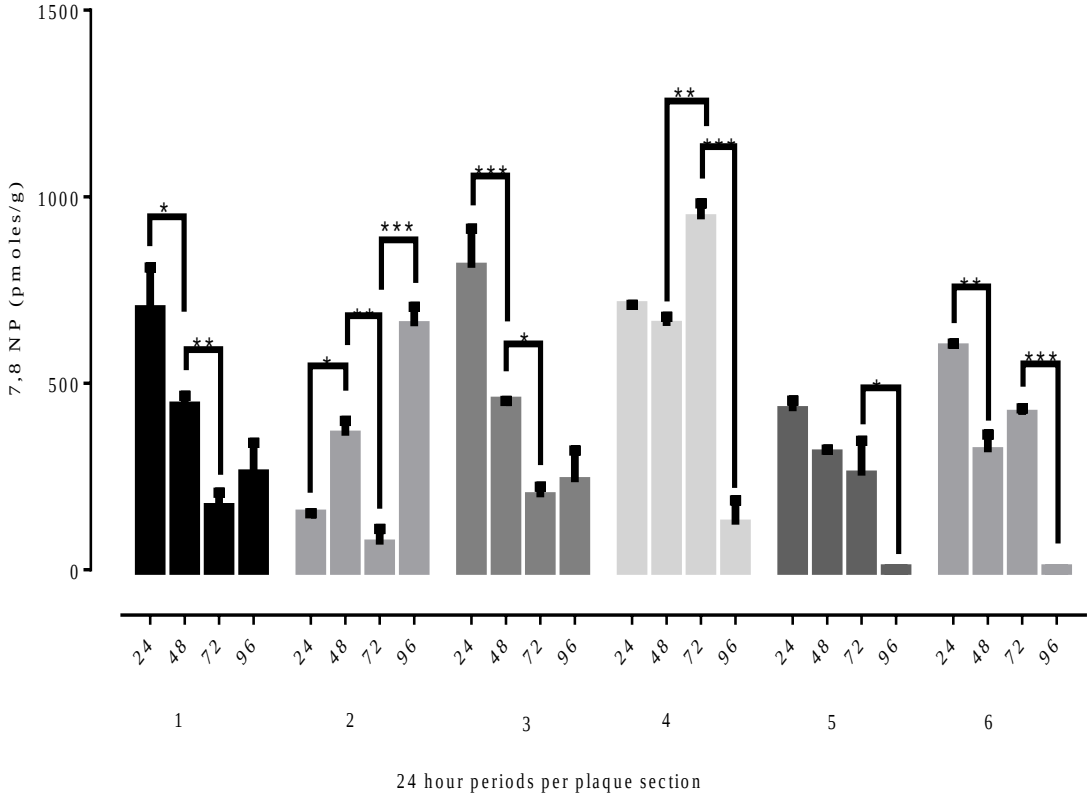

Fig 3.2.23. 7,8 NP produced per gram of PMA and IFN-γ treated live plaque. 200nM PMA media was added at 24 and 48 hour incubation periods. IFN- γ was added at the 72 hour incubation period. 2 way ANOVA: *= $p<0.05$, **= $p<0.01$, ***= $p<0.001$. Error bars= Mean ± SEM.

A general decrease in 7,8NP was observed, over the initial 72 hours of incubation, following two doses of PMA (Fig 3.2.23.). 7,8 NP levels significantly decreased in sections 1,

3 and 6 following the initial dose of PMA. In sections 5 and 4 levels of 7,8 NP were observed to decrease but this decrease was insignificant. An increase in 7,8 NP was observed in section 2 after the initial PMA treatment, but the increase also tended toward insignificance ($p<0.05$).

Following the second incubation with PMA, between 48 and 72 hours, levels of 7,8 NP significantly decreased in sections 1, 2 and 3, insignificantly decreased in section 5 and increased significantly in sections 4 and 6.

Incubation with IFN- γ, in the final 24 hours, resulted in a significant decrease in 7,8 NP found in sections 4, 5 and 6. 7,8 NP in sections 1 and 3 increased insignificantly after incubation with IFN- γ. Section 2 was the only section which produced significantly increased levels of 7,8 NP following IFN-γ treatment.

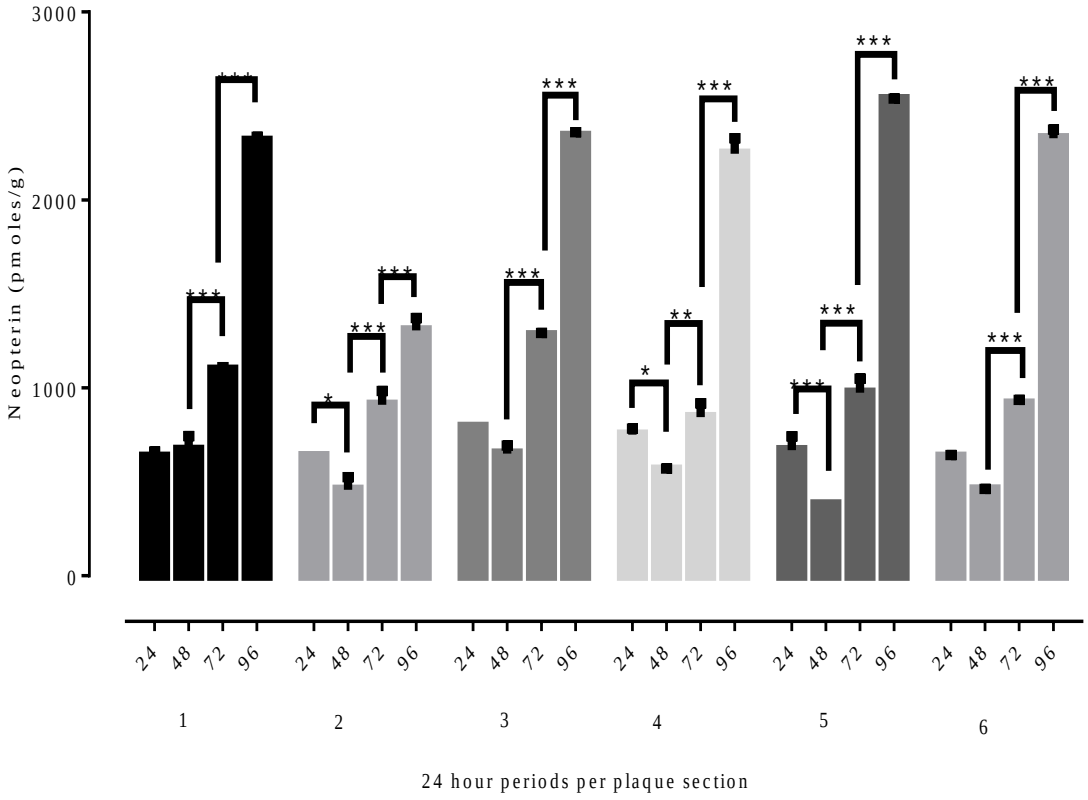

Fig 3.2.24. Neoterin produced per gram of PMA and IFN-γ treated live plaque. 200nM PMA media was added at 24 and 48 hour incubation periods. IFN- γ was added at the 72 hour incubation period. 2 way ANOVA: *= $p<0.05$, **= $p<0.01$, ***= $p<0.001$. Error bars= Mean ± SEM.

Levels of neopterin, as was observed in the analysis of total neopterin, generally increased after the second dose of PMA. The increase occurred following a lag period, during

which levels decreased after the first PMA dose. This lag period, after the initial dose of PMA, was observed in all plaque sections (Fig 3.2.24.).

IFN-γ treatment, in the last 24 hours of incubation, resulted in a significant increase in neopterin for all plaque sections.

Levels of neopterin did not vary greatly across the different plaque sections with the exception of section 2 and 5. After treatment with IFN-γ levels of neopterin found in section 2 were significantly lower than all other plaque sections. Section 5, on the other hand, had significantly higher levels of neopterin, after treatment with IFN-γ, compared to the other sections.

4

Discussion

4.1 Direct associations in the CDCS plasma between alcohol consumption and BNP versus the measured biomarkers neopterin, 7,8NP and sFlt-1

The VEGF system, generally comprising the major angiogenic molecules responsible for controlling vascular growth and function, is predominantly thought to have a protective role against atherosclerotic progression. However, contrary to this notion, studies have also shown that overexpression or chronic VEGF expression can contribute to pro-atherosclerotic processes (Couffinhal et al., 1997; Inoue et al., 1998). As sFlt-1 is known to sequester VEGFA molecules, preventing the downstream angiogenic response, it may exert differing effects on atherosclerotic progression. Using multiple regression analyses, attempts were made to assess whether a relationship existed between sFlt-1 and CVD events in acute coronary syndrome patients. In order to determine which known CVD risk factors may be used to account for variance, when assessing a potential association between sFlt-1 and CVD, a general linear model was used. Acute coronary syndrome patient plasma was analysed for sFlt-1 in association with other known associates of CVD including BNP, alcohol consumption per week, diastolic BP, heart rate, BMI and gender (Fig 3.1.2).

Markers of systemic immune system activation, neopterin and 7,8 NP, have also been associated with vascular inflammation and stenosis, which often leads to the development of severe cardiovascular events (Zouridakis et al., 2004). For this reason these markers were also compared to the same CVD risk factors in order to determine whether the same associations arose between neopterin (Fig 3.1.4), total neopterin (Fig 3.1.3) and 7,8NP (Fig 3.1.5) that occurred in sFlt-1.

Aside from gender and BMI which were insignificant and heart rate which tended toward insignificance ($p=0.035$), all other covariates were found to be highly associated in the general linear model of sFlt-1 associations. However, the same could not be said for the

neopterin data. The only covariate significantly associated with both, neopterin and sFlt-1, was BNP, which exhibited a marginally significant association (p=0.024) with neopterin and a highly significant association (p=0.007) with sFlt-1 (Table 3.1.2 and Table 3.1.4 in Results). In support of these findings recent results, from a study assessing the utility of multiple markers in determining the risk of chronic heart failure, also found a significant, but moderate (R=0.54), association between sFlt-1 and BNP (Ky et al., 2012). Similarly, a significant correlation was observed, between neopterin and BNP, in patients undergoing left ventricular remodelling after experiencing a MI (Dominguez-Rodriguez, Abreu-Gonzalez, Avanzas, Laynez-Cerdeña, & Kaski, 2010). Furthermore, when added to a multivariable Cox model of acute coronary syndrome event risk, containing C-reactive protein and BNP, the further addition of neopterin significantly improved the HF-risk prediction model (P = 0.005) (Nazer et al., 2011a). The results, therefore, suggest that the levels of sFlt-1 and neopterin, like BNP, may be associated with ventricular wall stress potentially occurring as a result of an acute coronary event. Interestingly BMI was significantly associated with neopterin, but not sFlt-1 (Table 3.1.2 and Table 3.1.4 in Results). Suggesting that oxidative stress (causing the increased oxidation of 7,8NP to neopterin) may be associated with an individual's BMI.

No covariates shared significance with both neopterin and 7,8NP. Likely due the production of neopterin being a direct result of 7,8NP oxidation. However, levels of 7,8 NP and total neopterin, like sFlt-1, were significantly associated with an individual's alcohol consumption. Typically alcohol is found to have a U-shaped association with inflammation, with non-drinkers and heavy drinkers having higher levels of inflammation (Kloner & Rezkalla, 2007). Past studies have shown that non-drinkers and heavy drinkers had higher C-reactive protein (CRP) concentrations and a higher risk of CVD than moderate drinkers (Imhof et al., 2001). The results derived from this dataset suggest that like CRP, produced in response to IL4 released from macrophages (Du Clos, 2000), 7,8 NP levels rise with higher levels of alcohol consumption. Suggesting that increased inflammation, with higher levels of alcohol consumption, may be in part be associated with increased macrophage activation.

The results of a recent study, also concerning the U-shaped association between alcohol and inflammation, indicate that ethanol stimulates endothelial angiogenic activity through cross talk between the notch and kinase insert domain (KDR) signalling pathways and also upregulates KDR (Morrow, Hatch, Hamm, Cahill, & Redmond, 2014). Excess alcohol consumption may therefore increase the risk of CVD, as a result of overactive

angiogenesis/vascular remodelling, causing chronic inflammation, mediated by the KDR receptor pathway. In agreement with these findings, a strong direct correlation (p=0.001) was observed between levels of sFlt-1 in the patient cohort and alcohol consumption per week. Since levels of sFlt-1 were lower at lower levels of alcohol consumption the ability of sFlt-1 to negate VEGF stimulated angiogenesis is less effective. For this reason the consumption of low levels of alcohol may contribute to VEGF stimulated angiogenesis, which is hindered to a lesser extent by sFlt-1, by upregulating KDR and further stimulating it. The data produced also potentially explains the protective effects of moderate alcohol consumption. Since sFlt-1 hinders the normal angiogenic effect, of VEGF binding to KDR, alcohol may provide an alternative route of angiogenic up-regulation resulting in a healthy level of vascular remodelling and repair.

Direct correlations also identified a significant association between levels of 7,8 NP, total neopterin and alcohol consumption, supporting the already identified relationship between alcohol and inflammation. Aside from alcohol consumption the only other direct correlations observed between measured variables were between sFlt-1 and BNP (p=0.027) (Fig 3.1.6). This may also be explained by the notion that sFlt-1 is upregulated in hypoxic conditions, which classically arise in ischaemia, a condition which can present significant stress on the ventricular walls such as in the case of MI (Goetze et al., 2003).

4.2 Predictive capacity of sFlt-1, neopterin, 7,8NP and total neopterin in determining ACD, TCVE and CVD death

Univariate analyses of all cause death (ACD) revealed that higher levels of total neopterin, 7,8 NP and sFlt-1 were all significantly associated with ACD, whereas, higher levels of neopterin were generally not. Total neopterin, 7,8 NP and sFlt-1 are therefore all independent markers of ACD post-acute coronary event.

sFlt-1 levels measured in a similar study, of patients with stable acute coronary disease, were not found to be a significant independent predictor (p=0.125) of any adverse outcomes (hazard ratio = 0.57) (Matsumoto et al., 2012). Contrary to this, plasma levels of sFlt-1 measured in the current study indicate that sFlt-1 is a highly significant independent predictor of ACD (p<0.001) (Fig 3.1.11, Table 3.1.25) and CVD death (p=0.001) (Fig 3.1.13, Table

3.1.29) over a 10-year period. Furthermore, a higher than median sFlt-1 level, when analysed in a Cox proportional analysis alongside higher than median BNP, alcohol consumption and age, corresponds to a 2-fold higher rate of mortality (Hazard ratio=1.990, p=0.003) (Table 3.1.26). Some of the relationship observed between ACD and sFlt-1 can be explained by the significant relationship between CVD death and sFlt-1 (p=0.001). The data suggests that sFlt-1 not only exhibits prognostic utility in determining the risk of ACD, but also exhibits predictive capabilities in determining the risk of CVD death. A notion which is further supported by its significant predictive capacity in association with the covariates BNP and age at baseline (Table 3.1.30). Since the risk of adverse events is 2 times higher in patients with elevated sFlt-1 (above 117.3 pg/ml), this level may be used clinically as a comparative standard in assessing the level of risk management required. Providing intensive management of coronary risk factors is essential for preventing secondary events. However, because the progression of atherosclerosis is slow, it is likely that continuous activation of intramural inflammation plays a role in the occurrence of cardiovascular events. This may not be accounted for by levels of sFlt-1 until a sufficient level of ischaemia occurs, to present a hypoxic condition, resulting in its up-regulation.

Levels of total neopterin and 7,8 NP, were found in this study, to be significantly associated with ACD (Fig 3.1.2, Fig 3.1.8), which is in agreement with past research relating inflammation to risk of death post CVD event (Andersson, Libby, & Hansson, 2010). Previous to this study neopterin has been presented as an independent marker of ACD and acute coronary events after an initial acute coronary event (Ray et al., 2007). However, it is unclear whether the study differentiates between 7,8NP and neopterin, suggesting that the two have been measured together as total neopterin. This being said enhanced T-cell activity, that results in increased production of interferon-γ, is implicated in the pathogenesis of CVD (Garcia-Moll, D. Cole, et al., 2000; Liuzzo et al., 2000). Total neopterin production, by monocytes and macrophages, is primarily in response to stimulation by interferon-γ released by activated T-lymphocytes (Berdowska & Zwirska-Korczala, 2001). Therefore, the levels of Total neopterin observed may reflect the level of cell-mediated immunity within individuals which could contribute to mortality post CVD event.

Both 7,8NP and total neopterin were not found to exhibit a significant individual capacity in predicting CVD death (Fig 3.1.4, Fig 3.1.10). However, in combination with alcohol consumption, age at baseline and BNP, higher levels of both 7,8NP and Total neopterin

did significantly (p=0.046 and p=.032 respectively) predict CVD death (Table 3.1.12, Table 3.1.24). Therefore, in combination with these factors, 7,8NP and Total neopterin show promise in their capacity for predicting the risk of CVD death, having the potential to aid in determining the need for management of coronary risk factors.

Although higher 7,8 NP was independently associated with ACD the case was not the same for neopterin. The risk of ACD is therefore suggested to have a lesser relationship to baseline oxidative stress. However, when combined in a Cox proportional hazard model, (Table 3.1.14) neopterin was indicated as a significant predictor (p=0.013) of ACD, alongside alcohol consumption, age at baseline and BNP, with a hazard ratio of 5.614. Neopterin may therefore be of more substantial prognostic use in combination with these other indicators compared to alone. Similarly Nazer *et al*., 2011 found that neopterin significantly improved the Cox proportional HF-risk prediction model (p = 0.005) already encompassing C-reactive protein and BNP. No relationship was observed between neopterin and CVD death, alone (Fig 3.1.7, Table 3.1.17) or in a Cox proportional regression model (Table 3.1.18), suggesting that the relationship between neopterin and ACD is not significantly contributed to by CVD death. Instead patients dying, in association with high levels of the neopterin, may be a result of alternative illness also associated with high levels of oxidative stress.

Despite the prognostic utility, exhibited by sFlt-1, 7,8 NP, neopterin and total neopterin, no significant association was found, alone or in combination with other CVD factors, between these markers and total cardiovascular events (TCVE). CVD is a dynamic process involving many factors, which may contribute to its progression and severity. In the case of an acute event certain markers may be elevated transiently, which has been shown in the case of sFlt-1 and total neopterin (Kaski et al., 2008; Onoue et al., 2009). A more accurate way, of determining an association with TCVE, would therefore be to serially evaluate levels in patients at risk indicating whether spikes in these markers correspond to an event. Likewise, the severity of an event in relation to these markers could also be assessed in this manner.

4.3 Plasma levels of sFlt-1, 7,8 NP, total neopterin and neopterin in patients with late stage atherosclerosis in the carotid artery

In comparison to age and gender matched healthy controls, levels of sFlt-1 were 38 times higher in males and 24 times higher in females (Fig 3.2.1), suggesting that sFlt-1 levels are significantly elevated in patients with a developed atherosclerotic occlusion. These elevated levels are likely due to the significant ischaemic condition downstream of the occlusion, which results in hypoxic up-regulation by HIF-1 (Sandner et al., 1997), supporting previous evidence of higher sFlt-1 levels in acute stages of CVD (Kapur et al., 2011). Levels of sFlt-1 were not significantly different between males and females or at different ages indicating that this up-regulation occurs regardless of age or gender. Levels of sFlt-1 were also significantly higher compared to levels found in the CDCS cohort, further indicating that a transient up-regulation of sFlt-1 is likely and that post recovery these levels decline. Although the two cohorts are from differing facets of CVD, similar results have been found upon comparing sFlt-1 in patients with acute ischaemia to sFlt-1 in the same patients after recovery (Chung, Lydakis, Belgore, Blann, & Lip, 2002).

Levels of total neopterin were also significantly elevated for both males and females in comparison to the healthy age and gender matched controls. Also no significant difference was observed between age groups and gender (Fig 3.2.4). Higher levels of total neopterin have been observed in patients with carotid atherosclerosis in a previous study (Weiss et al., 1994), indicating that the level of cell-mediated immunity within individuals which could be attributable to presence of atherosclerosis.

In comparison to levels observed in the CDCS cohort (median: 94.5 nM), levels found in the plasma of the carotid endarterectomy patients (median: 50.3 nM) were significantly lower. Therefore, macrophage activation may be a chronic response which occurs throughout atherosclerotic development and remains elevated long after a CVD event has occurred. However, due to differences in the two cohorts these levels are not directly relatable. In order for direct comparisons to be made, serially evaluated levels in advanced atherosclerosis patients, prior to and post recovery from an event, must be measured.

Levels of neopterin largely followed the same trend as total neopterin, suggesting that elevated oxidative stress occurs in CVD patients regardless of age or gender (Fig 3.2.2). However, levels of 7,8NP were significantly lower in the female control group than the female and male endarterectomy groups and the male control group. Males therefore appear to have higher healthy levels of macrophage activation, which do not significantly differ in atherosclerosis, as opposed to females whose levels appear to increase depending on atherosclerosis. This may partially, among other factors, account for the higher levels of CVD observed in males compared to females (Go et al., 2014) as inflammation has been closely related to the severity of CVD.

In patients prior to undergoing the endarterectomy procedure, a significant correlation was observed between plasma sFlt-1 and both total neopterin (Fig 3.2.7) and 7,8 NP (Fig 3.2.6). This relationship was not observed in patients post recovery from MI or unstable angina. Based on this finding, it would appear that levels of sFlt-1 increase somewhat proportionally to the amount of cell mediated inflammation in atherosclerosis and that these levels are reduced post recovery after the plaque has become unstable or an MI has occurred. Immune cell mediated inflammatory processes may therefore play a role in the hypoxia driven up-regulation of sFlt-1 by HIF-1. Also after recovery from an event oxygen reperfusion to the once ischaemic area, distal to the atherosclerotic plaque, may cause a down-regulation in sFlt-1. In support of this previous studies have identified a significant association between levels of the inflammation and sFlt-1 in, the systemic inflammatory disorder, pre-eclampsia, associated with placental hypoxia (McKeeman, Ardill, Caldwell, Hunter, & McClure, 2004; Nevo et al., 2006).

Plasma neopterin did not show the same relationship with sFlt-1 that 7,8NP did. Indicating that, although levels of oxidative stress may be elevated in these patients, little or no relationship exists between it and the hypoxic up-regulation of sFlt-1.

4.4 The presence of live inflammatory cell populations within atherosclerotic plaques

HMDM cells produce basal levels of both 7,8-NP and neopterin, which significantly increase with treatment of IFN-γ (Fig 3.2.9). Furthermore, the health of these cells was not significantly affected by the 96 hour incubation in RPMI or treatment with IFN-γ as a steady

state of lactate production was observed across the 24 hour incubation increments (Fig 3.2.8). Upon initial stimulation with IFN-γ a 2.4 fold increase in total neopterin concentration, produced by the HMDM cells, (From 40±3.54 nM to 94.4±9.516 nM) was observed, confirming previous results for the effectiveness of IFN-γ in stimulating total neopterin production (Werner et al., 1990; Wirleitner et al., 2002). The ratio of 7,8 NP to neopterin produced fell significantly in favour of neopterin, suggesting that much of the 7,8NP produced had been oxidized. Although a classical ratio of 2:1 for 7,8 NP to neopterin has been observed for arterial blood (Weiss et al., 1992), and the ratio observed in arterial blood here was more like 1:1, the levels observed here serve more to represent the potential for activation by IFN-γ as 7,8 NP produced may easily be effected by the surrounding testing conditions.

Compared to levels of total neopterin produced by HMDMs in a study by Wirleitner *et al.*, macrophages in this experiment produced significantly higher levels after treatment with half the dose of IFN-γ (1000 U/ml compared to 500 U/ml) (Wirleitner et al., 2002). However, basal levels of total neopterin were much higher in this study, which may explain, in part the higher levels observed after treatment.

Unsurprisingly, levels of total neopterin produced by a plaque section which had been freeze-thawed were negligible (Fig 3.2.10). Although significant amounts of 7,8NP were observed in the plaque culture media after 48 hours, these levels dropped below the limit of detection rapidly, suggesting that what was observed had been washed off the plaque rather than produced by its cellular constituents.

Without stimulation with IFN-γ or PMA levels of both 7,8 NP and neopterin, produced per gram of atherosclerotic plaque, significantly decreased within 24 hours of incubation (Fig 3.2.11). 7,8 NP levels, which significantly decreased after the first 48 hours of incubation, remained stable throughout the next 24 hours (Fig 3.2.12), whereas the decrease in neopterin consistently occurred over the three 24 hour incubation periods (Fig 3.2.13). Therefore, it would appear that the amount of macrophage activation taking place consistently decreases during the incubation procedure. Furthermore, a high proportion of the 7,8 NP produced oxidises to neopterin. Levels of both 7,8 NP and neopterin largely varied across the plaque sections, indicating that the proportion of inflammatory cell populations may have also varied between plaque sections, which was to be expected as atherosclerotic plaques do not usually consist of a uniform dispersion or cells.

Lactate production, although unchanged over 96 hours in the HMDM culture, generally increased in the plaque cell culture (Fig 3.2.14). This lactate increase is more likely due to gradual infiltration of the RPMI 1640 media into the plaque intima, than due to addition of IFN-γ, as the initial increase occurs prior to IFN-γ dosing.

After the initial dose of IFN-γ a general increase in total neopterin was observed in the live plaque sections (Fig 3.2.4). Like the HMDM cell culture a much more significant increase in both 7,8 NP (Fig 3.2.15) and neopterin (Fig 3.2.16) was observed after the final 500 U/ml dose of IFN-γ was administered. The macrophages may therefore either become primed by the first dose of INF-γ or experience some delay in production requiring longer than 24 hours before the full effect is observed. Much lower levels of both neopterin and 7,8 NP were produced, even after the final dose of IFN-γ , than those measured in the HMDM cell culture. Similarly, in past cell culture analysis, levels produced by HMDM cells were higher, even at lower (100 U/ml) doses of IFN-γ (Wirleitner et al., 2002). Suggesting that the immune cell populations within the plaque were either less sensitive to IFN-γ or that there were less of them. This being said levels of total neopterin measured 24 hours after the second dose of IFN-γ were in the nM concentration levels (ranging from 4.1±0.2 nM/g to 9.6±0.01 nM/g). These plaques are therefore capable of significant macrophage activation in the presence of IFN-γ, which may contribute to levels in the plasma higher than that identified in the blood of a healthy individual (6.7 ± 1.5 nM) (Murr. et al., 2005). Furthrmore, levels of 7,8 NP alone, produced by the plaque section, also ranged into the nM concentrations (from 1.7±0.06 nM/g to 6.8±0.0 nM/g) which could contribute to higher blood levels than healthy individuals (approximately 5.8 nM/L) (Flavall et al., 2008). This may indicate why much higher levels of 7,8 NP and neopterin were observed in the plasma of these endarterectomy patients.

Over the 96-hour incubation period levels of sFlt-1 either decreased gradually or did not change (Fig 3.2.17). Indicating that, although the cells were producing sFlt-1, IFN-γ had no significant effect on these levels. Taking into account the mechanism of sFlt-1 upregulation, the reason behind the gradual down-regulation may lie in the HIF-1 transcription factor. HIF-1 is a heterodimeric transcription factor consisting of subunit α, which is oxygen-sensitive and rapidly degraded/inactivated during normoxia, and subunit β, which is constitutively active (Semenza, 2000). Since the conditions of the plaque culture were atmospheric, the plaque experienced relative hyperoxia limiting HIF-1's ability for transcription of sFlt-1. In order to

determine whether levels of sFlt-1 could be upregulated within the plaque, incubation in hypoxia is required which could not be covered under the scope of this project. However, if sFlt-1 can be upregulated within the plaque, the upregulated levels may contribute to those observed in the plasma making it a valuable aspect of future research on the subject.

A 48-hour delay period was observed in total neopterin upregulation following initial dosing with 200nM PMA (Fig 3.2.18). However, following the second dose of PMA, a significant 6-fold increase was observed on average across the plaque sections. This delay period suggests that either the process of IFN-γ production by Th1 cells in the atheroma is not a rapid process or that the process of total neopterin production by macrophages in response to IFN-γ causes delay. Since we have shown previously, in the IFN-γ treated plaque, that the latter is not the case, it is likely that the PMA interaction with Th1 cells is responsible. However, the ultimate up-regulation of total neopterin to nM levels with the addition of PMA, shows that T-cell stimulation, by native molecules such as IL-12 or 18, may be another step in production of total neopterin levels observed in acute CVD patients. Supporting this statement, findings from a past study of monoclonal T-cell proliferation in atherosclerotic plaques, indicates that unstable angina is associated with the expansion of interferon-γ–producing T lymphocytes within the plaque (Liuzzo et al., 2000). Indicating that total neopterin, being upregulated by this IFN-γ, may be a valuable marker of these events.

Likewise, after a 48-hour delay, significant increases in both neopterin (Fig 3.2.20) and 7,8NP (Fig 3.2.19) were observed across all plaque sections. A decrease in 7,8 NP was observed in the majority of the plaque sections 24 hours after the 3rd dose of neopterin (at 96 hours), whilst an increase in neopterin was observed. Therefore, between 72 and 96 hours of incubation, there was a significant oxidative event suggesting the presence of radical species in the plaque sections. This is likely, as recent evidence shows advanced human atheroma contain high levels of myeloperoxidase containing macrophages capable of producing the pro-oxidant species, HOCl (Sugiyama et al., 2001).

The delay in total neopterin production was much more evident in the plaque culture analysis of PMA and IFN-γ together (Fig 3.2.21). Levels of total neopterin were observed to decrease 24 hours after the first dose of PMA whereas at 72 hours incubation (24 hours after the second dose) levels significantly increased. Providing more evidence for PMAs delayed upregulation of IFN-γ. Levels of both 7,8 NP and neopterin however were much lower in all

the plaque sections compared to other plaques. This is likely because cellular constituents vary between plaques. Making classification of an average plaques makeup difficult, if not impossible to derive. Similarly the cellular makeup between sections in a plaque are highly varied. This is supported by different levels of response to PMA in the plaque sections, with some sections producing significantly more 7,8 NP (Fig 3.2.22) than others. Although levels varied between sections a similar increase in oxidation of 7,8NP was observed over the plaque sections supporting that pro oxidants were being generated (Fig 3.2.23),

4.5 Summary

The results of this study have provided supportive evidence for the potential prognostic use of sFlt-1, total neopterin, and 7,8 NP via significant associations between these factors and ACD post-acute angina or MI. Furthermore sFlt-1 levels above 117 pg/ml were significantly associated with CVD death, supporting its predictive capacity in determining CVD risk using methods described in this research. The use of this marker alone or in combination with the covariates BNP, drinks per week and age at baseline may therefore, with further evidence, prove to be a valuable biomarker of CVD events. Alcohol consumption previously, shown to have a U shaped association with CVD, may in part be explained by its association with sFlt-1 levels in the plasma of acute coronary syndrome patients. Potentially linking the consumption of alcohol with angiogenesis via alternative activation of the VEGFR KDR. Significant associations observed between levels of sFlt-1 and total neopterin provides new evidence of a relationship between inflammatory cell activation and the hypoxic upregulation of sFlt-1. A process, which in future may support evidence for the association between sFlt-1 and CVD. Lastly the research indicating varied levels of live macrophage and T-cell populations within atherosclerotic plaques opens new avenues for research into the production of inflammatory biomarkers observed in the plasma of individuals with CVD.

5

Bibliography

Adachi, T., Naruko, T., Itoh, A., Komatsu, R., Abe, Y., Shirai, N., Kitabayashi, C. (2007). Neopterin is associated with plaque inflammation and destabilisation in human coronary atherosclerotic lesions. *Heart, 93*(12), 1537-1541.

Andersson, J., Libby, P., & Hansson, G. K. (2010). Adaptive immunity and atherosclerosis. *Clinical Immunology, 134*(1), 33-46.

Avanzas, P., Arroyo-Espliguero, R., Cosin-Sales, J., Quiles, J., Zouridakis, E., & Kaski, J. C. (2004). Prognostic value of neopterin levels in treated patients with hypertension and chest pain but without obstructive coronary artery disease. *The American journal of cardiology, 93*(5), 627-629.

Avanzas, P., Arroyo-Espliguero, R., Quiles, J., Roy, D., & Kaski, J. C. (2005). Elevated serum neopterin predicts future adverse cardiac events in patients with chronic stable angina pectoris. *European heart journal, 26*(5), 457-463.

Avanzas, P., & Kaski, J. C. (2009). Neopterin for risk assessment in angina pectoris. *Drug News Perspect, 22*(4), 215-219.

Banai, S., Shweiki, D., Pinson, A., Chandra, M., Lazarovici, G., & Keshet, E. (1994). Upregulation of vascular endothelial growth factor expression induced by myocardial ischaemia: implications for coronary angiogenesis. *Cardiovascular research, 28*(8), 1176-1179.

Belgore, F. M., Blann, A. D., & Lip, G. Y. (2001). Measurement of free and complexed soluble vascular endothelial growth factor receptor, Flt-I, in fluid samples: Development and application of two new immunoassays. *Clinical Science, 100*(5), 567-575.

Berdowska, A., & Zwirska-Korczala, K. (2001). Neopterin measurement in clinical diagnosis. *Journal of clinical pharmacy and therapeutics, 26*(5), 319-329.

Boyle, J. J., Weissberg, P. L., & Bennett, M. R. (2003). Tumor necrosis factor-α promotes macrophage-induced vascular smooth muscle cell apoptosis by direct and autocrine mechanisms. *Arteriosclerosis, thrombosis, and vascular biology, 23*(9), 1553-1558.

Cai, J., Jiang, W. G., Ahmed, A., & Boulton, M. (2006). Vascular endothelial growth factor-induced endothelial cell proliferation is regulated by interaction between VEGFR-2, SH-PTP1 and eNOS. *Microvascular research, 71*(1), 20-31.

Carmeliet, P. (2005). Angiogenesis in life, disease and medicine. *Nature, 438*(7070), 932-936.

Chung, N., Lydakis, C., Belgore, F., Blann, A., & Lip, G. (2002). Angiogenesis in myocardial infarction. An acute or chronic process? *European heart journal, 23*(20), 1604-1608.

Collart, M. A., Belin, D., Vassalli, J.-D., De Kossodo, S., & Vassalli, P. (1986). Gamma interferon enhances macrophage transcription of the tumor necrosis factor/cachectin, interleukin 1, and urokinase genes, which are controlled by short-lived repressors. *The Journal of experimental medicine, 164*(6), 2113-2118.

Couffinhal, T., Kearney, M., Witzenbichler, B., Chen, D., Murohara, T., Losordo, D. W., Isner, J. M. (1997). Vascular endothelial growth factor/vascular permeability factor (VEGF/VPF) in normal and atherosclerotic human arteries. *The American journal of pathology, 150*(5), 1673.

Davies, M. J. (2000). The pathophysiology of acute coronary syndromes. *Heart, 83*(3), 361-366.

De Boer, O. J., van der Wal, A. C., Verhagen, C. E., & Becker, A. E. (1999). Cytokine secretion profiles of cloned T cells from human aortic atherosclerotic plaques. *The Journal of pathology, 188*(2), 174-179.

Dominguez-Rodriguez, A., Abreu-Gonzalez, P., Avanzas, P., Laynez-Cerdeña, I., & Kaski, J. C. (2010). Neopterin predicts left ventricular remodeling in patients with ST-segment elevation myocardial infarction undergoing primary percutaneous coronary intervention. *Atherosclerosis, 211*(2), 574-578.

Du Clos. (2000). Function of C-reactive protein. *Annals of medicine, 32*(4), 274-278.

Eichmann, A., & Simons, M. (2012). VEGF signaling inside vascular endothelial cells and beyond. *Current opinion in cell biology, 24*(2), 188-193.

Epstein, F. H., Diaz, M. N., Frei, B., Vita, J. A., & Keaney Jr, J. F. (1997). Antioxidants and atherosclerotic heart disease. *New England Journal of Medicine, 337*(6), 408-416.

Ferrara, N., Gerber, H.-P., & LeCouter, J. (2003). The biology of VEGF and its receptors. *Nature medicine, 9*(6), 669-676.

Firth, C. A., Laing, A. D., Baird, S. K., Pearson, J., & Gieseg, S. P. (2008). Inflammatory sites as a source of plasma neopterin: measurement of high levels of neopterin and markers of oxidative stress in pus drained from human abscesses. *Clinical biochemistry, 41*(13), 1078-1083.

Flavall, E. A., Crone, E. M., Moore, G. A., & Gieseg, S. P. (2008). Dissociation of neopterin and 7,8-dihydroneopterin from plasma components before HPLC analysis. *Journal of Chromatography B, 863*(1), 167-171.

Fuchs, Avanzas, P., Arroyo-Espliguero, R., Jenny, M., Consuegra-Sanchez, L., & Kaski, J. (2009). The role of neopterin in atherogenesis and cardiovascular risk assessment. *Current medicinal chemistry, 16*(35), 4644-4653.

Fuchs, Milstien, S., Krämer, A., Reibnegger, G., Werner, E. R., Goedert, J. J., Wachter, H. (1989). Urinary neopterin concentrations vs total neopterins for clinical utility. *Clinical chemistry, 35*(12), 2305-2307.

Fuster, V., Moreno, P. R., Fayad, Z. A., Corti, R., & Badimon, J. J. (2005). Atherothrombosis and high-risk plaquePart I: evolving concepts. *Journal of the American College of Cardiology, 46*(6), 937-954.

Garcia-Moll, Coccolo, F., Cole, D., & Kaski, J. C. (2000). Serum neopterin and complex stenosis morphology in patients with unstable angina. *Journal of the American College of Cardiology, 35*(4), 956-962.

Garcia-Moll, Cole, D., Zouridakis, E., & Kaski, J. (2000). Increased serum neopterin: a marker of coronary artery disease activity in women. *Heart, 83*(3), 346-350.

Garcia-Moll, X., Cole, D., Zouridakis, E., & Kaski, J. (2000). Increased serum neopterin: a marker of coronary artery disease activity in women. *Heart, 83*(3), 346-350.

George, J. (2008). Mechanisms of disease: the evolving role of regulatory T cells in atherosclerosis. *Nature Clinical Practice Cardiovascular Medicine, 5*(9), 531-540.

Gerber, H.-P., Condorelli, F., Park, J., & Ferrara, N. (1997). Differential transcriptional regulation of the two vascular endothelial growth factor receptor genes Flt-1, but not Flk-1/KDR, is up-regulated by hypoxia. *Journal of Biological Chemistry, 272*(38), 23659-23667.

Germain, S., Monnot, C., Muller, L., & Eichmann, A. (2010). Hypoxia-driven angiogenesis: role of tip cells and extracellular matrix scaffolding. *Current opinion in hematology, 17*(3), 245-251.

Gieseg, S. P., Leake, D. S., Flavall, E. M., Amit, Z., Reid, L., & Yang, Y. T. (2009). Macrophage antioxidant protection within atherosclerotic plaques. *Frontiers in Bioscience, 14*, 1230-1246.

Glass, C. K., & Witztum, J. L. (2001). Atherosclerosis: The Road Ahead. *Cell, 104*(4), 503-516.

Go, A. S., Chertow, G. M., Fan, D., McCulloch, C. E., & Hsu, C.-y. (2004). Chronic kidney disease and the risks of death, cardiovascular events, and hospitalization. *New England Journal of Medicine, 351*(13), 1296-1305.

Go, A. S., Mozaffarian, D., Roger, V. L., Benjamin, E. J., Berry, J. D., Blaha, M. J., Franco, S. (2014). Heart disease and stroke statistics--2014 update: a report from the American Heart Association. *Circulation, 129*(3), e28.

Go, A. S., Mozaffarian, D., Roger, V. L., Benjamin, E. J., Berry, J. D., Borden, W. B., Fox, C. S. (2013). Executive Summary: Heart Disease and Stroke Statistics: 2013 Update: A Report From the American Heart Association. *Circulation, 127*(1), 143-146.

Goetze, J., Christoffersen, C., Perko, M., Arendrup, H., Rehfeld, J., Kastrup, J., & Nielsen, L. (2003). Increased cardiac BNP expression associated with myocardial ischemia. *The FASEB Journal, 17*(9), 1105-1107.

Gonzalez, R. M., Seurynck-Servoss, S. L., Crowley, S. A., Brown, M., Omenn, G. S., Hayes, D. F., & Zangar, R. C. (2008). Development and validation of sandwich ELISA microarrays with minimal assay interference. *Journal of proteome research, 7*(6), 2406-2414.

Gounopoulos, P., Merki, E., Hansen, L., Choi, S., & Tsimikas, S. (2007). Antibodies to oxidized low density lipoprotein: epidemiological studies and potential clinical applications in cardiovascular disease. *Minerva cardioangiologica, 55*(6), 821-837.

Grammer, T. B., Fuchs, D., Boehm, B. O., Winkelmann, B. R., & Maerz, W. (2009). Neopterin as a predictor of total and cardiovascular mortality in individuals undergoing angiography in the Ludwigshafen Risk and Cardiovascular Health study. *Clinical chemistry, 55*(6), 1135-1146.

Gross, C. P., Chaudhry, S. I., Leo-Summers, L., & Fried, T. R. (2011). Change in comorbidity prevalence with advancing age among persons with heart failure. *Journal of general internal medicine, 26*(10), 1145-1151.

Hansson, G. K. (2005). Inflammation, atherosclerosis, and coronary artery disease. *New England Journal of Medicine, 352*(16), 1685-1695.

Hansson, G. K., & Hermansson, A. (2011). The immune system in atherosclerosis. *Nature immunology, 12*(3), 204-212.

Hantash, J., Smidt, M., & Bowsher, R. R. (2009). The development, optimization and validation of an ELISA bioanalytical method for the determination of Cetuximab in human serum. *Analytical Methods, 1*(2), 144-148.

Harper, S. J., & Bates, D. O. (2008). VEGF-A splicing: the key to anti-angiogenic therapeutics? *Nature Reviews Cancer, 8*(11), 880-887.

Hay, D. R. (2002). *Cardiovascular disease in New Zealand, 2001: A summary of recent statistical information*: National Heart Foundation of New Zealand.

Hegyi, L., Skepper, J. N., Cary, N. R., & Mitchinson, M. J. (1996). Foam cell apoptosis and the development of the lipid core of human atherosclerosis. *The Journal of pathology, 180*(4), 423-429.

Henriksen, T., Mahoney, E. M., & Steinberg, D. (1981). Enhanced macrophage degradation of low density lipoprotein previously incubated with cultured endothelial cells: recognition by receptors for acetylated low density lipoproteins. *Proceedings of the National Academy of Sciences, 78*(10), 6499-6503.

Henriksen, T., Mahoney, E. M., & Steinberg, D. (1983). Enhanced macrophage degradation of biologically modified low density lipoprotein. *Arteriosclerosis, thrombosis, and vascular biology, 3*(2), 149-159.

Hessler, J. R., Morel, D. W., Lewis, L. J., & Chisolm, G. M. (1983). Lipoprotein oxidation and lipoprotein-induced cytotoxicity. *Arteriosclerosis, thrombosis, and vascular biology, 3*(3), 215-222.

Hiratsuka, S., Maru, Y., Okada, A., Seiki, M., Noda, T., & Shibuya, M. (2001). Involvement of Flt-1 tyrosine kinase (vascular endothelial growth factor receptor-1) in pathological angiogenesis. *Cancer Research, 61*(3), 1207-1213.

Hochholzer, W., Reichlin, T., Stelzig, C., Hochholzer, K., Meissner, J., Breidthardt, T., Winkler, K. (2011). Impact of soluble fms-like tyrosine kinase-1 and placental growth factor serum levels for risk stratification and early diagnosis in patients with suspected acute myocardial infarction. *European heart journal, 32*(3), 326-335.

Hornig, C., Behn, T., Bartsch, W., Yayon, A., & Weich, H. A. (1999). Detection and quantification of complexed and free soluble human vascular endothelial growth factor receptor-1 (sVEGFR-1) by ELISA. *Journal of immunological methods, 226*(1), 169-177.

Imhof, A., Froehlich, M., Brenner, H., Boeing, H., Pepys, M. B., & Koenig, W. (2001). Effect of alcohol consumption on systemic markers of inflammation. *The Lancet, 357*(9258), 763-767.

Inoue, M., Itoh, H., Ueda, M., Naruko, T., Kojima, A., Komatsu, R., Takaya, K. (1998). Vascular Endothelial Growth Factor (VEGF) Expression in Human Coronary Atherosclerotic Lesions Possible Pathophysiological Significance of VEGF in Progression of Atherosclerosis. *Circulation, 98*(20), 2108-2116.

Johnson, J. L., & Newby, A. C. (2009). Macrophage heterogeneity in atherosclerotic plaques. *Current opinion in lipidology, 20*(5), 370.

Kadl, A., Meher, A. K., Sharma, P. R., Lee, M. Y., Doran, A. C., Johnstone, S. R., Chen, W. (2010). Identification of a novel macrophage phenotype that develops in response to atherogenic phospholipids via Nrf2. *Circulation research, 107*(6), 737-746.

Kappas, N. C., Zeng, G., Chappell, J. C., Kearney, J. B., Hazarika, S., Kallianos, K. G., Bautch, V. L. (2008). The VEGF receptor Flt-1 spatially modulates Flk-1 signaling and blood vessel branching. *The Journal of cell biology, 181*(5), 847-858.

Kapur, N. K., Heffernan, K. S., Yunis, A. A., Nguyen, T. A., Aronovitz, M. J., Parpos, P., Shah, A. (2011). Elevated soluble fms-like tyrosine kinase-1 levels in acute coronary occlusion. *Arteriosclerosis, thrombosis, and vascular biology, 31*(2), 443-450.

Kaski, J. C., Consuegra-Sanchez, L., Fernandez-Berges, D. J., Cruz-Fernandez, J. M., Garcia-Moll, X., Marrugat, J., Guzmán-Martínez, G. (2008). Elevated serum neopterin levels and adverse cardiac events at 6 months follow-up in Mediterranean patients with non-ST-segment elevation acute coronary syndrome. *Atherosclerosis, 201*(1), 176-183.

Kerbel, R. S. (2008). Tumor angiogenesis. *New England Journal of Medicine, 358*(19), 2039-2049.

Khand, A., Gemmell, I., Rankin, A., & Cleland, J. (2001). Clinical events leading to the progression of heart failure: insights from a national database of hospital discharges. *European heart journal, 22*(2), 153-164.

Kim, S.-Y., Lee, S.-H., Park, S., Kang, S.-M., Chung, N., Shim, W.-H., Jang, Y. (2011). Vascular endothelial growth factor, soluble fms-like tyrosine kinase 1, and the severity of coronary artery disease. *Angiology, 62*(2), 176-183.

Kloner, R. A., & Rezkalla, S. H. (2007). To drink or not to drink? That is the question. *Circulation, 116*(11), 1306-1317.

Koch, S., & Claesson-Welsh, L. (2012). Signal transduction by vascular endothelial growth factor receptors. *Cold Spring Harbor perspectives in medicine,* a006502.

Kodama, Y., Kitta, Y., Nakamura, T., Takano, H., Umetani, K., Fujioka, D., Mende, A. (2006). Atorvastatin increases plasma soluble Fms-like tyrosine kinase-1 and decreases vascular endothelial growth factor and placental growth factor in association with improvement of ventricular function in acute myocardial infarction. *Journal of the American College of Cardiology, 48*(1), 43-50.

Ku, D. D., Zaleski, J. K., Liu, S., & Brock, T. A. (1993). Vascular endothelial growth factor induces EDRF-dependent relaxation in coronary arteries. *American Journal of Physiology, 265,* H586-H586.

Ky, B., French, B., Levy, W. C., Sweitzer, N. K., Fang, J. C., Wu, A. H., Cappola, T. P. (2012). Multiple biomarkers for risk prediction in chronic heart failure. *Circulation: Heart Failure, 5*(2), 183-190.

Ky, B., French, B., Ruparel, K., Sweitzer, N. K., Fang, J. C., Levy, W. C., Cappola, T. P. (2011). The vascular marker soluble fms-like tyrosine kinase 1 is associated with disease severity and adverse outcomes in chronic heart failure. *Journal of the American College of Cardiology, 58*(4), 386-394.

Lahoute, C., Herbin, O., Mallat, Z., & Tedgui, A. (2011). Adaptive immunity in atherosclerosis: mechanisms and future therapeutic targets. *Nature Reviews Cardiology, 8*(6), 348-358.

Langenkamp, A., Messi, M., Lanzavecchia, A., & Sallusto, F. (2000). Kinetics of dendritic cell activation: impact on priming of TH1, TH2 and nonpolarized T cells. *Nature immunology, 1*(4), 311-316.

Laurat, E., Poirier, B., Tupin, E., Caligiuri, G., Hansson, G., Bariety, J., & Nicoletti, A. (2001). In vivo downregulation of T helper cell 1 immune responses reduces atherogenesis in apolipoprotein E-knockout mice. *Circulation, 104*(2), 197-202.

Lee, J. W., Devanarayan, V., Barrett, Y. C., Weiner, R., Allinson, J., Fountain, S., Duan, L. (2006). Fit-for-purpose method development and validation for successful biomarker measurement. *Pharmaceutical research, 23*(2), 312-328.

Lee, J. W., & Hall, M. (2009). Method validation of protein biomarkers in support of drug development or clinical diagnosis/prognosis. *Journal of Chromatography B, 877*(13), 1259-1271.

Leitner, K., Meyer, M., Leimbacher, W., Peterbauer, A., Hofer, S., Heufler, C., Thony, B. (2003). Low tetrahydrobiopterin biosynthetic capacity of human monocytes is caused by exon skipping in 6-pyruvoyl tetrahydropterin synthase. *Biochem. J, 373*, 681-688.

Libby, P. (2001). Current concepts of the pathogenesis of the acute coronary syndromes. *Circulation, 104*(3), 365-372.

Libby, P. (2006). The immune response in atherosclerosis: a double-edged sword. *Nature Reviews Immunology, 6*(7), 508-519.

Libby, P., Ridker, P. M., & Hansson, G. K. (2011). Progress and challenges in translating the biology of atherosclerosis. *Nature, 473*(7347), 317-325.

Lip, G. Y. H., & Chung, I. (2005). Vascular endothelial growth factor and angiogenesis in heart failure. *Journal of Cardiac Failure, 11*(4), 285-287. doi: 10.1016/j.cardfail.2005.02.002

Liuzzo, G., Goronzy, J. J., Yang, H., Kopecky, S. L., Holmes, D. R., Frye, R. L., & Weyand, C. M. (2000). Monoclonal T-cell proliferation and plaque instability in acute coronary syndromes. *Circulation, 101*(25), 2883-2888.

Liuzzo, G., Kopecky, S. L., Frye, R. L., O'Fallon, W. M., Maseri, A., Goronzy, J. J., & Weyand, C. M. (1999). Perturbation of the T-cell repertoire in patients with unstable angina. *Circulation, 100*(21), 2135-2139.

Liuzzo, G., Vallejo, A. N., Kopecky, S. L., Frye, R. L., Holmes, D. R., Goronzy, J. J., & Weyand, C. M. (2001). Molecular fingerprint of interferon-γ signaling in unstable angina. *Circulation, 103*(11), 1509-1514.

Mallat, Z., Taleb, S., Ait-Oufella, H., & Tedgui, A. (2009). The role of adaptive T cell immunity in atherosclerosis. *Journal of lipid research, 50*(Supplement), S364-S369.

Matsumoto, T., Uemura, S., Takeda, Y., Matsui, M., Okada, S., Nishida, T., Ishigami, K.-i. (2012). An elevated ratio of placental growth factor to soluble fms-like tyrosine kinase-1 predicts adverse outcomes in patients with stable coronary artery disease. *Internal medicine (Tokyo, Japan), 52*(10), 1019-1027.

McKeeman, G. C., Ardill, J. E., Caldwell, C. M., Hunter, A. J., & McClure, N. (2004). Soluble vascular endothelial growth factor receptor-1 (sFlt-1) is increased throughout gestation in patients who have preeclampsia develop. *American journal of obstetrics and gynecology, 191*(4), 1240-1246.

Mestas, J., & Ley, K. (2008). Monocyte-Endothelial Cell Interactions in the Development of Atherosclerosis. *Trends in Cardiovascular Medicine, 18*(6), 228-232.

Moore, K. J., & Tabas, I. (2011). Macrophages in the pathogenesis of atherosclerosis. *Cell, 145*(3), 341-355.

Morel, & Chisolm, G. (1984). Endothelial and smooth muscle cells alter low density lipoprotein in vitro by free radical oxidation. *Arteriosclerosis, thrombosis, and vascular biology, 4*(4), 357-364.

Morel, Hessler, J. R., & Chisolm, G. M. (1983). Low density lipoprotein cytotoxicity induced by free radical peroxidation of lipid. *Journal of lipid research, 24*(8), 1070-1076.

Morrow, D., Hatch, E., Hamm, K., Cahill, P. A., & Redmond, E. M. (2014). Flk-1/KDR Mediates Ethanol-Stimulated Endothelial Cell Notch Signaling and Angiogenic Activity. *Journal of vascular research, 51*(4), 315-324.

Murr, Widner, B., Wirleitner, B., & Fuchs, D. (2002). Neopterin as a marker for immune system activation. *Current drug metabolism, 3*(2), 175-187.

Murr., Schroecksnadel, K., Schonitzer, D., Fuchs, D., & Schennach, H. (2005). Neopterin concentrations in blood donors differ between AB0 blood group phenotypes. *Clinical biochemistry, 38*(10), 916-919.

Murray, P. J., Allen, J. E., Biswas, S. K., Fisher, E. A., Gilroy, D. W., Goerdt, S., Lawrence, T. (2014). Macrophage activation and polarization: nomenclature and experimental guidelines. *Immunity, 41*(1), 14-20.

Nazer, B., Ray, K. K., Sloan, S., Scirica, B., Morrow, D. A., Cannon, C. P., & Braunwald, E. (2011a). Prognostic utility of neopterin and risk of heart failure hospitalization after an acute coronary syndrome. *European heart journal*, ehr032.

Nazer, B., Ray, K. K., Sloan, S., Scirica, B., Morrow, D. A., Cannon, C. P., & Braunwald, E. (2011b). Prognostic utility of neopterin and risk of heart failure hospitalization after an acute coronary syndrome. *European heart journal, 32*(11), 1390-1397.

Nevo, O., Soleymanlou, N., Wu, Y., Xu, J., Many, A., Zamudio, S., & Caniggia, I. (2006). Increased expression of sFlt-1 in in vivo and in vitro models of human placental hypoxia is mediated by HIF-1. *American Journal of Physiology-Regulatory, Integrative and Comparative Physiology, 291*(4), R1085-R1093.

Onoue, K., Uemura, S., Takeda, Y., Somekawa, S., Iwama, H., Nishida, T., Sung, J. H. (2009). Usefulness of soluble Fms-like tyrosine kinase-1 as a biomarker of acute severe heart failure in patients with acute myocardial infarction. *The American journal of cardiology, 104*(11), 1478-1483.

Orecchia, A., Lacal, P. M., Schietroma, C., Morea, V., Zambruno, G., & Failla, C. M. (2003). Vascular endothelial growth factor receptor-1 is deposited in the extracellular matrix by endothelial cells and is a ligand for theα 5β1 integrin. *Journal of cell science, 116*(17), 3479-3489.

Paulson, K. E., Zhu, S.-N., Chen, M., Nurmohamed, S., Jongstra-Bilen, J., & Cybulsky, M. I. (2010). Resident intimal dendritic cells accumulate lipid and contribute to the initiation of atherosclerosis. *Circulation research, 106*(2), 383-390.

Plata-Nazar, K., & Jankowska, A. (2011). Clinical usefulness of determining the concentration of neopterin. *Pteridines, 22*(1), 77-89.

Proctor, S. D., Vine, D. F., & Mamo, J. C. (2002). Arterial retention of apolipoprotein B48- and B100-containing lipoproteins in atherogenesis. *Current opinion in lipidology, 13*(5), 461-470.

Rader, D. J., & Daugherty, A. (2008). Translating molecular discoveries into new therapies for atherosclerosis. *Nature, 451*(7181), 904-913.

Rahimi, N. (2006). VEGFR-1 and VEGFR-2: two non-identical twins with a unique physiognomy. *Frontiers in bioscience: a journal and virtual library, 11*, 818.

Ray, K. K., Morrow, D. A., Sabatine, M. S., Shui, A., Rifai, N., Cannon, C. P., & Braunwald, E. (2007). Long-term prognostic value of neopterin a novel marker of monocyte activation in patients with acute coronary syndrome. *Circulation, 115*(24), 3071-3078.

Ross, Chen, J., Lin, Z. Q., Bueno, H., Curtis, J. P., Keenan, P. S., Vidán, M. T. (2009). Recent national trends in readmission rates after heart failure hospitalization. *Circulation: Heart Failure*, CIRCHEARTFAILURE. 109.885210.

Ross, Glomset, J., & Harker, L. (1977). Response to injury and atherogenesis. *The American journal of pathology, 86*(3), 675.

Sandner, P., Wolf, K., Bergmaier, U., Gess, B., & Kurtz, A. (1997). Induction of VEGF and VEGF receptor gene expression by hypoxia: divergent regulation in vivo and in vitro. *Kidney international, 51*(2), 448-453.

Sasaki, T., Takeishi, Y., Suzuki, S., Niizeki, T., Kitahara, T., Katoh, S., Kubota, I. (2010). High serum level of neopterin is a risk factor of patients with heart failure. *International Journal of Cardiology, 145*(2), 318.

Schaper, W., & Buschmann, I. (1999). VEGF and therapeutic opportunities in cardiovascular diseases. *Current opinion in biotechnology, 10*(6), 541-543.

Searle, J., Slagman, A., Gwosc, S., Vollert, J. O., Holert, F., Müller, C., Möckel, M. (2012). Soluble fms-like tyrosine kinase-1 (sFlt-1) predicts post-percutaneous coronary intervention (PCI) myocardial infarction (MI type 4a). *Biomarkers, 17*(8), 730-737.

Seki, H. (2014). Balance of antiangiogenic and angiogenic factors in the context of the etiology of preeclampsia. *Acta obstetricia et gynecologica Scandinavica, 93*(10), 959-964.

Selim, A. M., Velankar, P., Soghier, I., & Zolty, R. (2011). short term mortality and re-admission rates in patients hospitalized for acute heart failure: a comparison between

the specialized cardiology services and general medicine. *Journal of the American College of Cardiology, 57*(14), E1153.

Semenza, G. L. (2000). Expression of hypoxia-inducible factor 1: mechanisms and consequences. *Biochemical pharmacology, 59*(1), 47-53.

Shashkin, P., Dragulev, B., & Ley, K. (2005). Macrophage differentiation to foam cells. *Current pharmaceutical design, 11*(23), 3061-3072.

Shchepetkina, A. (2013). Mechanisms of 7,8-dihydroneopterin protection from cytotoxicity. *Masters Thesis, University Of Canterbury, Christchurch, New Zealand*.

Shimada, K. (2009). Immune system and atherosclerotic disease: heterogeneity of leukocyte subsets participating in the pathogenesis of atherosclerosis. *Circulation journal: official journal of the Japanese Circulation Society, 73*(6), 994-1001.

Siegel, D., Devaraj, S., Mitra, A., Raychaudhuri, S. P., Raychaudhuri, S. K., & Jialal, I. (2013). Inflammation, atherosclerosis, and psoriasis. *Clinical reviews in allergy & immunology, 44*(2), 194-204.

Stemme, S., Faber, B., Holm, J., Wiklund, O., Witztum, J. L., & Hansson, G. K. (1995). T lymphocytes from human atherosclerotic plaques recognize oxidized low density lipoprotein. *Proceedings of the National Academy of Sciences, 92*(9), 3893-3897.

Stocker, R., & Keaney Jr, J. F. (2004). Role of oxidative modifications in atherosclerosis. *Physiological reviews, 84*(4), 1381-1478.

Stoner, L., Lucero, A. A., Palmer, B. R., Jones, L. M., Young, J. M., & Faulkner, J. (2013). Inflammatory biomarkers for predicting cardiovascular disease. *Clinical biochemistry, 46*(15), 1353-1371.

Sucher, R., Schroecksnadel, K., Weiss, G., Margreiter, R., Fuchs, D., & Brandacher, G. (2010). Neopterin, a prognostic marker in human malignancies. *Cancer letters, 287*(1), 13-22.

Sugioka, K., Naruko, T., Matsumura, Y., Shirai, N., Hozumi, T., Yoshiyama, M., & Ueda, M. (2010). Neopterin and atherosclerotic plaque instability in coronary and carotid arteries. *Journal of atherosclerosis and thrombosis, 17*(11), 1115-1121.

Sugiyama, S., Okada, Y., Sukhova, G. K., Virmani, R., Heinecke, J. W., & Libby, P. (2001). Macrophage myeloperoxidase regulation by granulocyte macrophage colony-stimulating factor in human atherosclerosis and implications in acute coronary syndromes. *The American journal of pathology, 158*(3), 879-891.

Thorp, E., Subramanian, M., & Tabas, I. (2011). The role of macrophages and dendritic cells in the clearance of apoptotic cells in advanced atherosclerosis. *European journal of immunology, 41*(9), 2515-2518.

Thorp, E., & Tabas, I. (2009). Mechanisms and consequences of efferocytosis in advanced atherosclerosis. *Journal of leukocyte biology, 86*(5), 1089-1095.

Tse, K., Tse, H., Sidney, J., Sette, A., & Ley, K. (2013). T cells in atherosclerosis. *International immunology, 25*(11), 615-622.

Vásquez-Vivar, J. (2009). Tetrahydrobiopterin, superoxide, and vascular dysfunction. *Free Radical Biology and Medicine, 47*(8), 1108-1119.

Verlohren, S., Galindo, A., Schlembach, D., Zeisler, H., Herraiz, I., Moertl, M. G., . . . Stepan, H. (2010). An automated method for the determination of the sFlt-1/PIGF ratio in the assessment of preeclampsia. *American journal of obstetrics and gynecology, 202*(2), 161. e161-161. e111.

Vissers, M., Gunningham, S. P., Morrison, M. J., Dachs, G. U., & Currie, M. J. (2007). Modulation of hypoxia-inducible factor-1 alpha in cultured primary cells by intracellular ascorbate. *Free Radical Biology and Medicine, 42*(6), 765-772.

Walter, R., Schaffner, A., & Schoedon, G. (2001). Tetrahydrobiopterin in the vascular system. *Pteridines-Berlin, 12*(3), 93-120.

Wang, Y., Zhou, Y., He, L., Hong, K., Su, H., Wu, Y., . . . Cheng, X. (2011). Gene delivery of soluble vascular endothelial growth factor receptor-1 (sFlt-1) inhibits intra-plaque angiogenesis and suppresses development of atherosclerotic plaque. *Clinical and experimental medicine, 11*(2), 113-121.

Weiss, G., Glaser, K., Kronberger, P., Ambach, E., Fuchs, D., Bodner, E., & Wachter, H. (1992). Distinct distributions of D-erythro-neopterin in arteries and veins and its recovery by an enterohepatic circulation. *Biological chemistry Hoppe-Seyler, 373*(1), 289-294.

Weiss, G., Willeit, J., Kiechl, S., Fuchs, D., Jarosch, E., Oberhollenzer, F., . . . Wachter, H. (1994). Increased concentrations of neopterin in carotid atherosclerosis. *Atherosclerosis, 106*(2), 263-271.

Werner, E. R., Werner-Felmayer, G., Fuchs, D., Hausen, A., Reibnegger, G., Yim, J., . . . Wachter, H. (1990). Tetrahydrobiopterin biosynthetic activities in human macrophages, fibroblasts, THP-1, and T 24 cells. GTP-cyclohydrolase I is stimulated by interferon-gamma, and 6-pyruvoyl tetrahydropterin synthase and sepiapterin reductase are constitutively present. *Journal of Biological Chemistry, 265*(6), 3189-3192.

Westermeier, R., & Marouga, R. (2005). Protein detection methods in proteomics research. *Bioscience reports, 25*, 19-32.

Widner, B., Mayr, C., Wirleitner, B., & Fuchs, D. (2000). Oxidation of 7, 8-dihydroneopterin by hypochlorous acid yields neopterin. *Biochemical and biophysical research communications, 275*(2), 307-311.

Williams, K. J., & Tabas, I. (1995). The response-to-retention hypothesis of early atherogenesis. *Arteriosclerosis, thrombosis, and vascular biology, 15*(5), 551-561.

Wirleitner, B., Reider, D., Ebner, S., Böck, G., Widner, B., Jaeger, M., Fuchs, D. (2002). Monocyte-derived dendritic cells release neopterin. *Journal of leukocyte biology, 72*(6), 1148-1153.

Witztum, J. L., & Steinberg, D. (2001). The Oxidative Modification Hypothesis of Atherosclerosis: Does It Hold for Humans? *Trends in Cardiovascular Medicine, 11*(3–4), 93-102.

Xu, Li, J., Simons, M., Li, J., Laham, R. J., & Sellke, F. W. (2001). Expression of vascular endothelial growth factor and its receptors is increased, but microvascular relaxation is impaired in patients after acute myocardial ischemia. *The Journal of thoracic and cardiovascular surgery, 121*(4), 735-742.

Xu, L., Kanasaki, K., Kitada, M., & Koya, D. (2012). Diabetic angiopathy and angiogenic defects. *Fibrogenesis Tissue Repair, 5*(1), 13-13.

Zangar, R. C., Varnum, S. M., & Bollinger, N. (2005). Studying cellular processes and detecting disease with protein microarrays. *Drug metabolism reviews, 37*(3), 473-487.

Zethelius, B., Berglund, L., Sundström, J., Ingelsson, E., Basu, S., Larsson, A., . . . Ärnlöv, J. (2008). Use of multiple biomarkers to improve the prediction of death from cardiovascular causes. *New England Journal of Medicine, 358*(20), 2107-2116.

Zhou, X., & Hansson, G. (1999). Detection of B cells and proinflammatory cytokines in atherosclerotic plaques of hypercholesterolaemic apolipoprotein E knockout mice. *Scandinavian journal of immunology, 50*(1), 25-30.

Zouridakis, E., Avanzas, P., Arroyo-Espliguero, R., Fredericks, S., & Kaski, J. C. (2004). Markers of inflammation and rapid coronary artery disease progression in patients with stable angina pectoris. *Circulation, 110*(13), 1747-1753.

6

Appendix

Patient number	Age	Gender	Plaque location	Symptoms	Stenosis
42	64	M	Left ICA	TIA	75%
44	63	F	Left ICA	TIA	80-95%
50	88	M	Left ICA	Stroke, TIA	70-80%
51	78	M	Right ICA	TIA	79%
53	64	M	Left ICA	Critical limb ischaemia	70-79%
55	76	M	Right ICA	Stroke	70%
58	70	M	Left ICA	TIA	70-79%
60	81	M	Right ICA	Stroke	70-79%
63	63	F	Left ICA	Stroke	80-95%
66	81	M	Right ICA	TIA	90%
67	55	F	Left ICA	TIA	60-69%
68	81	F	Left ICA	TIA	80-95%
69	83	M	Left ICA	TIA	60-69%
70	72	F	Left ICA	Dysphasia, Slurred speech	60-69%
74	67	M	Right ICA	Stroke, left side weakness, TIA	80-95%
76	68	M	Left ICA	Stroke	85-90%
77	71	M	Right ICA	Stroke	80-95%
79	75	M	Left ICA	Stroke	80-95%
83	54	F	Right ICA	TIA/left arm weakness	79%
86	81	M	Left ICA	Stroke	70%
87	67	M	Right ICA	Stroke	70-79%
89	72	M	Right ICA	TIA	90%
*95	49	M	Left ICA	Stroke, Retinal Ischemia, Familial Hypercholesterolemia	60-69%
*97	84	M	Left ICA	TIA	70%
98	69	M	Right ICA	TIA, Left sided weakness	50-69%
*99	76	M	Right ICA	Stroke	70%
100	67	F	Right ICA	TIA	70-79%
101	87	F	Left ICA	Stroke	80%
102	81	M	Left ICA	TIA	70%
*103	71	F	Right ICA	TIA	70-79
*106	79	F	Right ICA	TIA, Stroke	80%

Table 6.1. General summary of endarterectomy patients. General medical information regarding the endarterectomy patients. TIA (Transient ischaemic attacks), ICA (Internal carotid artery). * Plaque was used for tissue culture analysis.

Patient number	sFlt-1 (pg/ml)	Neopterin (nM)	7,8 NP (nM)	Total neopterin (nM)
42	429.00	-	-	-
44	2.00	20.63	12.96	33.59
50	8342.00	31.18	11.62	42.80
51	359.00	21.44	7.10	28.54
53	169.00	13.01	10.87	23.88
55	8559.00	27.61	22.65	50.25
58	15543.00	24.72	34.91	59.63
60	5554.00	37.09	31.38	68.47
63	12221.00	39.99	17.98	57.97
66	11536.00	37.40	20.41	57.81
67	2734.00	26.28	24.25	50.54
68	8313.00	22.22	24.19	46.41
69	11186.00	35.29	29.48	64.78
70	12994.00	33.00	19.58	52.59
74	5079.00	25.27	11.24	36.51
76	20453.00	23.10	45.17	68.27
77	18887.00	17.73	39.15	56.88
79	9847.00	12.02	11.23	23.25
83	14754.00	30.23	18.31	48.53
86	11981.00	30.59	28.92	59.52
87	10461.00	57.03	24.55	81.58
89	17043.00	10.11	26.66	36.77
98	8961.00	30.93	34.83	65.77
99	9536.00	12.38	46.02	58.40
100	6206.00	29.14	30.98	60.12
101	10016.0	15.30	35.37	50.67
102	2.00	6.18	18.15	24.34

Table 6.2. General summary of endarterectomy patient's plasma. Levels of sFlt-1, neopterin 7,8 NP and total neopterin measured in patients plasma. Levels expressed as the average of duplicate sample testing. Levels of pterin measured in patient 42 were ignored as results indicated contamination.

Patient number	sFlt-1 (pg/ml)	Neopterin (nM)	7,8 NP (nM)	Total neopterin (nM)
42	2.00	-	-	-
44	294.00	20.19	8.63	28.82
50	52.39	14.95	31.81	46.76
51	9.82	11.16	28.67	39.84
53	2.00	6.38	22.85	29.23
55	28.00	13.46	30.77	44.23
58	294.00	20.41	18.48	38.89
60	60.39	6.72	24.39	31.11
63	294.00	14.99	12.06	27.05
66	6.00	17.14	8.55	25.70
67	197.00	20.87	12.93	33.80
68	462.00	25.87	15.79	41.66
69	769.00	13.18	45.21	58.39
70	335.00	27.72	16.62	44.34
74	638.00	9.82	19.27	29.09
76	710.00	11.55	16.67	28.22
77	72.73	20.78	36.70	57.49
79	171.00	16.83	15.01	31.85
83	548.00	14.41	30.28	44.69
86	320.00	21.51	16.95	38.47
87	279.00	14.82	27.75	42.57
89	874.00	13.12	30.58	43.70
98	0.0	8.13	30.24	38.37
99	29.0	13.46	30.77	44.23
100	0.0	11.72	34.10	45.82
101	0.0	16.00	31.34	47.34
102	6.00	17.14	8.55	25.70

Table 6.3. Age and gender matched healthy control patient plasma. Levels of sFlt-1, neopterin 7,8 NP and total neopterin measured in healthy control patients plasma. Levels expressed as the mean of duplicate sample testing. Levels of pterin measured in patient 42 were ignored as results from the endarterectomy plasma indicated contamination.